

**SUSTAINED MIXED MODE CRACK GROWTH
IN FLAT PLATES**

By

MICHAEL ALLEN MAGILL

Bachelor of Science
Oklahoma State University
Stillwater, Oklahoma
1980

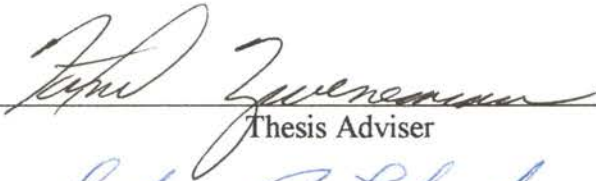
Master of Science
Oklahoma State University
Stillwater, Oklahoma
1988

Submitted to the Faculty of the
Graduate College of the
Oklahoma State University
in partial fulfillment of
the requirements for
the Degree of
DOCTOR OF PHILOSOPHY
May, 1995

Thesis
1945D
M1945

**SUSTAINED MIXED MODE CRACK GROWTH
IN FLAT PLATES**

Thesis Approved:

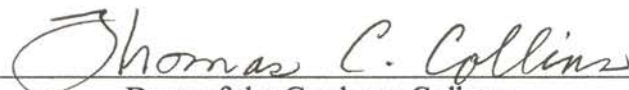


Thesis Adviser









Dean of the Graduate College

ACKNOWLEDGMENTS

A special thanks goes to Dr. Farrel Zwerneman for his support, leadership, patience, and genuine caring. In spite of the long hours and incredible amount of work, he made my five years an excellent experience. I consider myself extremely fortunate to have worked with him.

My committee was comprised of men I greatly respect and admire: Dr. Keith Good, Dr. Tim Hogue, and Dr. John Lloyd. They are great role models.

A "Thanks again!" goes to my parents. Through the years they have loved, shaped, directed, and encouraged me. They introduced me to the Faith that I now hold. I am who I am because of them.

To my kids I say, "Daddy will now be home at night! Some of my greatest emotions surround you guys. I started this long journey a month after Jessica was born with a goal of finishing by her fifth birthday. Sorry, I went two months over. I love you Jessica, Tyler, and Marshall!"

Finally, to my favorite person in the whole world, my wife, Lisa, "You made the unseen sacrifices that have no apparent reward or earthly recognition. It wasn't the desire for a lofty title or the praise of men that prompted your actions, but a genuine love for your husband. I am forever grateful." Because of her, I've become a philologist by osmosis.

TABLE OF CONTENTS

Chapter	Page
1. INTRODUCTION	1
1.1 Objective of the Study	1
1.2 Chronological Outline of the Study	2
2. LITERATURE REVIEW	4
2.1 Review of Mixed Mode Fracture Mechanics	4
2.2 Literature Search	6
2.2.1 "Equivalent" SIF Calculations/Driving Force Parameters	6
2.2.2 Mixed Mode Specimens	9
2.2.3 Specimen Considerations	17
2.2.3.1 Specimen Materials	17
2.2.3.2 Specimen Side-Grooves	18
2.2.3.3 Specimen Thickness	20
2.2.3.4 Specimen Heat Treating	20
2.2.3.5 Modes II and III Friction	20
2.2.3.6 Interface Cracks Between Dissimilar Materials	21
2.2.4 Experimental Techniques	21
2.2.4.1 Crack Measurement	21
2.2.4.2 Load Magnitude and Frequency	22
2.2.5 Finite Element Analysis	23
2.2.6 Mixed Mode Experimental Data for Comparison	24
2.3 Other Relevant Research Currently in Progress	24
2.3.1 L.P. Pook	24
2.3.2 D. Bowness and M.M.K. Lee	25
3. EXPERIMENTAL PROCEDURE	28
3.1 Background	28
3.2 The Final Specimen	32
3.3 Manufacturing the Specimens	35
3.4 Loading Procedure	38
3.5 Crack Front Shape Measurement	40
3.6 Comparison of Crack Growth Rates	40
3.7 Observations on Procedure	41

Chapter	Page
4. COMPUTER MODELING	43
4.1 The Software	43
4.2 Verification of SIF Calculations	43
4.3 Plate Length Check	44
4.4 Model Details and Procedures	44
4.5 The Programs	53
4.6 Mode I/Mode III Specimen	56
4.7 Observations on Modeling	56
5. RESULTS	58
5.1 Mode I/Mode II Specimen	58
5.2 Mode I/Mode III Specimen	69
5.3 Crack Growth Rate Comparison	72
6. CONCLUSIONS	76
7. RECOMMENDATIONS FOR FUTURE RESEARCH	78
BIBLIOGRAPHY	79
APPENDICES	88
APPENDIX A--ANSYS SIF VERIFICATIONS	89
APPENDIX B--TABULAR VALUES OF PLATE STRESS INTENSITY FACTORS	98
APPENDIX C--PLOTS OF PLATE STRESS INTENSITY FACTORS	125
APPENDIX D--PROGRAMS FOR USE WITH ANSYS	129
APPENDIX E--CRACK GROWTH RATE DATA	165
APPENDIX F--FORTRAN PROGRAM TO CALCULATE CRACK GROWTH RATES	170
APPENDIX G--STRESS INTENSITY FACTORS FOR SLANTED CRACKS PROJECTED TO HORIZONTAL	174

LIST OF TABLES

Table	Page
I. STRESS INTENSITY FACTORS VERSUS PLATE DEPTH Plate #25 - Crack Length= 2.188 in	99
II. STRESS INTENSITY FACTORS VERSUS PLATE DEPTH Plate #25 - Crack Length= 2.625 in	100
III. STRESS INTENSITY FACTORS VERSUS PLATE DEPTH Plate #25 - Crack Length= 2.850 in	101
IV. STRESS INTENSITY FACTORS VERSUS PLATE DEPTH Plate #20 - Crack Length= 2.317 in	102
V. STRESS INTENSITY FACTORS VERSUS PLATE DEPTH Plate #20 - Crack Length= 2.688 in	103
VI. STRESS INTENSITY FACTORS VERSUS PLATE DEPTH Plate #21 - Crack Length= 2.657 in	104
VII. STRESS INTENSITY FACTORS VERSUS PLATE DEPTH Plate #21 - Crack Length= 2.657 in (Straight Crack Front)	105
VIII. STRESS INTENSITY FACTORS VERSUS PLATE DEPTH Plate #21 - Crack Length= 2.969 in	106
IX. STRESS INTENSITY FACTORS VERSUS PLATE DEPTH Plate #22 - Crack Length= 2.281 in	107
X. STRESS INTENSITY FACTORS VERSUS PLATE DEPTH Plate #22 - Crack Length= 2.594 in	108
XI. STRESS INTENSITY FACTORS VERSUS PLATE DEPTH Plate #17 - Crack Length= 2.309 in	109
XII. STRESS INTENSITY FACTORS VERSUS PLATE DEPTH Plate #17 - Crack Length= 2.309 in (Straight Crack Front)	110

Table	Page
XIII. STRESS INTENSITY FACTORS VERSUS PLATE DEPTH Plate #17 - Crack Length= 2.625 in	111
XIV. STRESS INTENSITY FACTORS VERSUS PLATE DEPTH Plate #17 - Crack Length= 2.813 in	112
XV. STRESS INTENSITY FACTORS VERSUS PLATE DEPTH Plate #23 - Crack Length= 2.938 in	113
XVI. STRESS INTENSITY FACTORS VERSUS PLATE DEPTH Plate #23 - Crack Length= 3.031 in	114
XVII. STRESS INTENSITY FACTORS VERSUS PLATE DEPTH Plate #24 - Crack Length= 2.750 in	115
XVIII. STRESS INTENSITY FACTORS VERSUS PLATE DEPTH Plate #24 - Crack Length= 2.750 in (Straight Crack Front)	116
XIX. STRESS INTENSITY FACTORS VERSUS PLATE DEPTH Plate #24 - Crack Length= 3.250 in	117
XX. STRESS INTENSITY FACTORS VERSUS PLATE DEPTH Plate #26 - Crack Length= 2.594 in	118
XXI. STRESS INTENSITY FACTORS VERSUS PLATE DEPTH Plate #26 - Crack Length= 3.063 in	119
XXII. STRESS INTENSITY FACTORS VERSUS PLATE DEPTH Plate #27 - Crack Length= 3.125 in	120
XXIII. STRESS INTENSITY FACTORS VERSUS PLATE DEPTH Plate #27 - Crack Length= 3.125 in (Straight Crack Front)	121
XXIV. STRESS INTENSITY FACTORS VERSUS PLATE DEPTH Plate #27 - Crack Length= 3.347 in	122
XXV. STRESS INTENSITY FACTORS VERSUS PLATE DEPTH Plate #28 - Crack Length= 2.344 in (12 Element Layers)	123
XXVI. STRESS INTENSITY FACTORS VERSUS PLATE DEPTH Plate #28 - Crack Length= 2.344 in (22 Element Layers)	124

Table	Page
XXVII. CRACK LENGTH VERSUS NUMBER OF CYCLES ALPHA= 0 DEGREES	166
XXVIII. CRACK LENGTH VERSUS NUMBER OF CYCLES ALPHA= 20 DEGREES	168
XXIX. DA/DN VERSUS DELTA K ALPHA= 0 & 20 DEGREES	169
XXX. SIF'S FOR SLANTED CRACKS PROJECTED TO HORIZONTAL	175

LIST OF FIGURES

Figure		Page
1.	Coordinate System and Stresses Near the Crack Tip	4
2.	Basic Modes of Loading	5
3.	Remote Stress Applied to a Cracked Body	6
4.	Crack Rotation to Mode I Growth	7
5.	Mixed Mode Specimens	10
6.	Loading Device for CTS Specimen in a Tensile Testing Machine	11
7.	Fixture and Specimen Used by Chell and Yishu	12
8.	Fixture and Specimen Used by Richard	13
9.	Specimen Used by Pook	13
10.	Specimen Used by Miglin	14
11.	Specimen Used by Tschegg	14
12.	Specimen Used by Baloch and Hua	15
13.	Specimen Used by Nunomura	15
14.	Specimen and Testing Machine Used by Tschegg	16
15.	Specimen and Testing Facility Used by Found	16
16.	Specimen Used by Hojfeldt	17
17.	Mode II or Mode III Loading	19
18.	Mode II Friction	20

Figure	Page
19. Potential Drop Method	22
20. Example of Potential Drop Method	22
21. Crack Front Modeled With Quarter-Point 20-Node Wedge Elements	23
22. Example of the Mesh Used in Bowness and Lee Study	25
23. Modeled Crack Curvatures (Not to Scale)	26
24. Results of Bowness and Lee Study	27
25. Specimen for Maintaining Mixed Mode Crack Growth	29
26. Definition of Alpha and Beta Angles	30
27. Crack Growth Perpendicular to Tensile Load	31
28. Specimen With V-Shaped Side Grooves	31
29. Specimen With Staggered Rectangular Side Grooves	33
30. Specimens With V-Shaped and Symmetric Rectangular Side Grooves	33
31. Modified Chevron Notch	34
32. The Mode I/Mode II Specimens	36
33. The Mode I/Mode III Specimen	37
34. 20 Kip MTS Fatigue Testing Machine	39
35. Curved Crack Front	39
36. Plate Length Check	45
37. Finite Element Model of Specimen Using Symmetry	46
38. First Submodel of Crack Front	48
39. Second Submodel of Crack Front	49

Figure	Page
40. Third Submodel of Crack Front	50
41. Quarter-Point Wedge Elements at the Crack Tip	52
42. Submodel Generated by CURVECRK	54
43. Submodel Generated by WARPCRKR	55
44. Plots of Normalized SIF's vs. Plate Depth for Alpha= 10-30 Degrees	59
45. Plots of Normalized SIF's vs. Plate Depth for Alpha= 40 Degrees	60
46. Plot of Normalized SIF's vs. Plate Depth for Alpha= 0 Degrees	60
47. Contour of the Maximum Principal Stress in 30 Degree Plate	62
48. Strain Distribution Near Crack Tip for Curved Crack Front (Alpha= 30 Deg.)	63
49. Strain Distribution Near Crack Tip for Curved Crack Front (Alpha= 20 Deg.)	64
50. Strain Distribution Near Crack Tip for an Assumed Straight Crack Front	65
51. Maximum Principal Stress Direction for Actual Curved Crack Front	67
52. Maximum Principal Stress Direction for Assumed Straight Crack Front	68
53. Plots of Normalized SIF's vs. Plate Depth for Beta= 20 Degrees	69
54. Strain Distribution Near Crack Tip for Curved Crack Front (Beta= 20 Deg.)	70
55. Maximum Principal Stress Direction for Mode I/Mode III Specimen	71
56. Crack Growth Data for The Specimen With Alpha=0 Degrees	73
57. Crack Growth Data for The Specimen With Alpha=20 Degrees	74
58. Crack Growth Rate Versus Delta K	75
59. 2-D Compact Specimen	91
60. 2-D Plate With Center Through Crack	93

Figure	Page
61. 3-D Plate With Edge Crack in Tension	95
62. 2-D Plate With Edge Crack in Mode II Shear	97
63. Normalized SIF's vs. Plate Depth for Alpha=0 Degrees	126
64. Normalized SIF's vs. Plate Depth for Alpha=5 Degrees	126
65. Normalized SIF's vs. Plate Depth for Alpha=10 Degrees	126
66. Normalized SIF's vs. Plate Depth for Alpha=15 Degrees	127
67. Normalized SIF's vs. Plate Depth for Alpha=20 Degrees	127
68. Normalized SIF's vs. Plate Depth for Alpha=25 Degrees	127
69. Normalized SIF's vs. Plate Depth for Alpha=30 Degrees	128
70. Normalized SIF's vs. Plate Depth for Alpha=35 Degrees	128
71. Normalized SIF's vs. Plate Depth for Alpha=40 Degrees	128
72. Handbook Solution for SIF's[94]	175

NOMENCLATURE

a	crack length
A	dimensionless constant that is a function of geometry and material
B	specimen thickness
C	dimensionless constant that is a function of geometry and type of loading
E	modulus of elasticity
f_{ij}	dimensionless function
K_c	equivalent stress intensity factor
K_I	mode one stress intensity factor
K_{II}	mode two stress intensity factor
K_{III}	mode three stress intensity factor
K_{Ic}	critical value of K_I , plane-strain fracture toughness
m	exponent in Paris Growth Law that is a function of material, temperature, etc.
N	number of cycles
P	axial load on the specimen
r	radial distance from crack tip
S	strain energy density factor
SIF	stress intensity factor
SIGMA	nominal far field stress
α	angle of crack plane for Mode I/Mode II specimen

β	angle of crack plane for Mode I/Mode III specimen
ΔK	difference of maximum K and minimum K
ΔP	difference of maximum P and minimum P
θ	angle describing location relative to crack tip
ν	Poisson's ratio
σ	nominal far field stress
σ_{ij}	stress near the crack tip
σ_{kl}	nominal far field stress (i.e. σ_{xx} , σ_{yy} , σ_{xy})
σ_{YS}	material yield strength

CHAPTER 1

INTRODUCTION

1.1 Objective of the Study

The objectives of this study are to better understand what causes fatigue crack growth under mixed mode loading and to develop a suitable method for calculating the driving force parameter or verify an existing method. These objectives were accomplished by developing and analyzing a specimen that is capable of maintaining mixed mode crack growth. Several specimens were built and exposed to controlled fatigue loading in the lab. These specimen were then modeled on the computer using finite elements to determine the stress intensity factors (SIF). The computed stress intensity factors were used to determine what actually forced the crack growth (i.e. an "equivalent" SIF, the Mode I SIF, etc.).

This study was initiated in response to questions regarding fatigue crack growth control parameters and crack growth direction (including warping) in tubular joints. Because of the lack of geometric symmetry in tubular joints, even simple loads can cause predominantly mixed mode behavior. Given this complex geometry it is difficult to predict fatigue crack growth behavior. Much of the current literature [1,2] points to the fact that if mixed mode crack growth were better understood many of the fracture mechanics problems facing the offshore industry could be solved more reliably.

1.2 Chronological Outline of the Study

The original plan for the study was to use the Paris Growth Law to determine the "equivalent" SIF's developed from the forced crack growth. This plan was dependent on the specimen crack front being straight and flat. After testing several specimens it became obvious a curved crack front was the norm with this mixed mode loading. As a result the new strategy became to calculate the SIF's along the stabilized curved crack front and establish an algebraic expression for the "equivalent" SIF . This algebraic expression could then be verified by applying it to other curved crack fronts to determine if the "equivalent" SIF was satisfied.

The chronology of the study is as follows:

1. Conducted intensive literature search on mixed mode fracture mechanics
2. Ran simple crack model on finite element software (SESAM and ANSYS)
3. Calculated SIF's using handbook solutions
4. Validated computer SIF's by comparing them to handbook solutions
5. Built several types of mixed mode specimens
6. Fatigue loaded the cracked specimens to determine which would function best for maintaining the desired crack growth direction
7. Built a fixture for the traveling microscope to allow observation of slanted cracks
8. Wrote several programs to create a finite element model of the specimen with a curved crack front
9. Ran several finite element models with curved crack fronts to ensure error free calculation of SIF's

10. Built final specimens in the machine shop
11. Fatigue tested each specimen on the MTS tensile machine
12. Measured the coordinates along the curved crack fronts on each specimen
13. Calculated the SIF's for each specimen using the finite element programs
14. Analyzed the results and theorized the driving force parameter
15. Fatigue loaded a Mode I specimen and a Mode I/Mode II specimen to compare their growth rates

CHAPTER 2

LITERATURE REVIEW

2.1 Review of Mixed Mode Fracture Mechanics

The stress in a linear elastic cracked body is defined by [51,74,84,85]

$$\sigma_{ij} = \left(\frac{K_i}{\sqrt{2\pi r}} \right) f_{ij}(\theta)$$

where σ_{ij} is the stress near the crack tip, K_i is the stress intensity factor, f_{ij} is a dimensionless function and r and θ are described by Figure 1. The stress near a crack tip varies with a $\frac{1}{\sqrt{r}}$ singularity, regardless of the configuration of the cracked body.

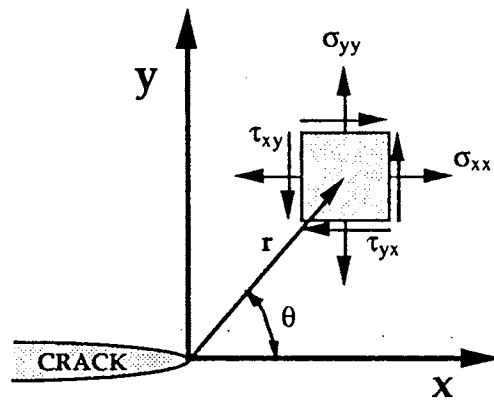


Figure 1. Coordinate System and Stresses Near the Crack Tip

A crack can experience three types of loading as shown in Figure 2. In Mode I the load is applied perpendicular to the crack faces. This is called the opening mode. In

Mode II the load is applied parallel to the crack faces and tends to cause in-plane shear.

This is called the sliding mode. In Mode III the load is also applied parallel to the crack faces but tends to force out-of-plane shear. This is called the tearing mode.

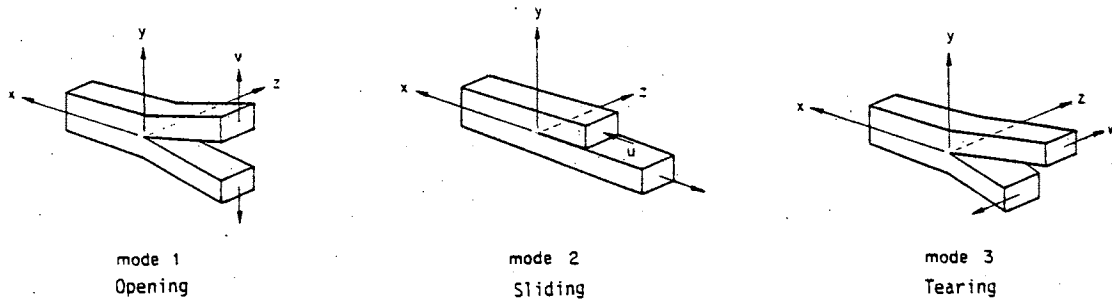


Figure 2. Basic Modes of Loading

Stress intensity factors are most useful if they are defined relative to the remote loading and the geometry. The general equations for stress intensity factors can then be written as follows:

$$\begin{aligned}
 K_I &= C_I \sigma_{kl} \sqrt{\pi a} \\
 K_{II} &= C_{II} \sigma_{kl} \sqrt{\pi a} \\
 K_{III} &= C_{III} \sigma_{kl} \sqrt{\pi a}
 \end{aligned}$$

where σ is the remote stress, a is the crack length, and C is a dimensionless constant that is a function of the geometry and type of loading. Refer to Figure 3.

Paris [66] has postulated that the stress intensity factor is the overall controlling factor in the fatigue crack propagation process. That postulate has become known as the Paris Growth Law and is mathematically stated as follows:

$$\frac{da}{dN} = A(\Delta K)^m$$

where $\frac{da}{dN}$ is the fatigue growth rate, ΔK is the stress intensity factor range

($\Delta K = K_{\max} - K_{\min}$), and A and m are constants that are a function of the material,

environment, frequency, temperature, and stress ratio. This growth law applies for Mode I, II, or III. [95]

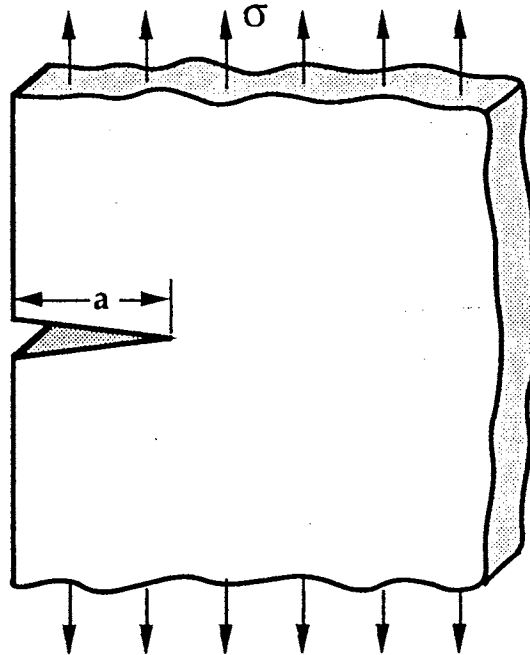


Figure 3. Remote Stress Applied to a Cracked Body

2.2 Literature Search

The results of the literature search are broken into the five major categories that follow:

2.2.1 "Equivalent" SIF Calculations/Driving Force Parameters

The objective of this portion of the literature search is to locate all research directed at developing an "Equivalent" SIF or Driving Force Parameter for mixed mode

subcritical crack growth. There is substantial literature on mixed mode crack growth and behavior. Nearly all the papers apply to symmetric and uniform specimens where the crack is free to grow in any direction. It is well established [3] that in subcritical mixed mode crack growth the crack will rotate until it reaches fully mode I growth (Figure 4). Baloch, Erdogan, Iida, Pook, Richard, Shah, Sih, Stanzl, Tschegg, Yishu and a host of others have observed and analyzed crack growth in this situation. Some of the more prominent studies are listed as references [3] through [30]. There is also literature that discusses predicting fracture in mixed mode loading [31-35,49].

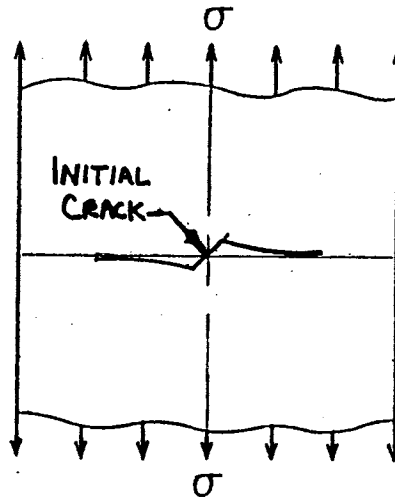


Figure 4. Crack Rotation to Mode I Growth

There is minimal literature describing subcritical crack growth if the crack is forced by geometry to maintain a mixed mode growth. Rhee [1,36-40] has written several papers that describe the need for more research on this subject as it applies to the offshore structure industry. Han [48] came to the same conclusion as a result of his work. Pook

[2] has also stated this specific need and goes on to say that the design of mixed mode specimens with a desired degree of crack path constraint has not been addressed.

At present there is not a firmly established mixed mode crack driving parameter that is universally accepted. The following is a list of the crack driving parameters found in the literature:

Broek [41] has predicted a two dimensional equivalent SIF:

$$K_{Ieq} = K_I \cos^3 \frac{\theta_m}{2} - 3K_{II} \cos^2 \frac{\theta_m}{2} \sin \frac{\theta_m}{2}$$

Rhee [37, 40, 42] and de Freitas and Carvalho [43] have used an equivalent SIF defined by the crack energy release rate:

$$K_e = \left[K_I^2 + K_{II}^2 + \frac{K_{II}^2}{(1-\nu)} \right]^{\frac{1}{2}}$$

Sih [44] and Badaliane [45] have applied the strain energy density factor to predict crack growth as follows:

$$\frac{da}{dN} = f(\Delta S_{min})$$

$$S = a_{11}k_1^2 + 2a_{12}k_1k_2 + a_{22}k_2^2 + a_{33}k_3^2$$

where:

$$a_{11} = (3 - 4\nu - \cos \theta)(1 + \cos \theta)/16\mu$$

$$a_{12} = 2 \sin \theta (\cos \theta - 1 + 2\nu)/16\mu$$

$$a_{22} = [4(1 - \nu)(1 - \cos \theta) + (3 \cos \theta - 1)(1 + \cos \theta)]/16\mu$$

$$a_{33} = 1/4\mu$$

$\mu = E/2(1 + \nu)$
 ν is Poisson Ratio
 θ is the crack angle with the horizontal
 k_1, k_2, k_3 are stress intensity factors

Tongo, Otsuka, and Yoshida [46] predict crack growth for modes II and III to be a function of the summation of the two SIF's.

$$\frac{da}{dN} = \left(\frac{da}{dN} \right)_{II} + \left(\frac{da}{dN} \right)_{III} = A_{II}(\Delta K_{II})^m + A_{III}(\Delta K_{III})^n$$

Roberts and Kibler [47] suggested a two dimensional approach:

$$\frac{da}{dN} = \frac{C_1(\Delta k)^{n_1} + C_2(\Delta k_2)^{n_2}}{\left[\left[\frac{k_{1max}}{k_{1c}} \right]^2 + \left[\frac{k_{2max}}{k_{2c}} \right]^2 - 1 \right]}$$

2.2.2 Mixed Mode Specimens

The literature search revealed numerous types and configurations of mixed mode specimens. Richard [33] has a paper that summarizes many of the more common mixed mode specimens. Figure 5 shows the specimens he evaluated. He critiques each of the specimens using the following criteria:

- C1 Full range of mixed Mode I/Mode II combinations
- C2 Compactness of specimen
- C3 Ease of manufacture
- C4 Ability to form fatigue precracks under Mode I loading
- C5 Clamping and loading conditions must be easy to achieve
- C6 Simple test procedure and evaluation
- C7 Realizability of a state of plane strain
- C8 Small minimum dimensions to give small fracture loads

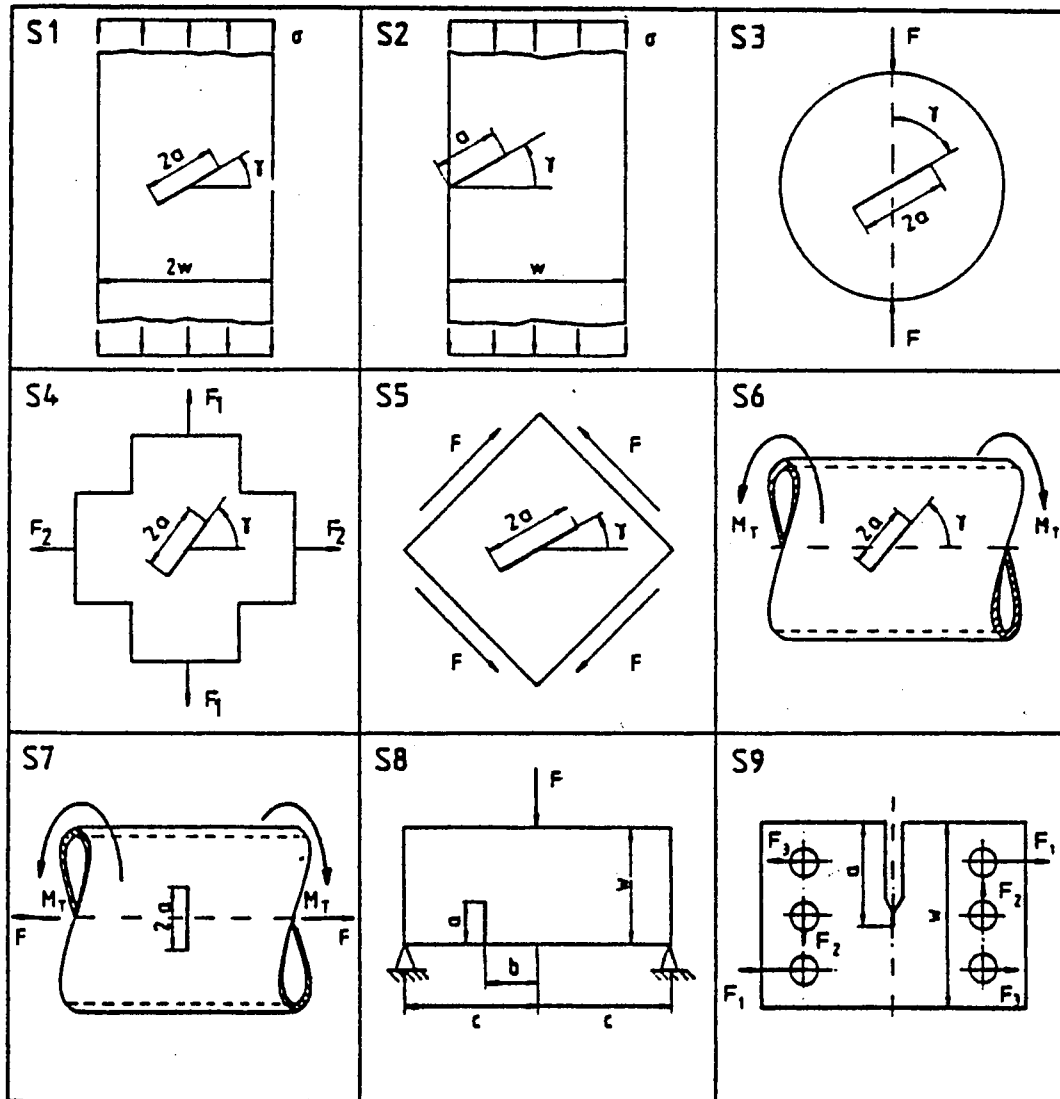


Figure 5. Mixed Mode Specimens

All of these mixed mode specimens will produce mode I crack propagation under subcritical loading. There are numerous papers on each listed in the Literature Library that was developed for this project. Richard [21] also has another paper that expands on each of these specimens in more detail. In this and another of Richard's papers [33] a

fixture is illustrated that can be used for holding compact test specimens at different angles to produce mixed mode loading (Figure 6).

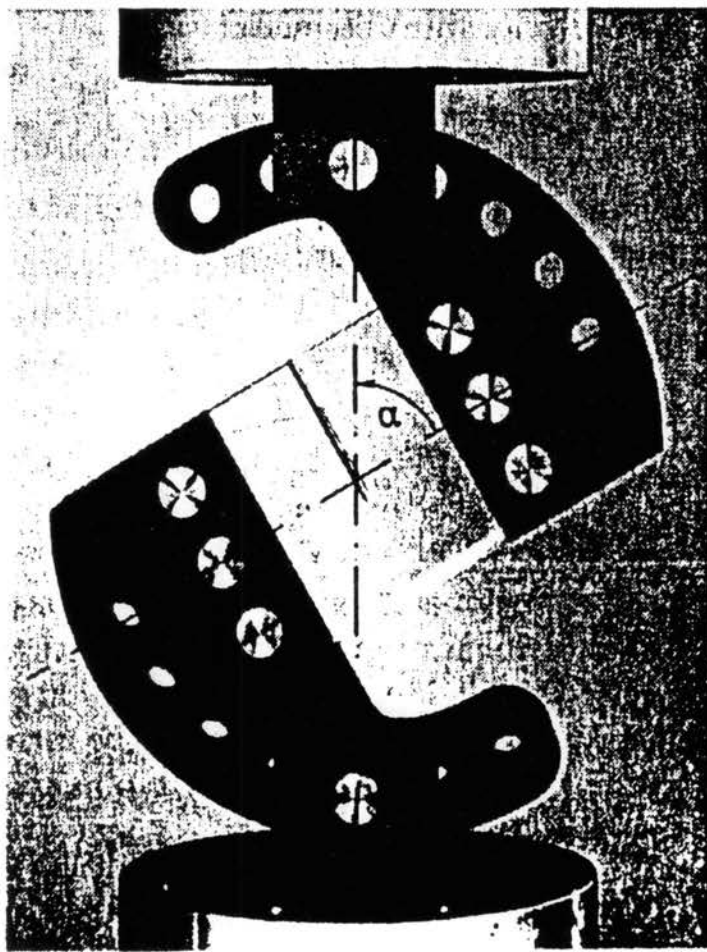


Figure 6. Loading Device for CTS Specimen in a Tensile Testing Machine

The following are additional specimens that were found in the literature.

Chell [49] and Yishu [35] used the specimen and fixture in Figure 7 to produce different combinations of modes I, II, and III for static fracture.

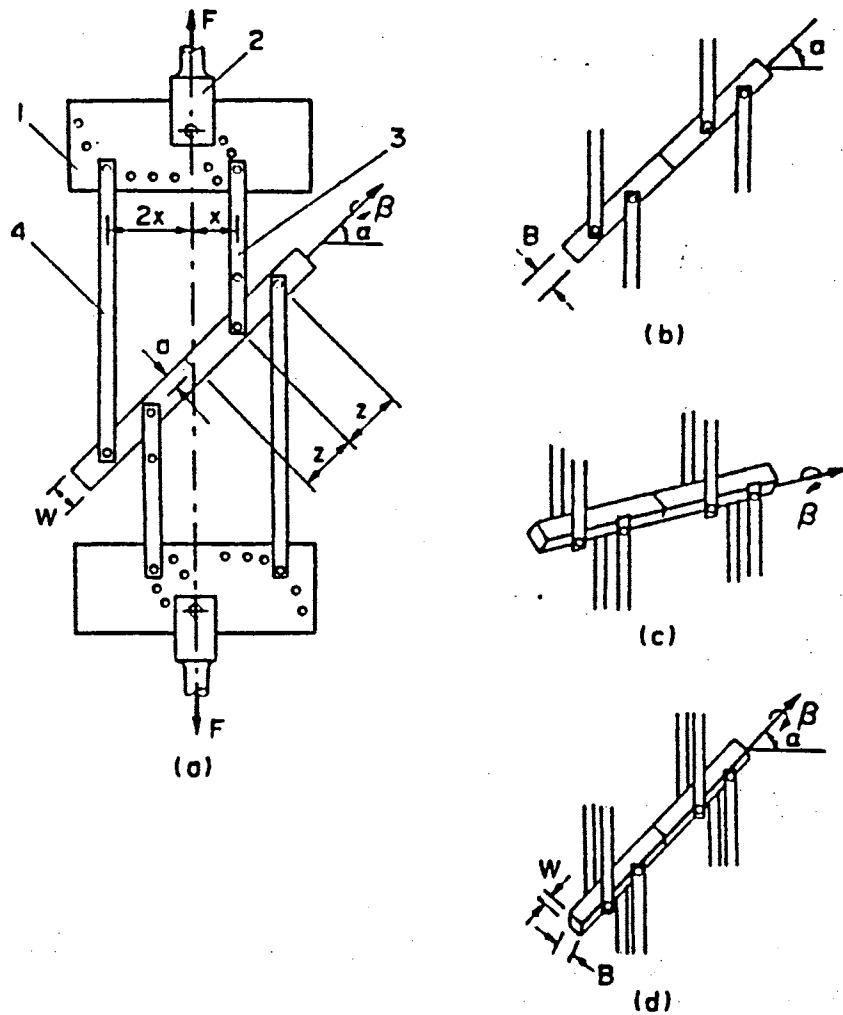


Figure 7. Fixture and Specimen Used by Chell and Yishu

Richard [32] used the specimen and fixture in Figure 8 to produce different combinations of modes I, II, and III for static fracture.

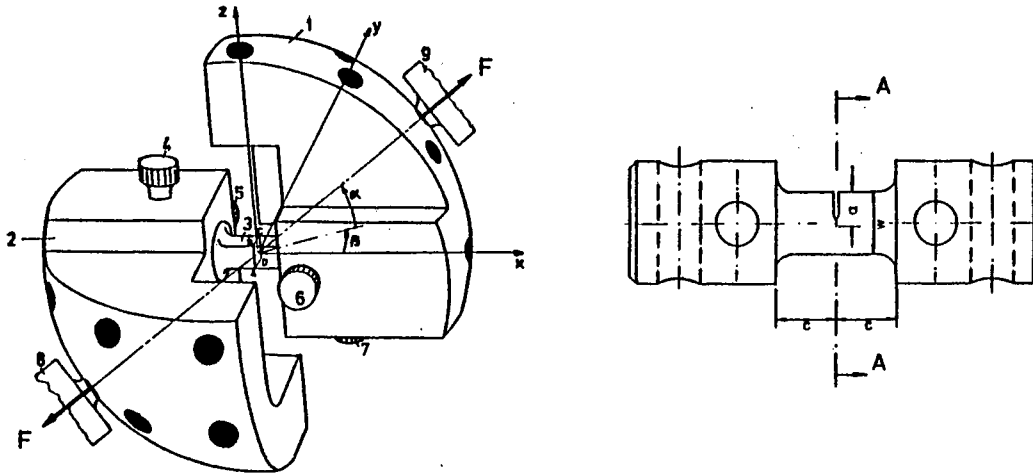


Figure 8. Fixture and Specimen Used by Richard

Pook [14, 15, 17, 18, 19, 20] used the specimens in Figure 9 to produce modes I and III.

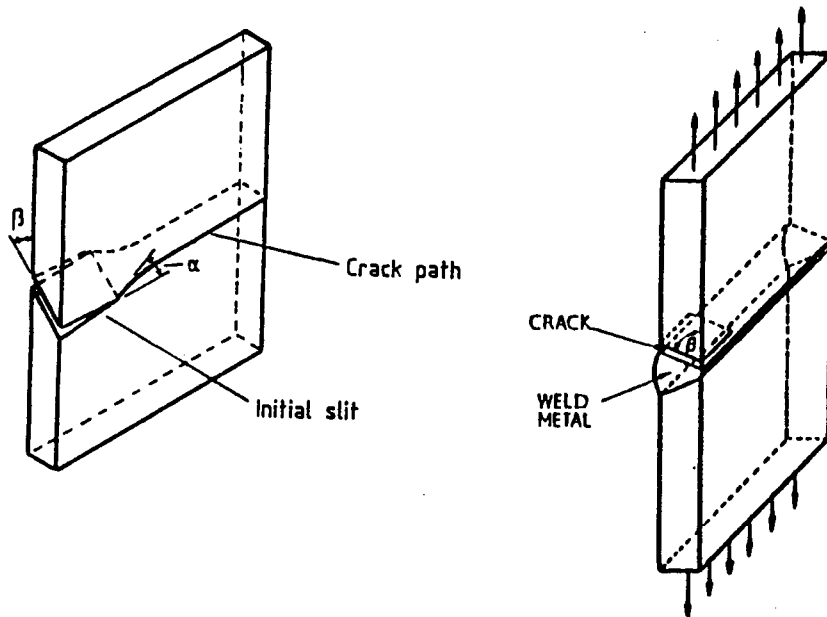


Figure 9. Specimen Used by Pook

Miglin [12] used the specimen in Figure 10 to produce modes I and III loading.

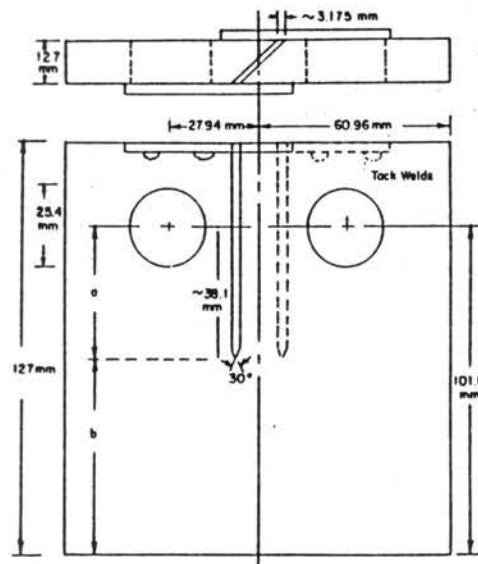


Figure 10. Specimen Used by Miglin

Tschegg [25, 28, 29, 30] used the specimen in Figure 11 to produce mode I with static mode III.

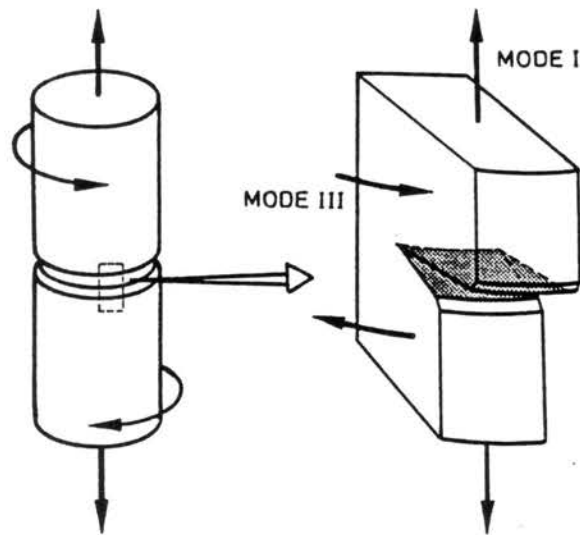


Figure 11. Specimen Used by Tschegg

Baloch [4] and Hua [9] used the specimen in Figure 12 to produce modes I and II.

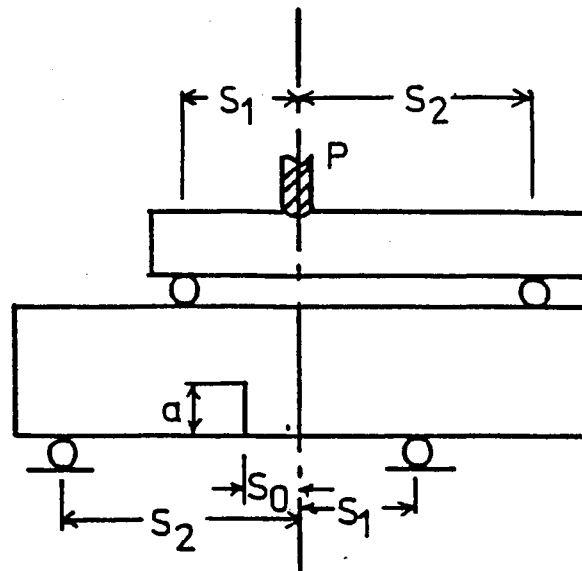


Figure 12. Specimen Used by Baloch and Hua

Nunomura [13] used the specimen in Figure 13 to produce modes I and II loading.

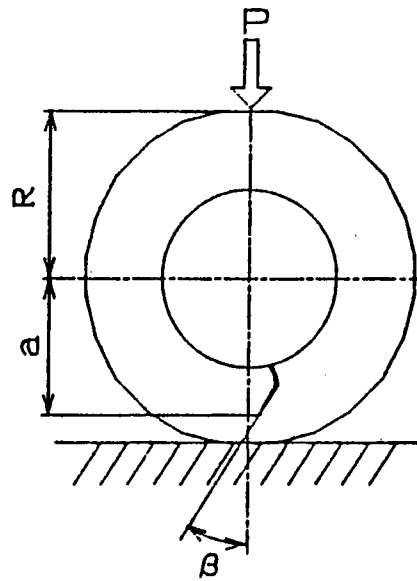


Figure 13. Specimen Used by Nunomura

Tschegg [26] used the rotating bending machine to produce reversed-repeated modes I and II (Figure 14).

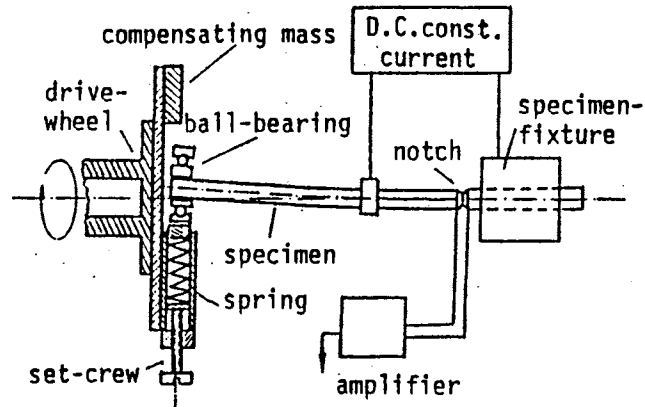


Figure 14. Specimen and Testing Machine Used by Tschegg

Found [50] developed a fatigue testing facility for producing axial loads, torsional loads, and internal and external pressures in thin-walled tubes (Figure 15).

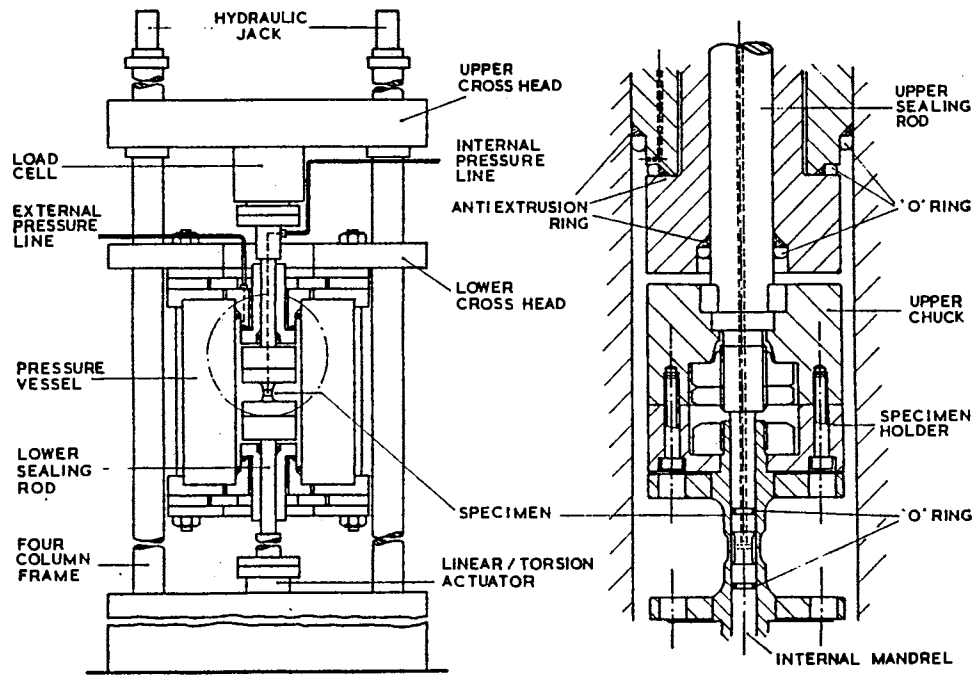


Figure 15. Specimen and Testing Facility Used by Found

Hojfeldt [8] used the specimen in Figure 16 to produce modes I, II, and III at the shoulder fillet where the precrack is located. The primary loading is mode I.

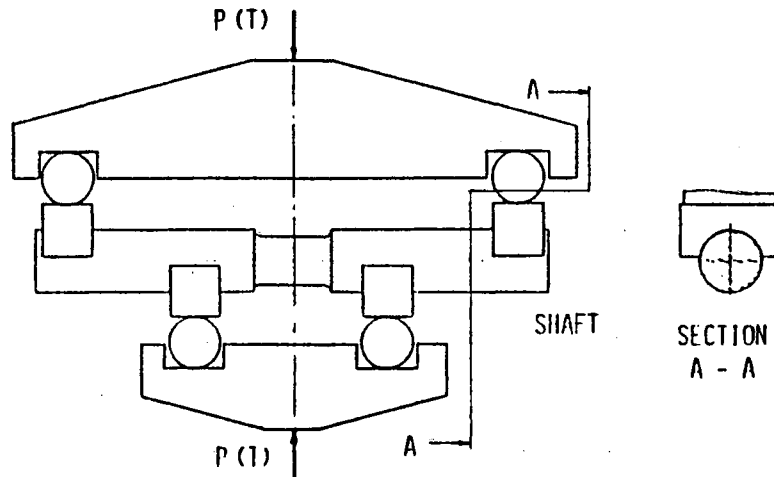


Figure 16. Specimen Used by Hojfeldt

2.2.3 Specimen Considerations

2.2.3.1 Specimen Materials. The following is a list of the different types of materials used for mixed mode studies and their associated references.

<u>Material</u>	<u>Reference</u>
Steel	
AISI 4140	[64]
AISI 4340	[23,27,28,30,64,65]
AISI C1018	[27,29,56,65]
BS4360 50D	[14,15,55]
ASTM A36	[61]
ASTM A469	[64,65]
ASTM A470	[64]
ASTM A508CL3	[62]
ASTM A514	[61]
ASTM A588	[61]

ASTM A710	[12]
AISI 304 Stainless	[13,26,60,69]
AISI 316 Stainless	[4,9,16]
AISI 420 Stainless	[25,26,35,59]

Aluminum

2017-T3	[67]
2024-T3	[13,31,57,63]
6061-T6	[69,70]
7075-T651	[13]
7075-T6	[10,11,66,67]
7475-T7351	[58]

Titanium	[68]
Plexiglas	[32,35]
Inconel 718	[22]

2.2.3.2 Specimen Side-Grooves. Specimen side-grooves can be used to force crack direction by causing a reduced cross-sectional area. Specimen side-grooves also have the "effect" of thickening the specimen and producing primarily a plane strain state [51,62,73]. Zhang [62] and Havas [71] both state there exists an optimal side-groove depth for producing the "maximum thickness". Zhang says the optimal side-groove depth is 33% of the specimen's total thickness. This also allows the specimen size to be smaller.

The following literature concerns specimens using side-grooves:

Gillemot [71] used side-grooves with compact tension specimens in mode I loading:

Deshayes [56] used side-grooves to control the crack growth direction in flat plates.

Tschegg [29,30] and Ritchie [64] used "circumferential notches" side-grooves on cylindrical specimens loaded in mode III and static mode I (Figure 11).

Wright [70] used side-grooves to produce mode III crack propagation (Figure 17).

There are two articles by Pook [72,17] where he states this is actually mode II loading.

His reasoning is that the cracked body acts like three cantilevered "beams". The bending action produces large normal strain on the top and bottom surfaces of the "beams". This normal strain causes in-plane shear at the crack tip which is mode II loading. The magnitude of the mode II loading will inherently be a function of the crack length. The longer the crack the greater the mode II loading.

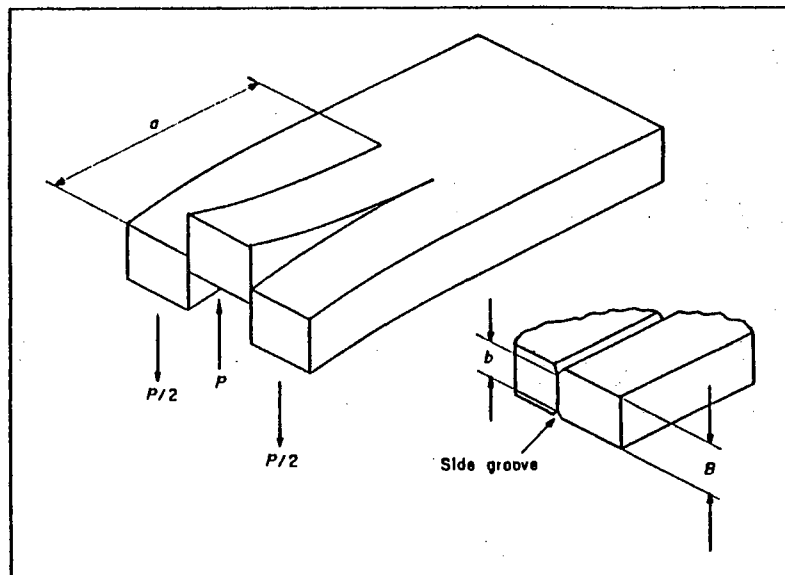
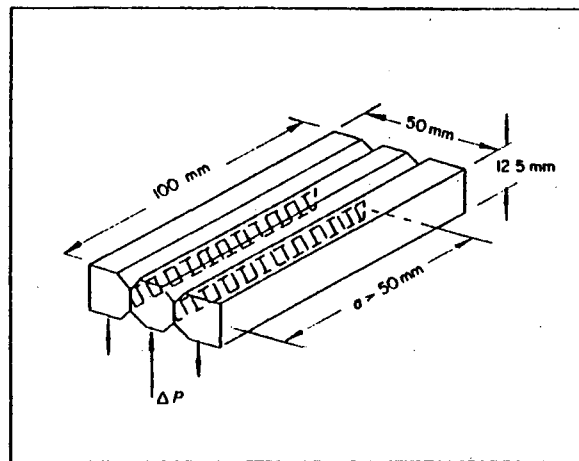


Figure 17. Mode II or Mode III Loading

2.2.3.3 Specimen Thickness. ASTM E-399 [74] and Munz [75] give the thickness requirements to produce plain strain constraint.

$$B=2.5\left(\frac{K_{Ic}}{\sigma_{YS}}\right)^2$$

2.2.3.4 Specimen Heat Treating. References [12,23,30,64,76] contain heat treating techniques that were used to change specimen fracture toughness and strength properties. Heat treating was also used to eliminate the plastic zone after precracking [25] before beginning the fatigue crack propagation process.

2.2.3.5 Modes II and III Friction. References [22,77] discuss the significance of surface rubbing caused by mode II crack growth (Figure 18). References [17,27,30,64,65] seem to indicate this also occurs in mode III.

There appear to be no quantitative methods for determining the effect of this friction. The magnitude of this effect is greatly dependent on the accompanying mode I load. It is also possible that this effect is a function of the magnitude of the minimum load relative to the maximum load.

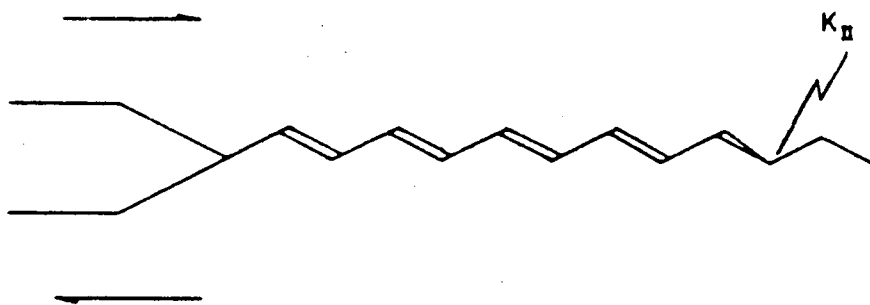


Figure 18. Mode II Friction

2.2.3.6 Interface Cracks Between Dissimilar Materials. It is possible to force a crack to grow mixed mode between two dissimilar materials. References [78,79,80] discuss the nature of crack growth at the interface between these materials. This appears to be a very complicated fracture mechanics situation and would produce a specimen difficult to accurately model on the computer. As a result dissimilar materials were not used to force the crack direction on the specimens used in this project.

2.2.4 Experimental Techniques

2.2.4.1 Crack Measurement. Based on the literature it appears the electric potential drop method (EP) is a very successful and popular method for measuring crack growth. The potential drop technique simply involves applying a constant current through a cracked specimen or structure in such a way that a change in crack length alters the potential difference at contact points in the vicinity of the crack, as shown in Figure 19 and 20. Expected accuracy can be as high as 0.0005 in. References [51] through [54] contain specific information on how to use this method and its accuracy. References [4,14,26,30,55,56,57] contain fatigue tests that used this method.

This method works well with straight crack fronts but would require complicated calibration with a curved crack front.

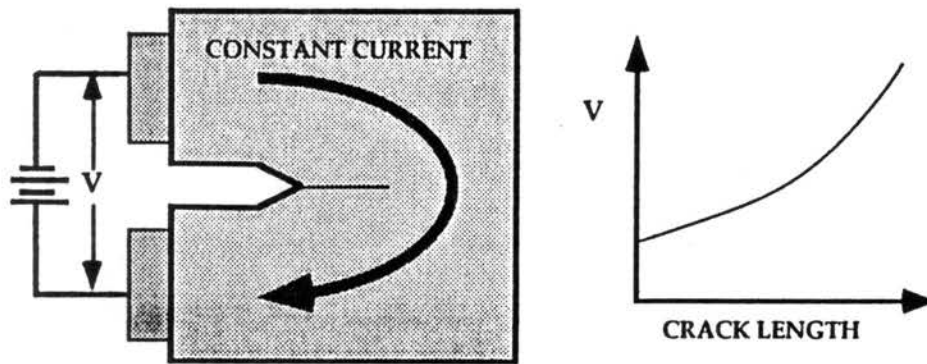


Figure 19. Potential Drop Method

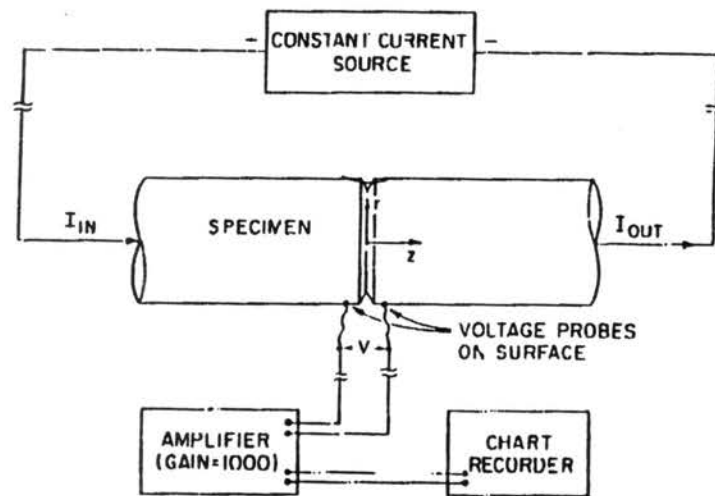


Figure 20. Example of Potential Drop Method

2.2.4.2 Load Magnitude and Frequency. The literature shows a wide range of values for the cyclic fatigue loads. It is common to set the minimum load at one-tenth of the maximum load [19,70]. To maintain subcritical crack growth the maximum stresses are generally kept below 70% of the yield strength. All loading is in tension to prevent closure effects.

The loading frequencies used in the literature varied from 0.1 Hz to 100 Hz without any apparent preferred range [4,9,15,16,19,26,30,64,70]. The exception to this was a study performed by Stanzl [60] using ultrasonic frequencies at 20kHz. After comparing his results to a loading frequency of 100 Hz he observed there were no pronounced frequency effects.

2.2.5 Finite Element Analysis

Rhee [81,82] and Ingraffea [83] have presented a technique for calculating the SIF's using the displacements from a finite element analysis. This technique uses three-dimensional quarter-point elements lined along the crack front. The quarter-point elements are actually 20-node block elements that are collapsed to a wedge and have the mid-side nodes moved to the quarter point (Figure 21). The advantage of these elements are that they produce the $\frac{1}{\sqrt{r}}$ singularity at the crack tip. This technique is used in many commercially purchased software packages such as ANSYS [86] and SESAM [87].

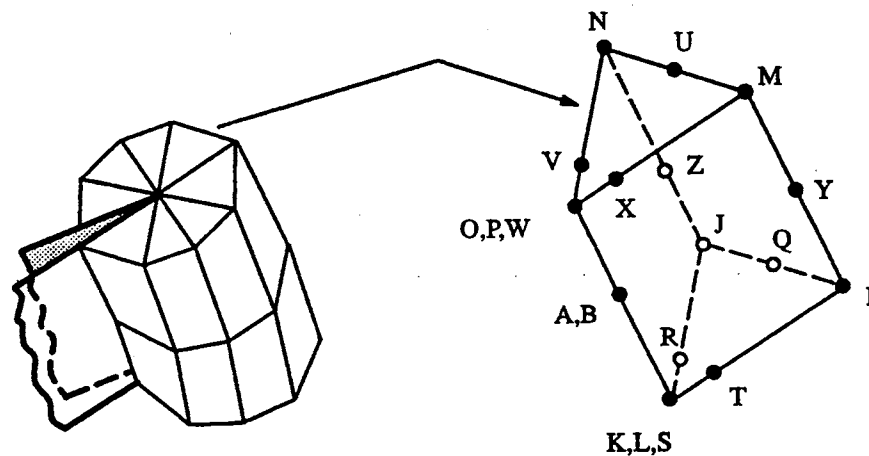


Figure 21. Crack Front Modeled With Quarter-Point 20-Node Wedge Elements

2.2.6 Mixed Mode Experimental Data for Comparison

No experimental data was found that could be used for a direct comparison with the specimen used in the current study.

2.3 Other Relevant Research Currently in Progress

2.3.1 L.P. Pook

An article was found in the May 1992 issue of "NDE Centre News" [88] from the University College at London. It states that the Science and Engineering Research Council has awarded a three year grant for the study of mixed mode fatigue and fracture cracking of offshore steels. The research will be conducted by L.P. Pook.

The article goes on to say the following. "The purpose of the project is to study the behavior of fatigue cracks in offshore steels, using small scale specimens, under the types of mixed mode loading often experienced by offshore tubular welded structures. Crack growth rates and the paths taken by cracks will be examined in detail, and data analyzed in the light of results of finite element analysis. The results obtained from the small scale specimens will be compared with data from large scale tests on tubular welded joints, including results which are becoming available from sequential multiaxial tests. It is expected that this will lead to the development of methods of predicting mixed mode fatigue crack growth behavior in practical structures, such as tubular welded joints, from the results of small scale laboratory tests."

2.3.2 D. Bowness and M.M.K. Lee

Bowness and Lee have recently performed research [89,90] at the University College of Swansea, United Kingdom that is pertinent to this study. The focus of their research was to determine the driving force parameter for the "mixed mode" crack growth in a T-joint (See Figure 22). The researchers used a locally developed program and ABAQUS to model the joint and crack. Only axial loads were applied. Eight finite element runs were made using eight different assumed crack shapes (See Figure 23). The first four runs used straight shallow cracks at different angles. The other four runs were deep cracks with two cracks being straight at different angles and the other two having curvature. The authors state that the actual crack front shape for a joint of this type is closest to curve D3. The results of their runs can be seen in Figure 24. From this figure it can be seen that K_I is the dominant mode and K_{II} and K_{III} are very close to zero except where the crack intersects the surface. The authors' conclusion is that a cracked tubular joint under axial loading is governed by the Mode I SIF and the crack grows perpendicular to the maximum principal stress. The authors also indicated that they are continuing their study to include moment loaded joints.

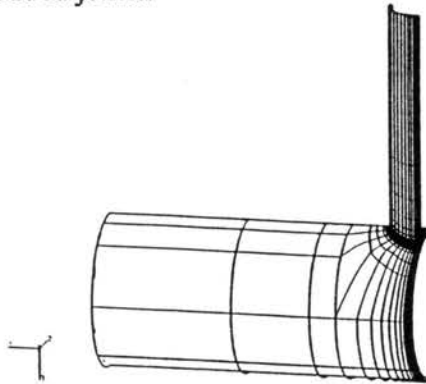
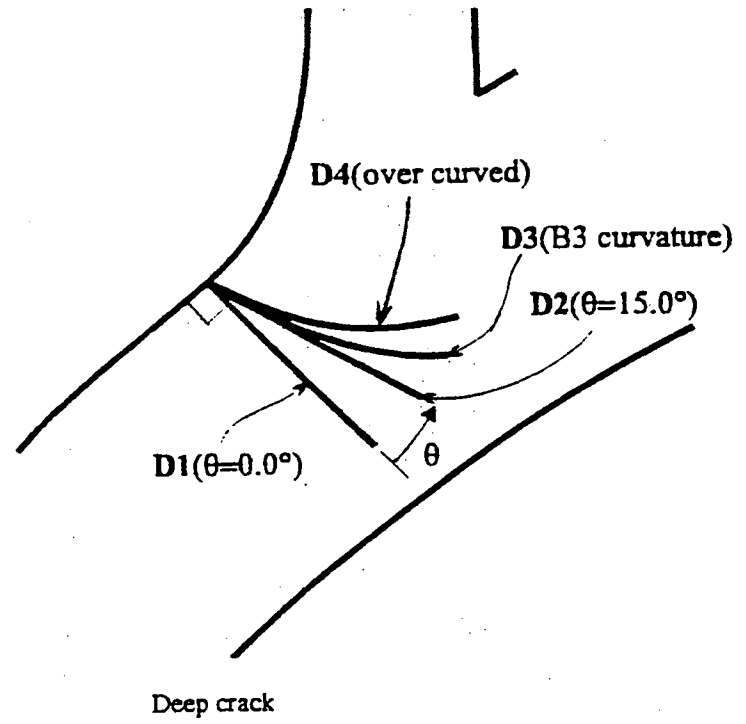
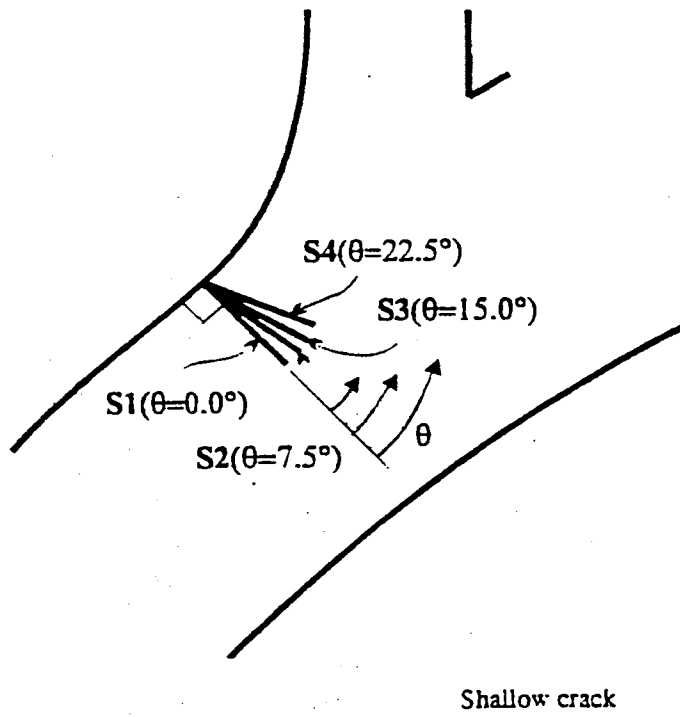


Figure 22. Example of the Mesh Used in Bowness and Lee Study

Figure 23. Modeled Crack Curvatures (Not to Scale)



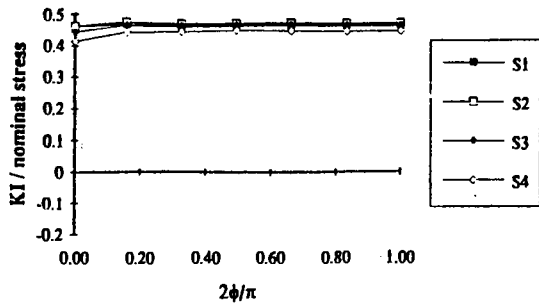


Figure 3 - Mode I SIF distribution for the shallow crack.

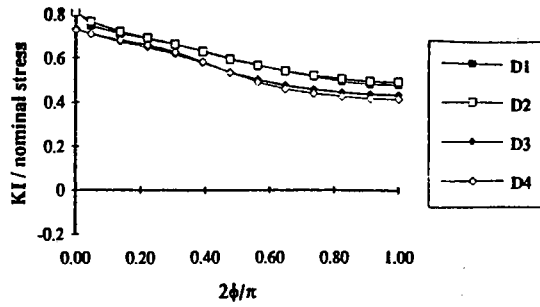


Figure 6 - Mode I SIF distribution for the deep crack.

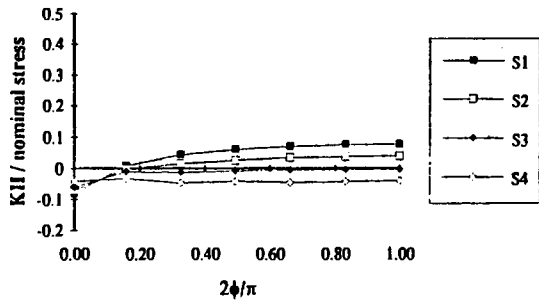


Figure 4 - Mode II SIF distribution for the shallow crack.

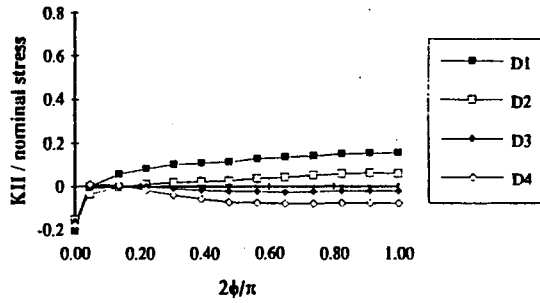
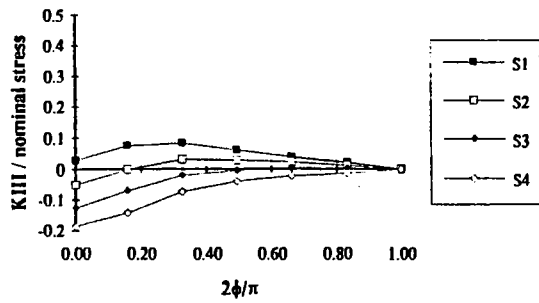
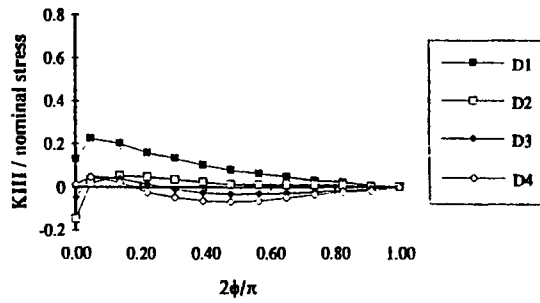


Figure 7 - Mode II SIF distribution for the deep crack.



Mode III SIF distribution for the shallow crack.



Mode III SIF distribution for the deep crack.

Figure 24. Results of Bowness and Lee Study

CHAPTER 3

EXPERIMENTAL PROCEDURE

3.1 Background

The first step in the experimental phase was to develop a specimen that could maintain "mixed mode" growth. None of the specimens found in the literature had this ability. For ease of computer modeling, fabrication, and load application, flat plates with slanted side grooves were used to force the desired crack direction (Figure 25 and 26). Seventeen specimens were built and tested one by one before a specimen was developed that could maintain the proper crack growth direction. While testing these seventeen specimens it was immediately observed that the crack has a strong tendency to grow perpendicular to the load. Even with the reduced cross section at the side grooves, the crack would quite often veer and grow normal to the load (Figure 27).

The rationale for the side grooves was to increase the stress due to the reduced cross sectional area and also to produce a stress concentration at the side groove tip. These higher stresses in turn increased the stress intensity factors in this region and controlled the crack growth direction. A variety of side groove shapes, depths and angles were tried with one inch plate. To simplify the problem, the specimen was changed to just a "Mode I/Mode II" configuration. The following side groove types were tried:

- 1) V-grooves with depths of .1", .125", .250", and .375" (Figure 28)

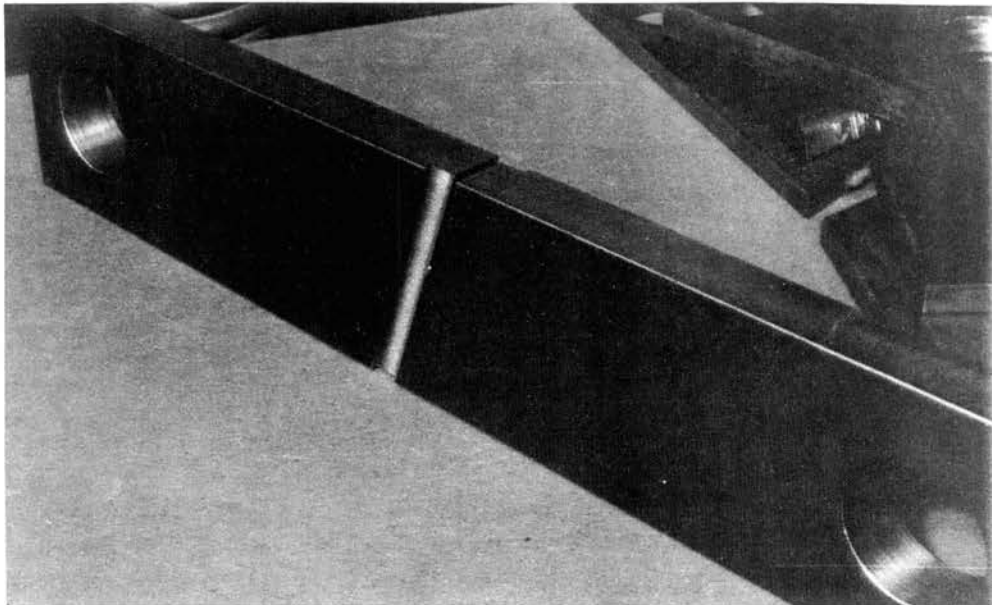
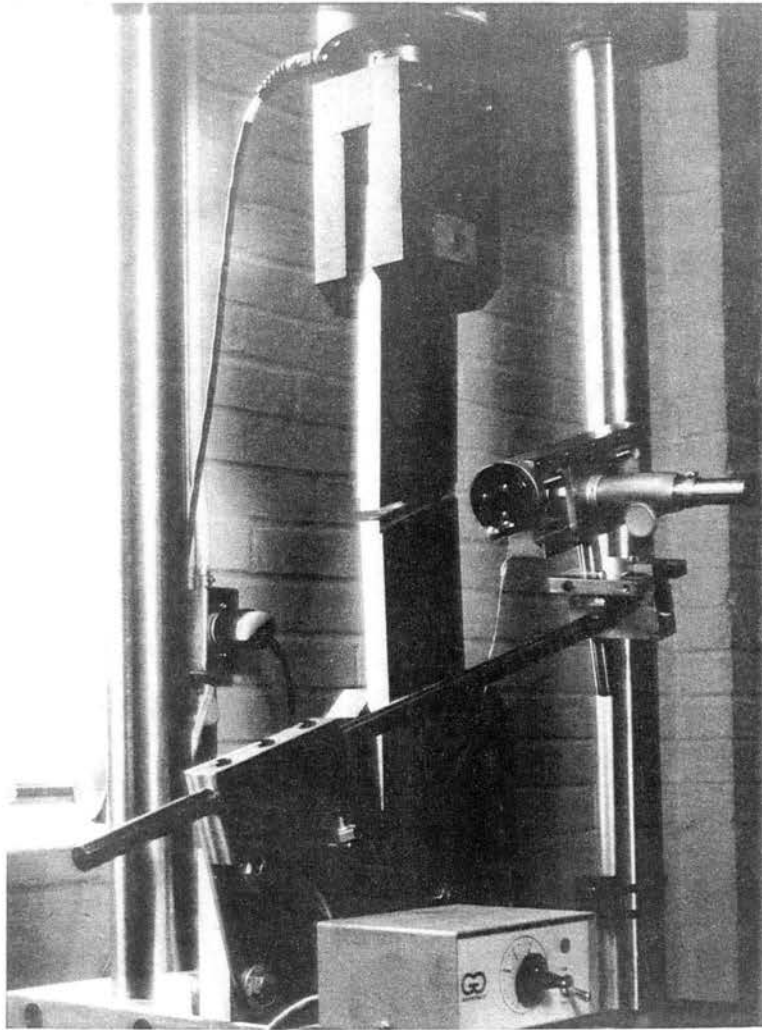


Figure 25. Specimen for Maintaining Mixed Mode Crack Growth

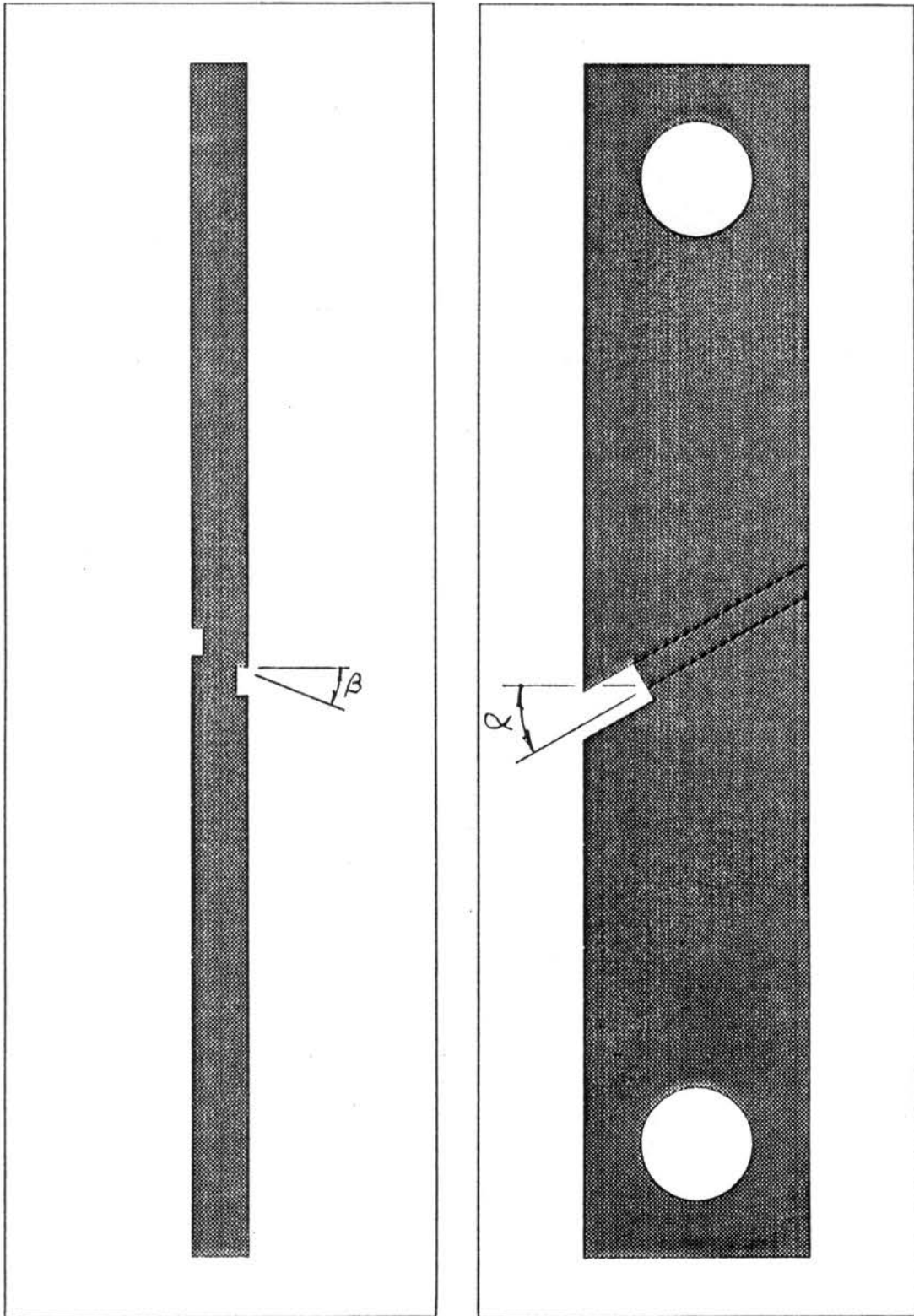


Figure 26. Definition of Alpha and Beta Angles

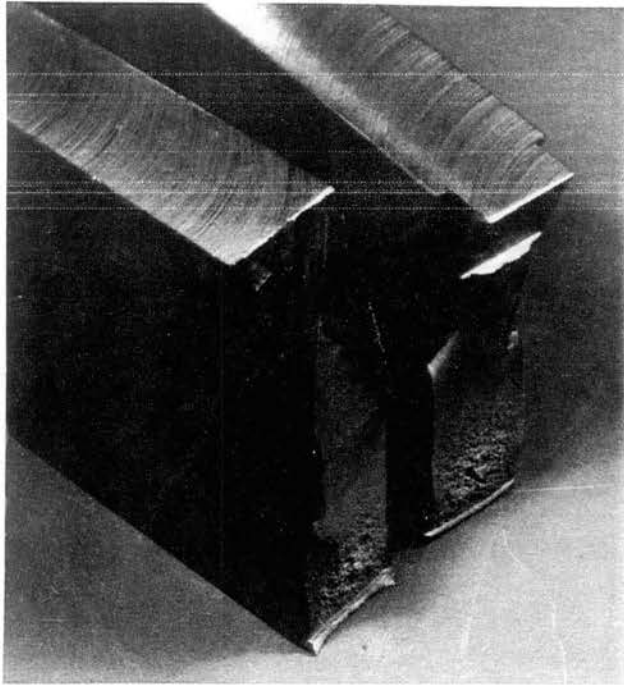


Figure 27. Crack Growth Perpendicular to Tensile Load

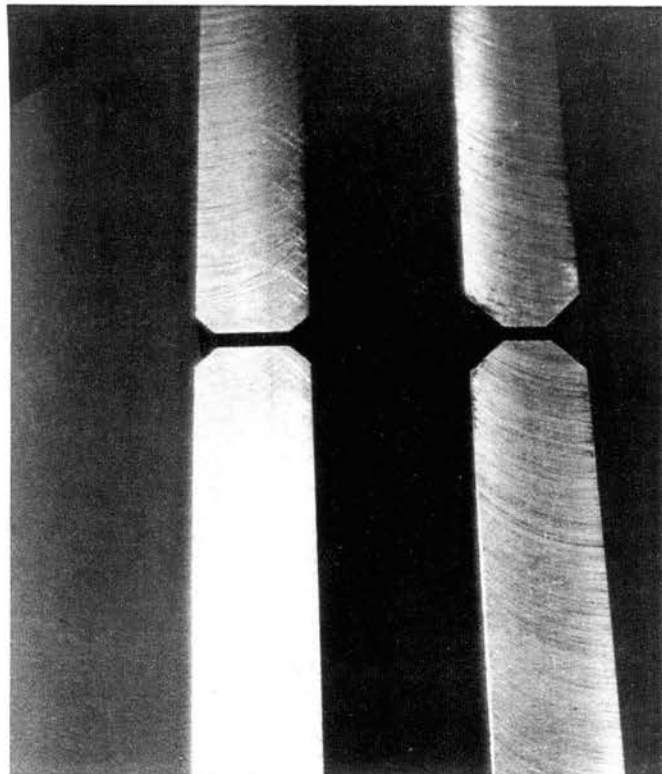


Figure 28. Specimen With V-Shaped Side Grooves

- 2) Radiused V-grooves with a depth of .250"
- 3) Rectangular grooves staggered with depths of .1" and .125" (Figure 29)
- 4) Rectangular grooves symmetrical with depths of .125" and .200"

(Figure 30)

A specimen with V-grooves (Figure 30) was developed that properly forced the crack growth but the crack front curvature was very extreme and difficult to measure. The desired crack growth direction was not able to be maintained when staggered rectangular grooves were used.

3.2 The Final Specimen

The specimens used for the final tests were made of A572, 50 ksi steel plate. This material was chosen because of its immediate availability, its machinability, and its high fracture toughness allowing for long subcritical crack growth. The specimen size was 21" x 4" x 1". This size was selected to produce plane strain through the thickness yet not have a large cross section that required excessive loads to produce crack growth. The length was chosen to limit bending effects. The specimens were loaded through two-inch diameter holes at the ends. Half inch wide symmetric side grooves were machined 0.200 inches deep on both sides at the middle of the plate. A modified chevron notch (Figure 31) was machined at one edge of the plate to force the starting location for the crack. The mill scale pattern on all the specimens was maintained in the same direction to ensure that the rolled grain direction of the material was the same in all the specimens.

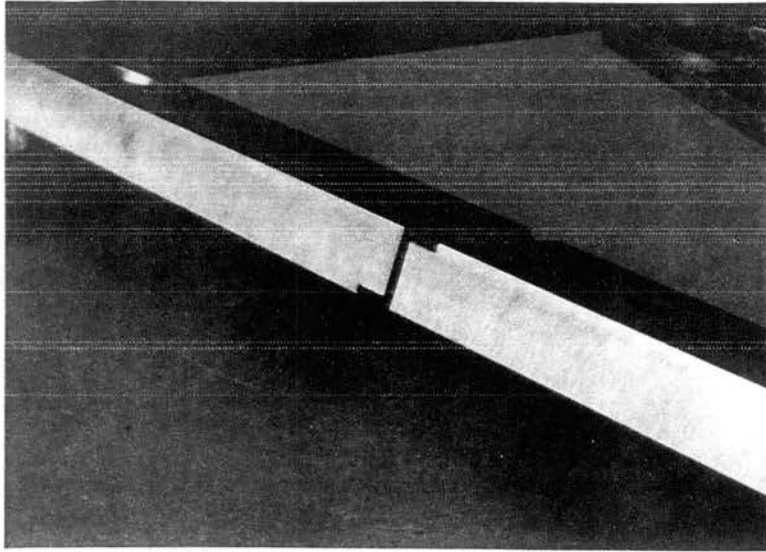


Figure 29. Specimen With Staggered Rectangular Side Grooves

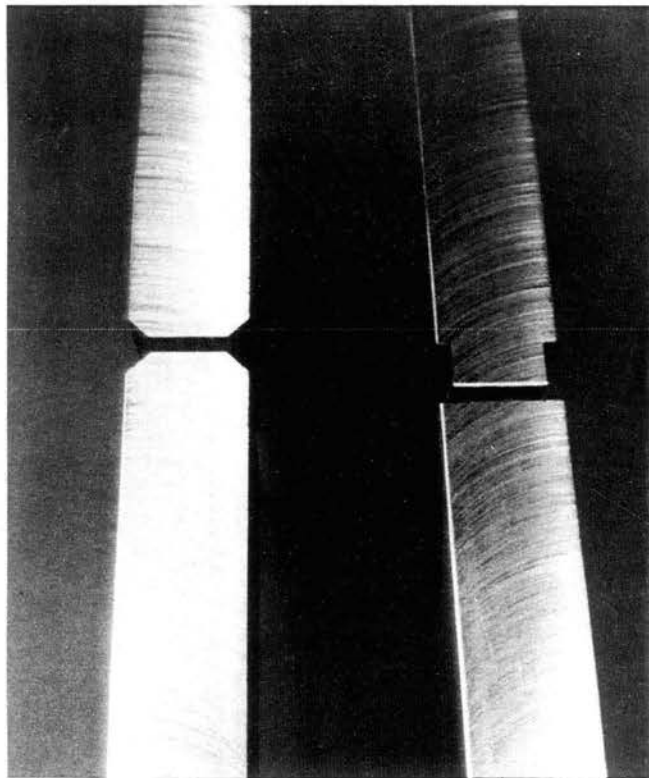


Figure 30. Specimens With V-Shaped and Symmetric Rectangular Side Grooves

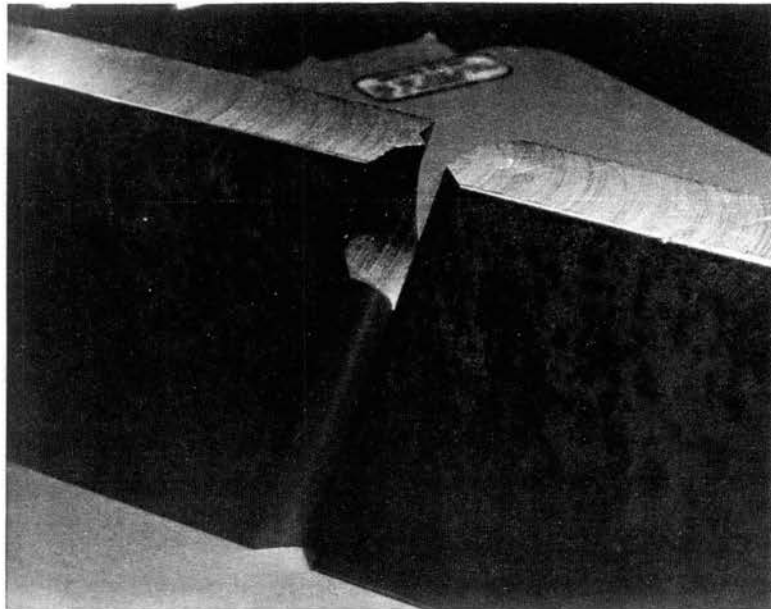
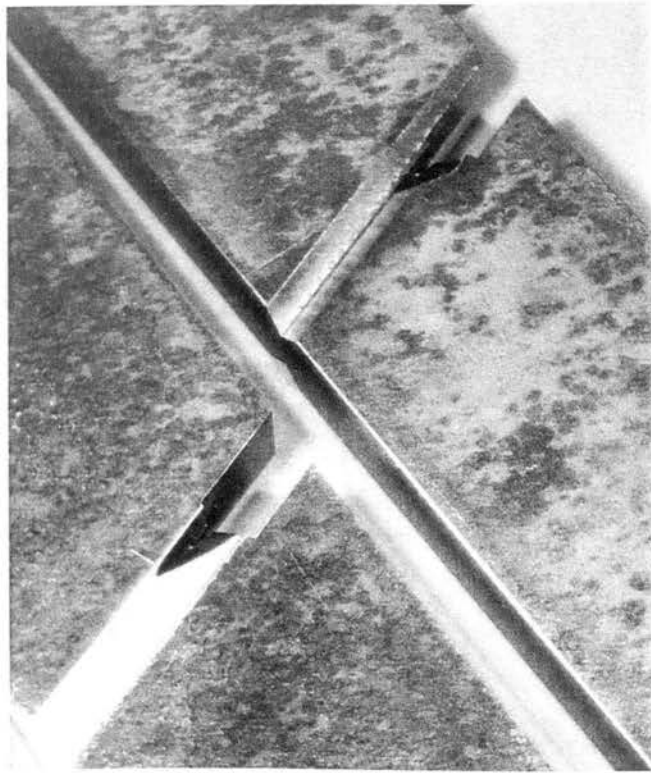


Figure 31. Modified Chevron Notch

Nine specimens were developed with side grooves to produce modes I and II loading. These specimens were machined with alpha angles of 0, 5, 10, 15, 20, 25, 30, 35, and 40 degrees (Figure 26). Figure 32 shows the final Mode I/Mode II plates.

One specimen was developed and tested to produce modes I and III loading. This specimen had a beta angle of 20 degrees (Figure 26). See Figure 33 for the Mode I/Mode III specimen.

For both specimen types the crack length (a) refers to the distance from the plate edge to the crack tip measured along the side groove.

3.3 Manufacturing the Specimens

Specimens were flame cut from large flat plates. Flame cut edges were then milled smooth on a horizontal milling machine. Holes were drilled with a two inch twist drill. Following the drilling, the holes were bored to 2.030 inches on a vertical milling machine. The purpose of boring the holes was to ensure that the hole surface was very smooth and also perpendicular to the plate longitudinal axis. Next the side grooves were milled on a vertical milling machine with a 1/2-inch two-fluted end mill. A swivel base vise allowed for milling the alpha angle accurately. At this point an opening was machined at one end of the side grooves to make room for cutting the modified chevron notch. Machining the modified chevron notch was the most tedious procedure. The vertical milling machine, with a 45 degree angle cutter, was used to cut this notch. The final step was to deburr all the machined edges and clean the specimens in a solvent tank. The approximate time for making each specimen was 6 hours. A total of 31 specimens were built.

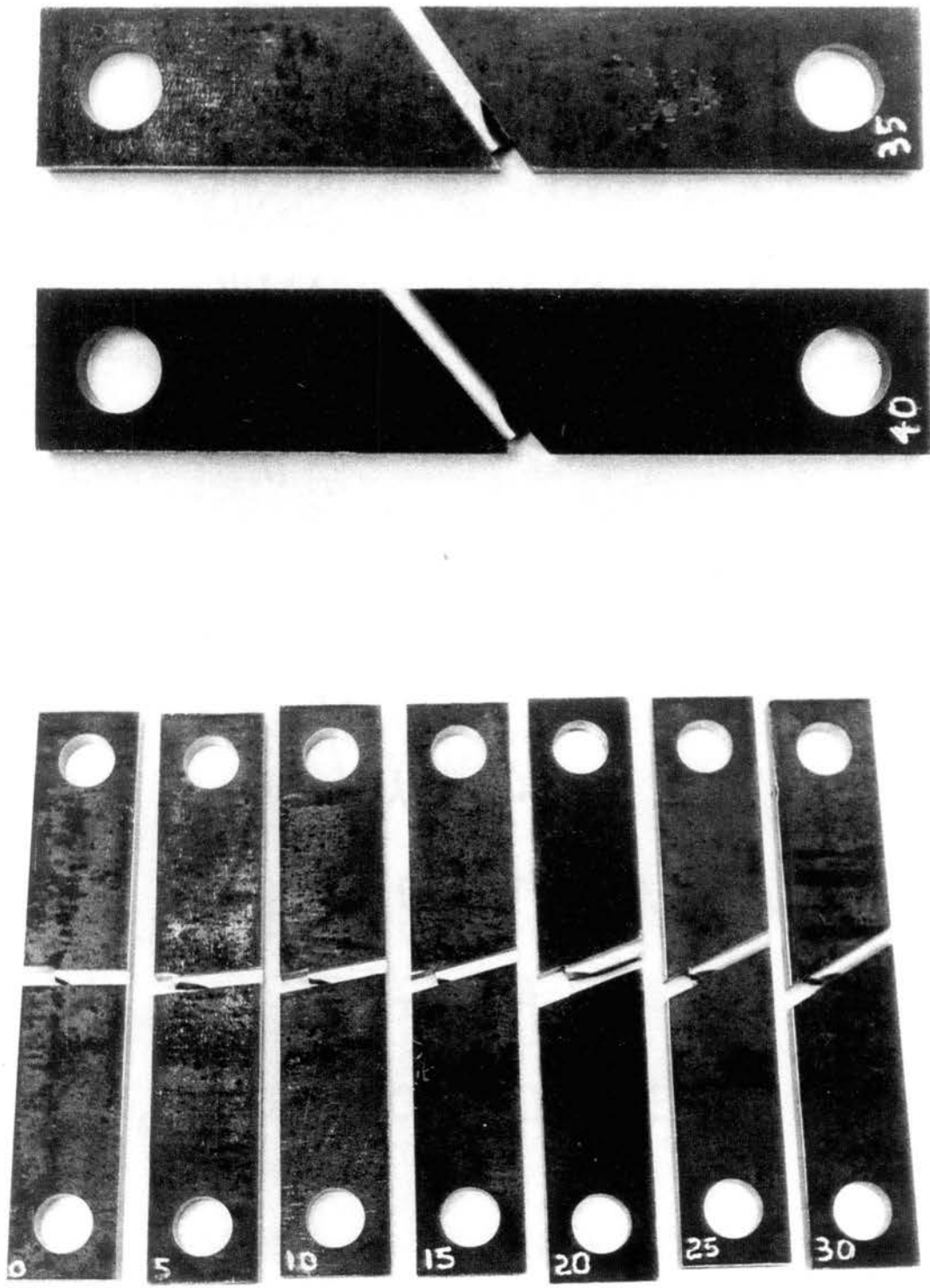


Figure 32. The Mode I/Mode II Specimens

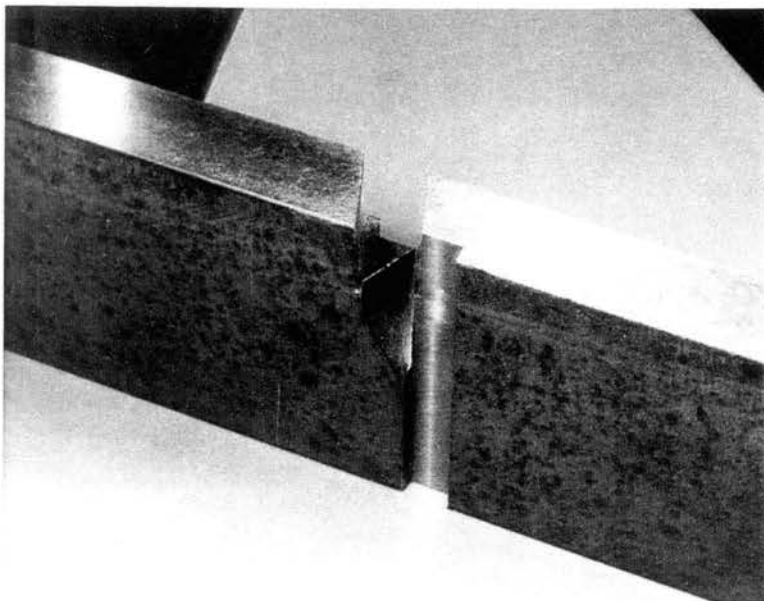
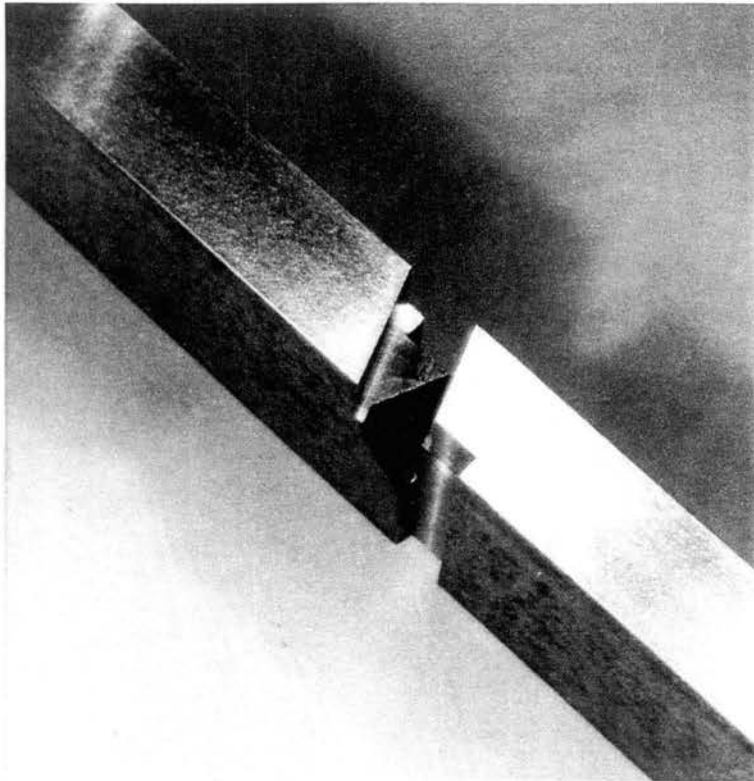


Figure 33. The Mode I/Mode III Specimen

In addition, an adjustable fixture was built to hold the traveling microscope (Figure 25). This fixture allowed for adjusting and holding the microscope at different angles and locations.

3.4 Loading Procedure

The specimens were fatigue loaded in uniaxial tension in a 20 kip MTS testing machine (Figure 34). The testing was performed under load control. One of the objectives of the experimental phase was to produce visible crack front marks on the fracture surface of the specimens (Figure 35). This was accomplished by having a systematic procedure of allowing crack growth and then changing the load range.

For each specimen the crack was permitted to grow approximately .100 to .200 inches at a constant ΔP and then the ΔP loading was changed. This procedure was repeated until the crack had grown the length of the specimen. The ΔP loading was alternately increased and decreased being careful not to produce plastic deformation with a large P_{max} . The ΔP loads applied to the specimens varied from one kip to 17 kips depending on the desired rate of crack growth.

The loading frequency was set at 5, 10, or 20 hertz during the crack growth phase, depending on the crack length and P_{max} . The frequency was set at one or two hertz while reading the traveling microscope. The load was applied in a haversine wave form.

The specimens were carefully centered in the MTS machine to ensure that bending was not present. Also, the specimen fracture surfaces were observed after failure to ensure that the crack fronts were symmetrical which would indicate the plates were not in bending.

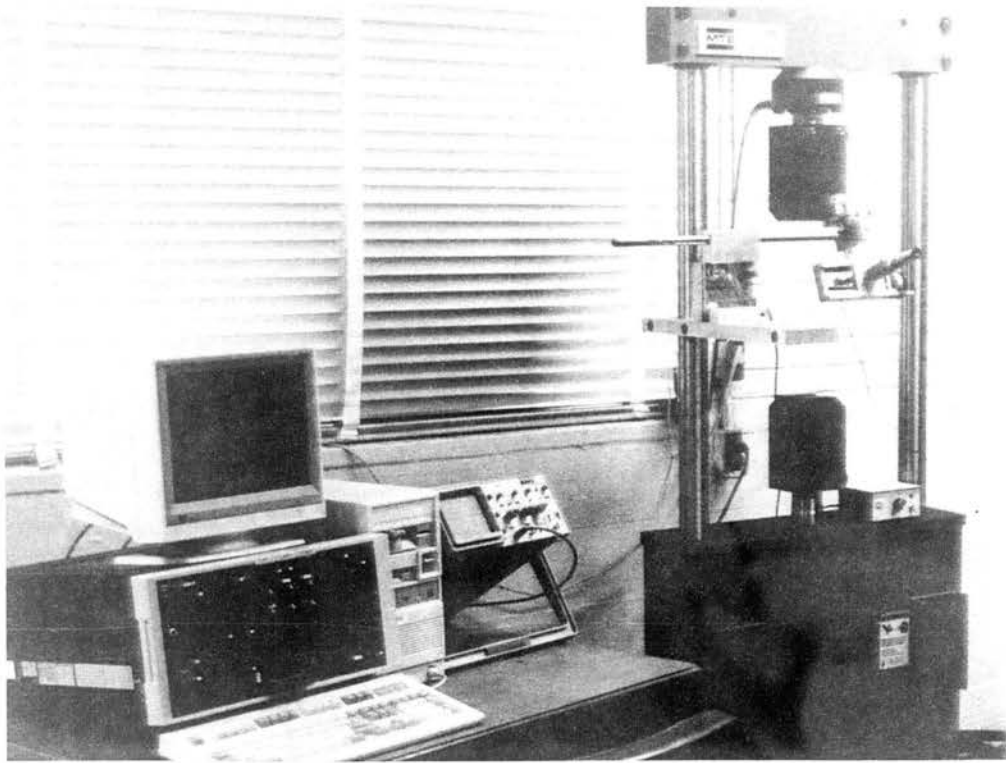


Figure 34. 20 Kip MTS Fatigue Testing Machine

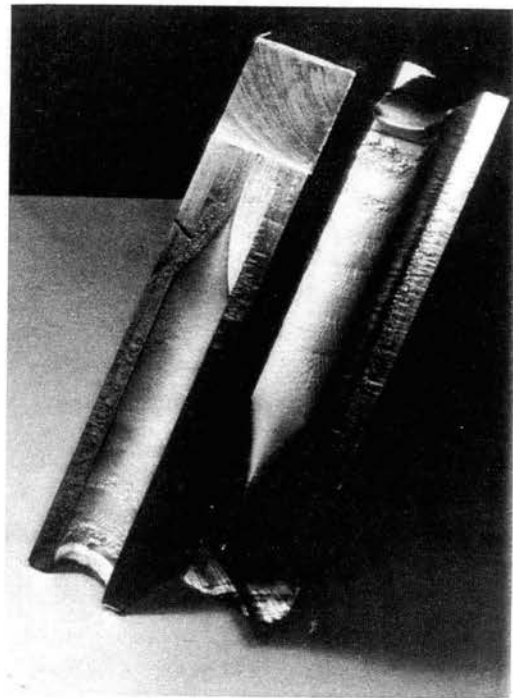
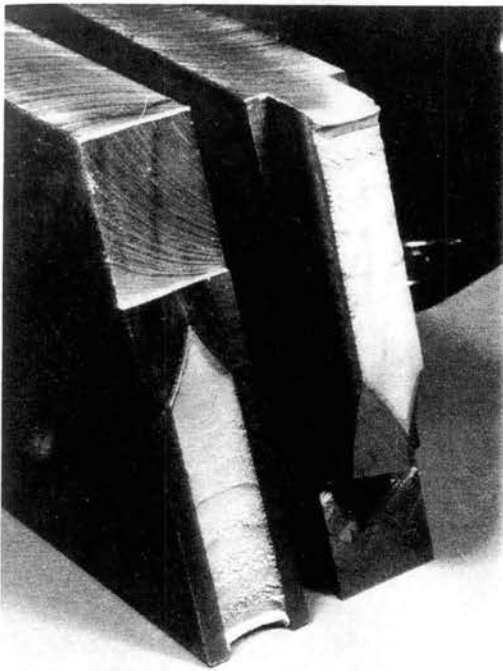


Figure 35. Curved Crack Front

The crack movement was observed and measured using the traveling microscope held in the adjustable fixture. The crack location was then recorded with respect to the number of cycles. After failure each specimen was sprayed with acrylic to preserve the fracture surface.

3.5 Crack Front Shape Measurement

Next the crack front shape (Figure 35) of each specimen was measured using a Bridgeport vertical milling machine. A sharp steel scribe was placed in the spindle and used to locate the crack front. The coordinate values were observed from the digital displays for the milling table location. These coordinate locations were recorded and then used for input into the computer models.

3.6 Comparison of Crack Growth Rates

Two additional Mode I/Mode II plates were developed to compare crack growth rates. The plates had alpha angles of 0 degrees and 20 degrees. Both plates were fatigue loaded in the MTS tensile testing machine following the guidelines of ASTM Standard E647 [74]. The crack was allowed to grow freely with no load change for about half an inch on both plates. The plates were loaded to produce ΔK values gradually increasing from 15 to 50 $\text{ksi}\sqrt{\text{in}}$. The 0 degree plate was fatigue loaded with a P_{max} of 7 kips and a P_{min} of 2 kips. The 20 degree plate was fatigue loaded with a P_{max} of 12 kips and a P_{min} of 4 kips.

The crack length was monitored and measured using the traveling microscope. The exact location of the crack tip was very difficult to monitor. At the surface, the crack moved in the sharp corner of the side groove. This made it visually difficult to measure. As a result, the recorded crack length data is sometimes erratic.

3.7 Observations on Procedure

The following are items that were observed during the experimental phase of the project:

- 1) The crack tended to leave the desired path if the growth rate was slow. The crack would tend to grow at an alpha angle less than the side grooves. This would cause the crack to grow or "tunnel" into the material without growth on the surface. It appeared this phenomenon was dependent on ΔP (i.e. ΔK) and not the absolute load. The crack seemed to have a stronger tendency to grow perpendicular to the load when the growth rate was slow.
- 2) The corner of the side groove must be machined very sharp or the crack will tend to wander and not stay down in the side groove corner.
- 3) The modified chevron starter notch must be very sharp and it must be located exactly or the crack will tend to grow in the wrong direction or secondary cracks will start at the side grooves.
- 4) Stray scratches and machining marks can redirect the crack.

5) Crack growth rate data recorded for each specimen was approximate because of the difficulty in visually locating and measuring the exact crack tip location in the corner of the side groove. This data is also approximate because of the continual changing of the load range.

CHAPTER 4

COMPUTER MODELING

4.1 The Software

The software used to model the specimens was ANSYS Version 5.0 [86]. This software was obtained following the discovery that SESAM [87] and its preprocessors PREFEM and PRETUBE were totally unacceptable for modeling the specimens. The SESAM modeling package was originally proposed because it had already been purchased and was in use for other research in this Joint Industry Project. The ANSYS software is an extremely powerful package and easy to use. The version of ANSYS used was limited to a wavefront of 1200 which controlled the mesh density.

ANSYS software does not have the ability to directly create 3-dimensional cracks or curved cracks. As a result, eight programs were written to run within ANSYS that create the curved cracks. Most of these programs are specific to this specimen and its crack shapes. The time required to write these programs was approximately 400-500 hours. A similar set of programs could be written for the Mode I/Mode III specimen.

4.2 Verifications of Stress Intensity Factor Calculations

Various 2-dimensional and 3-dimensional crack configurations were modeled with ANSYS and the SIF's were compared to handbook solutions. The purpose was to

confirm that ANSYS was calculating K_I , K_{II} , and K_{III} properly. ANSYS calculates the SIF's with the nodal displacements at the crack tip using the procedure outlined by Ingrassia [83]. In all cases except one, the values calculated by ANSYS differed from the handbook solutions by less than two percent. The one exception varied by only 3.9%. Appendix A contains the results of the computer runs for various configurations.

4.3 Plate Length Check

A finite element model was analyzed to verify that the specimens were long enough to produce a uniform stress distribution in the middle of the plate. St. Venant's principle would suggest that if the plates were long enough the large stresses around the holes would redistribute before reaching the center of the plate. Figure 36 shows that the stresses in the middle of the plate vary by less than ± 2 psi at an average stress of 500 psi. The stress contours in this plate at the middle are between 498 and 502 psi.

4.4 Model Details and Procedures

Each specimen was modeled with a series of four consecutive finite element runs. The first step was to model the plate to its exact dimensions with the holes, side grooves, pre-notch opening, and crack included. Since each plate has a plane of symmetry only half of each plate was modeled. Figure 37 shows an example plate with its elements included. The boundary conditions include a fixed node at the bottom of the lower hole and a node restriction against x-translation on the top of the upper hole. The plane of symmetry was restricted against z-translation and the load was applied at one node at the top of the upper hole. For this model of the plate, the crack front was straight and was not modeled

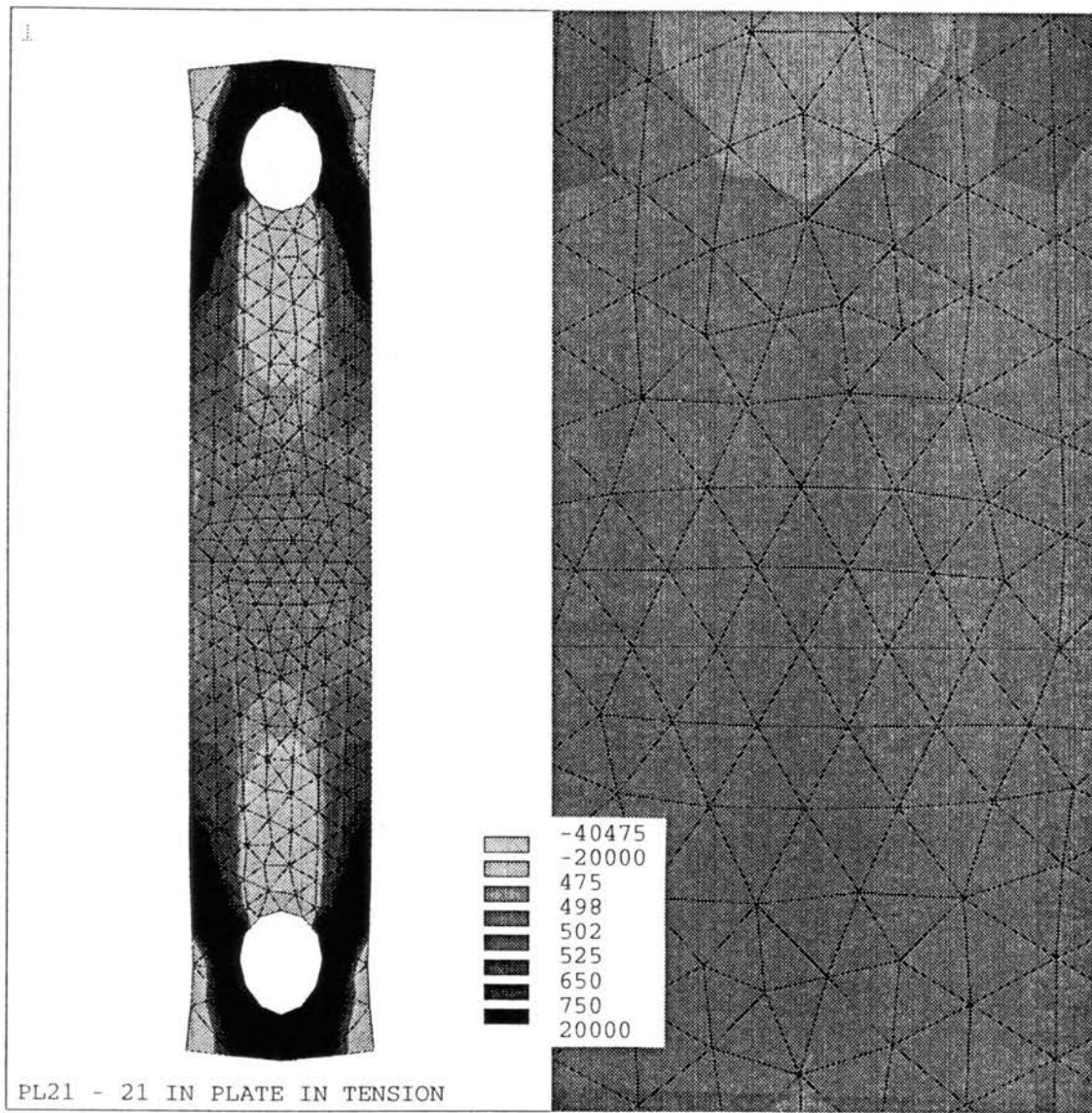


Figure 36. Plate Length Check

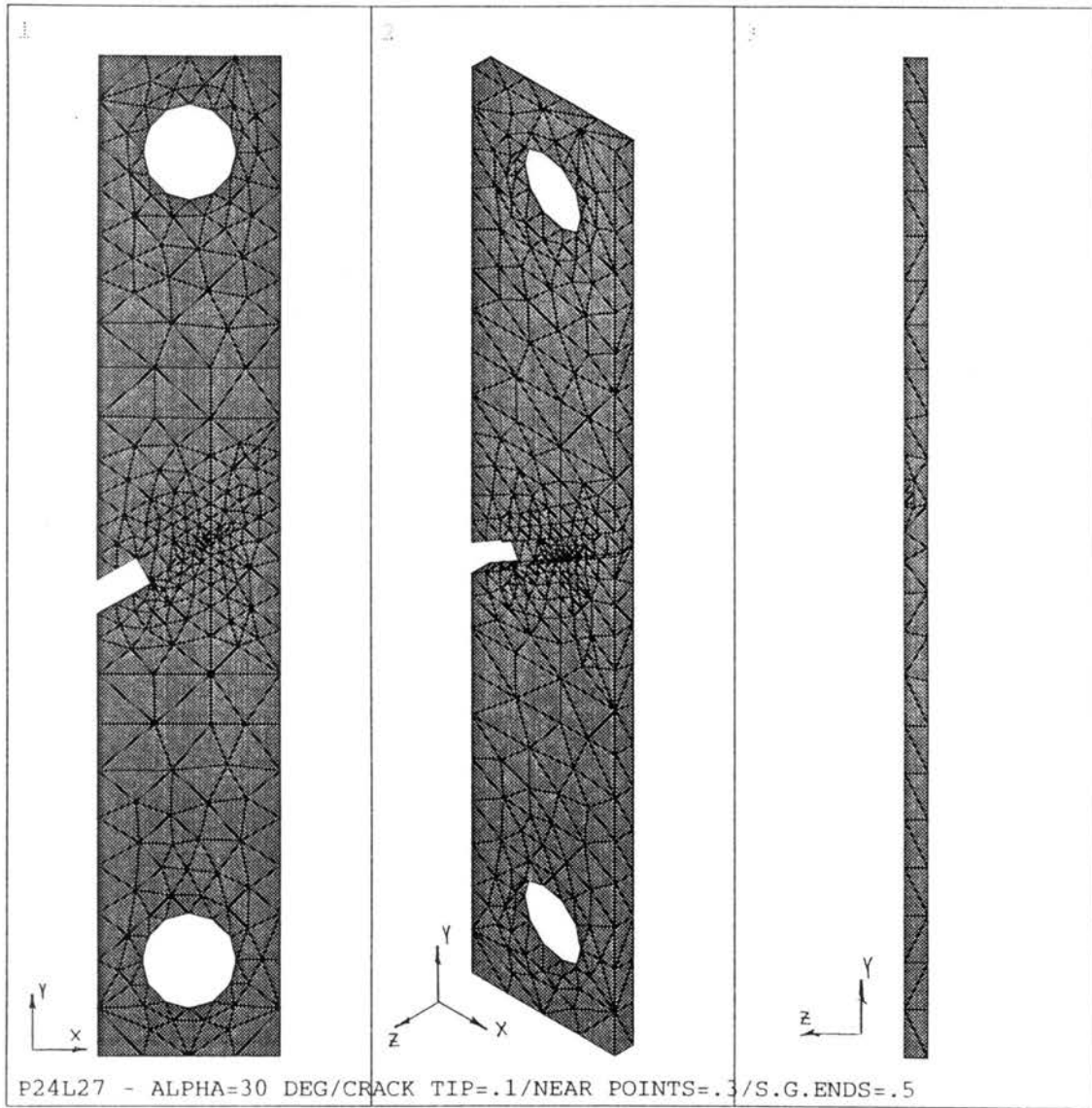


Figure 37. Finite Element Model of Specimen Using Symmetry

with wedge elements.

The second step was to build a two-inch diameter submodel of the crack area. This diameter was chosen to ensure that crack stress concentrations and singularities had redistributed before reaching the submodel boundary. This model had the exact crack front shape and for ease of modeling wedge elements were used at the crack tip. The elements in this submodel lie in planes parallel to the long axis of the plate. Because the wedge elements were not perpendicular to the curved crack front they could not be used to calculate the SIF's in ANSYS. Figure 38 shows an example of this submodel. ANSYS has a very powerful feature that allows the boundary of this submodel to be specified and located relative to the coarse model (the plate). Then ANSYS uses this information to interpolate the forced displacements for the boundary of the submodel.

The third step was to build a one inch diameter submodel of the cracked area. This submodel also had the exact crack front shape and included wedge elements at the crack tip. Figure 39 shows an example of this second submodel. The forced displacements at the boundary on this submodel were calculated from the first submodel. Again these wedge elements were not perpendicular to the curved crack front so they could not be used to calculate the SIF's.

The fourth and final step was to build a .075 inch diameter submodel of the cracked area. This submodel had the exact crack front shape and its wedge elements were rotated so that they were perpendicular to the crack front at all locations. Figure 40 shows an example of this submodel. The SIF's were calculated from this model. The total time to build and run the complete model for each specimen was approximately 15 hours.

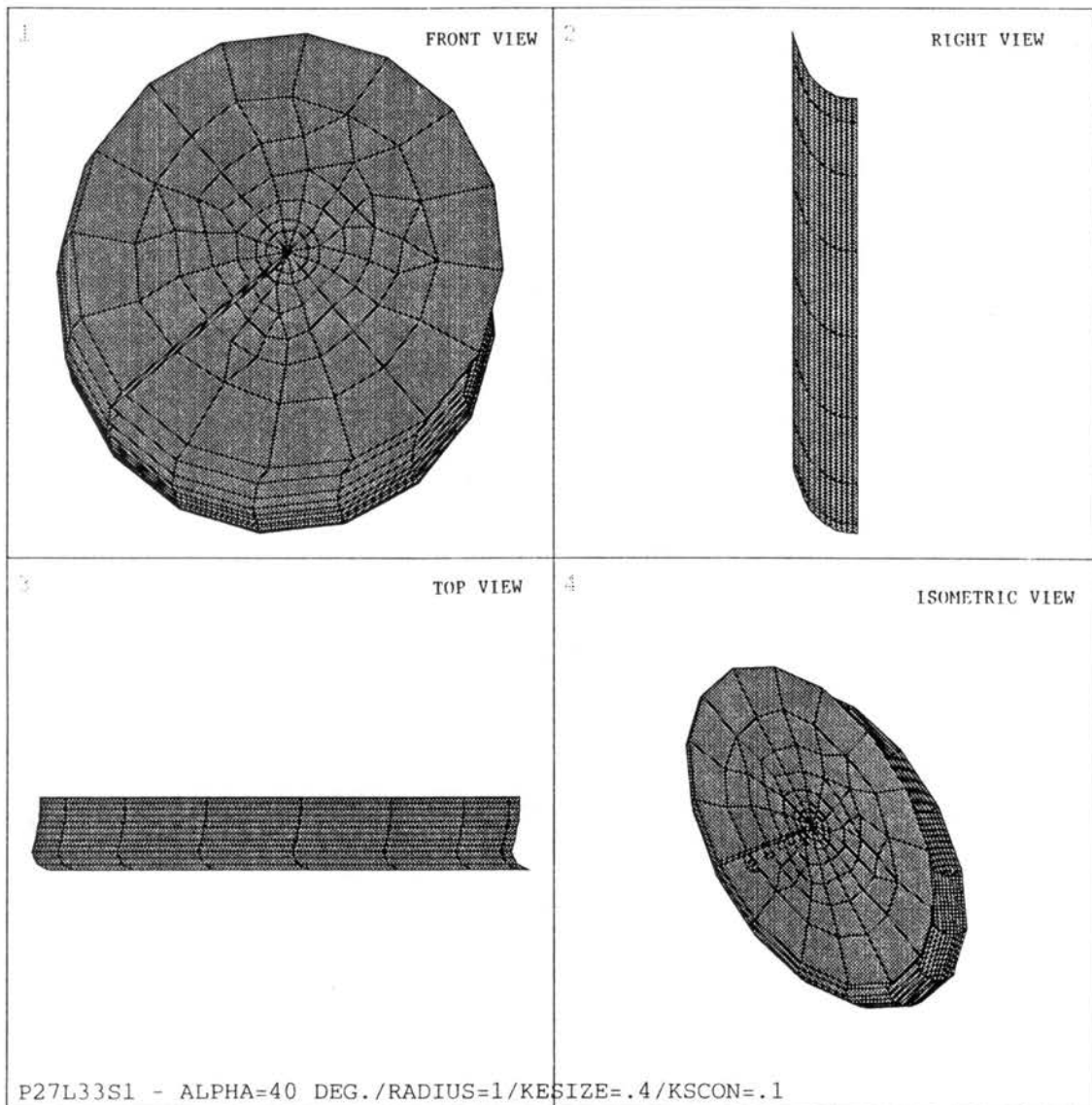


Figure 38. First Submodel of Crack Front

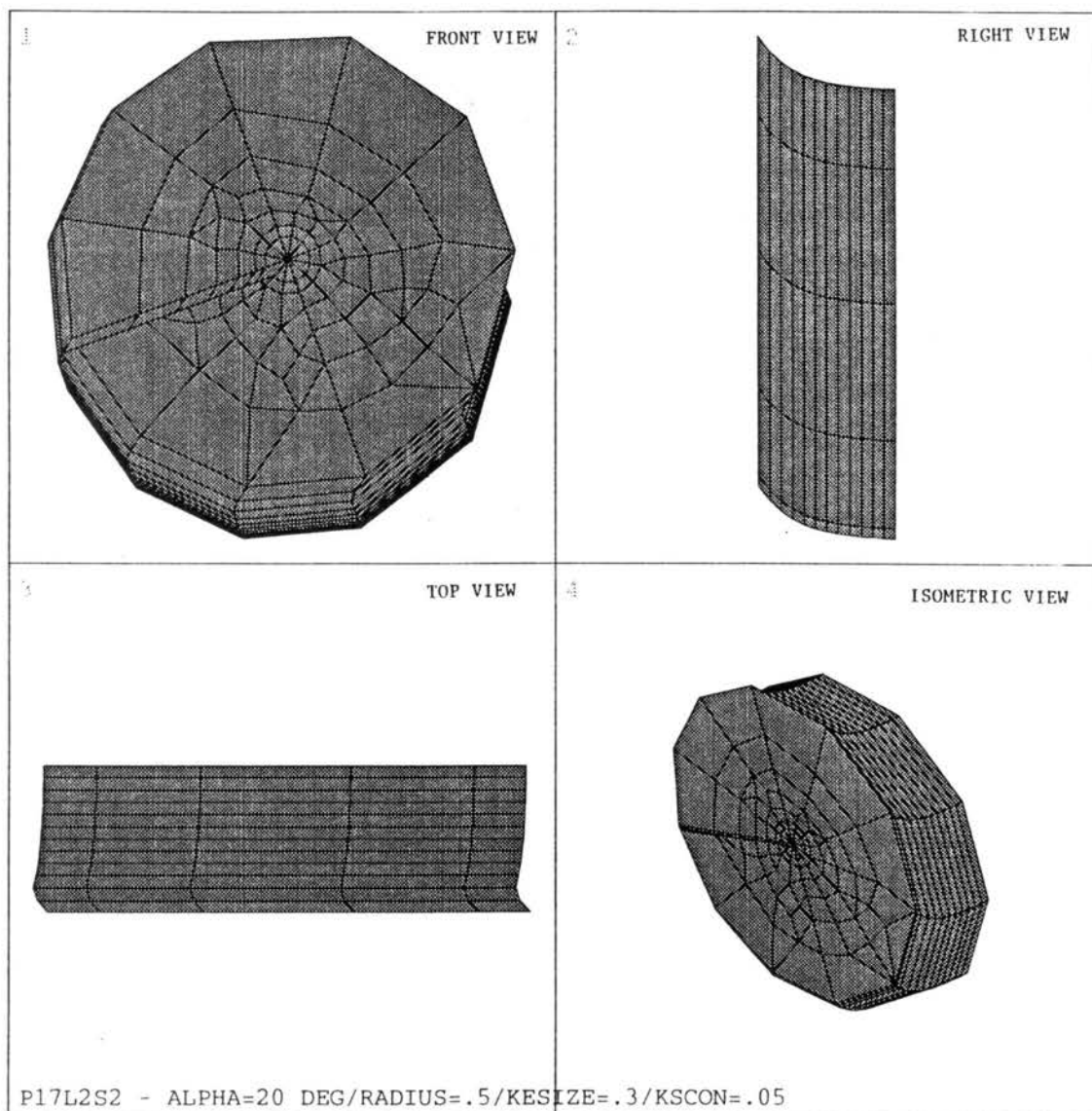


Figure 39. Second Submodel of Crack Front

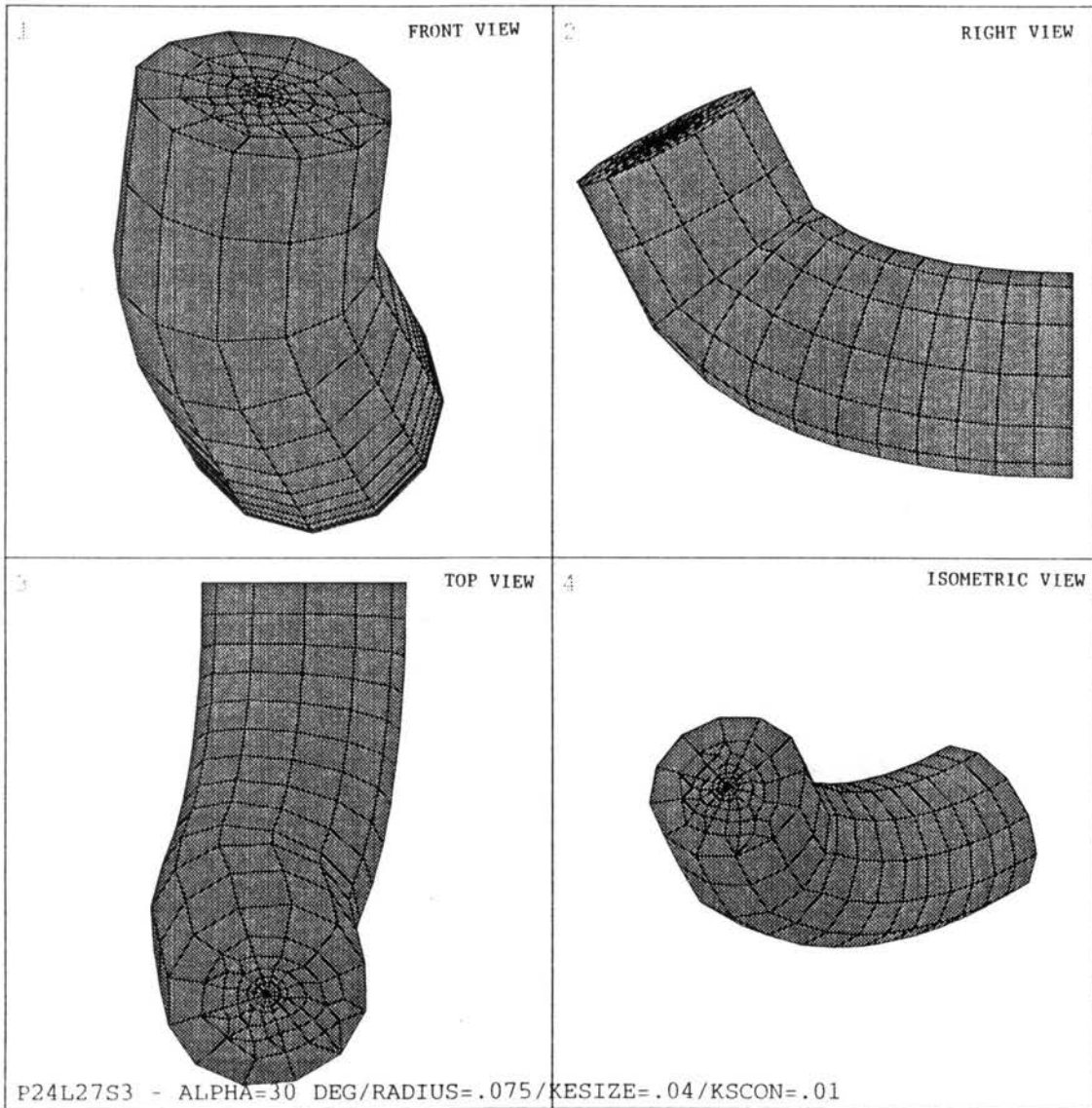


Figure 40. Third Submodel of Crack Front

The four step procedure of building a coarse model with three submodels was used for the following reasons: 1) ANSYS did not allow direct solids modeling of the exact plate configuration with the curved crack front and its wedge elements all in one model. 2) The size of the first curved crack submodel was restricted by the wavefront limit. The wavefront limit thus forced the building of the second submodel. 3) The reason for the third submodel was to include "rotated" quarter-point wedge elements that are perpendicular to the crack front so the SIF's can be calculated. When the wedge elements are perpendicular to the curved crack front, the diameter of the total model must be very small to produce elements with reasonable aspect ratios.

The elements in the coarse model of the plate were all 20-node quadratic brick elements collapsed to tetrahedrons. The coarse models typically had 2500 to 4000 elements. The elements used in the three submodels were full 20-node bricks except at the crack tip. The submodels typically had 1200 to 1400 elements. The elements used at the crack tip were 20-node quadratic brick elements collapsed to a wedge and the mid-side nodes were moved to the quarter-point. Figure 41 shows a close-up view of the quarter-point wedge elements at the crack tip.

Numerous preliminary computer runs were made to determine the best model configurations that would fit within the wavefront limit.

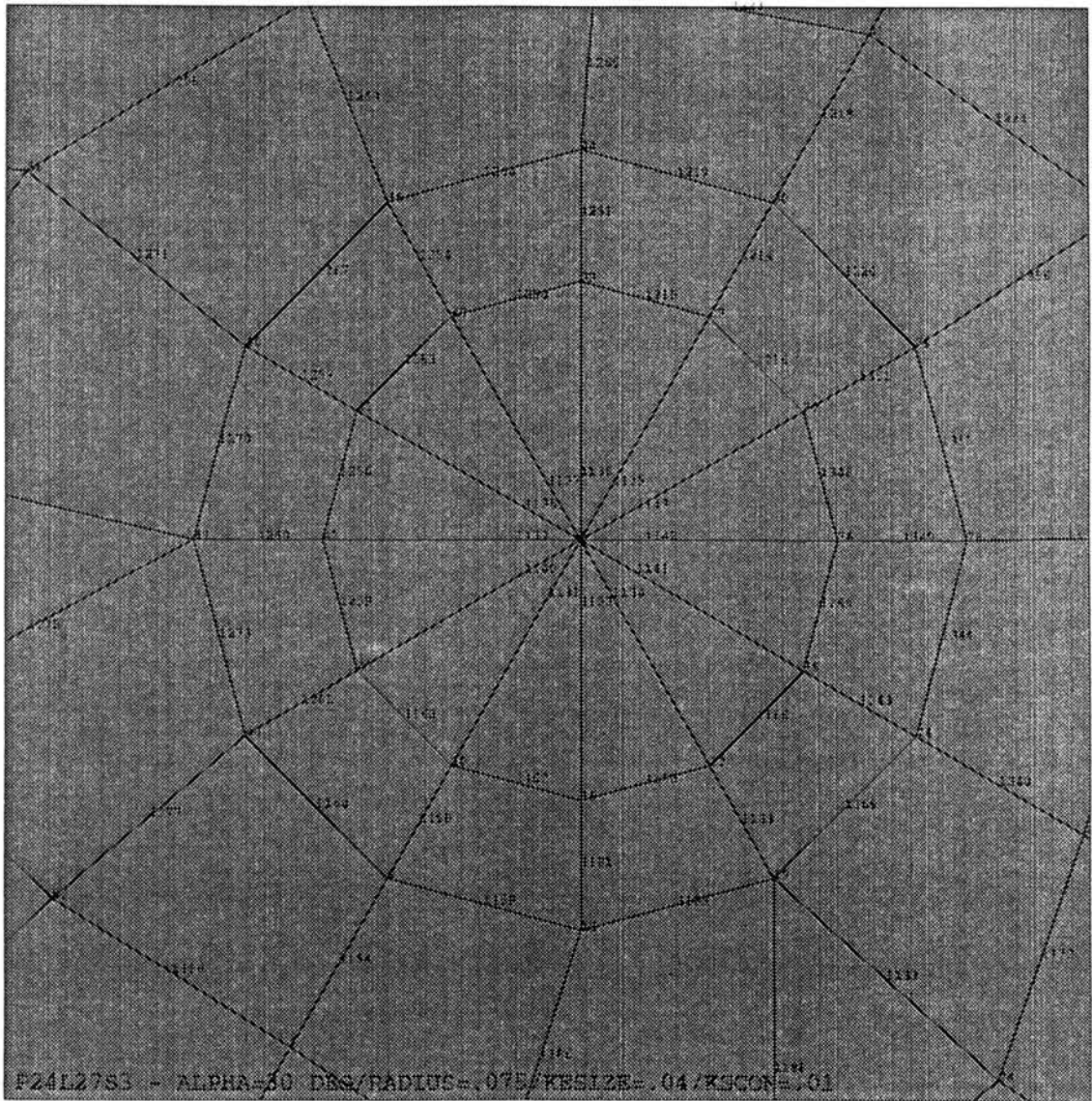


Figure 41. Quarter-Point Wedge Elements at the Crack Tip

4.5 The Programs

The following programs were written to run from within ANSYS:

1. **CURVECRK** - generates the elements around a curved crack front and keeps the elements in planes parallel to the specimen's long axis (See Figure 42)
2. **CURVEQP** - moves the midside nodes to the quarter-point for the wedge elements created by **CURVECRK**
3. **CURVEBD** - finds the nodes on the submodel boundary for the elements created by **CURVECRK**
4. **CURVEK** - finds the nodes in the wedge elements created by **CURVECRK** and then calculates the SIF's using the node displacements
5. **WARPCRKR** - generates the elements around a curved crack front and keeps the elements perpendicular to the crack front (See Figure 43)
6. **WARPQPR** - moves the midside nodes to the quarter-point for the wedge elements created by **WARPCRKR**
7. **WARPBDR** - finds the nodes on the submodel boundary for the elements created by **WARPCRKR**
8. **WARPKR** - finds the nodes in the wedge elements created by **WARPCRKR** and then calculates the SIF's using the node displacements

The code for these programs is listed in Appendix D.

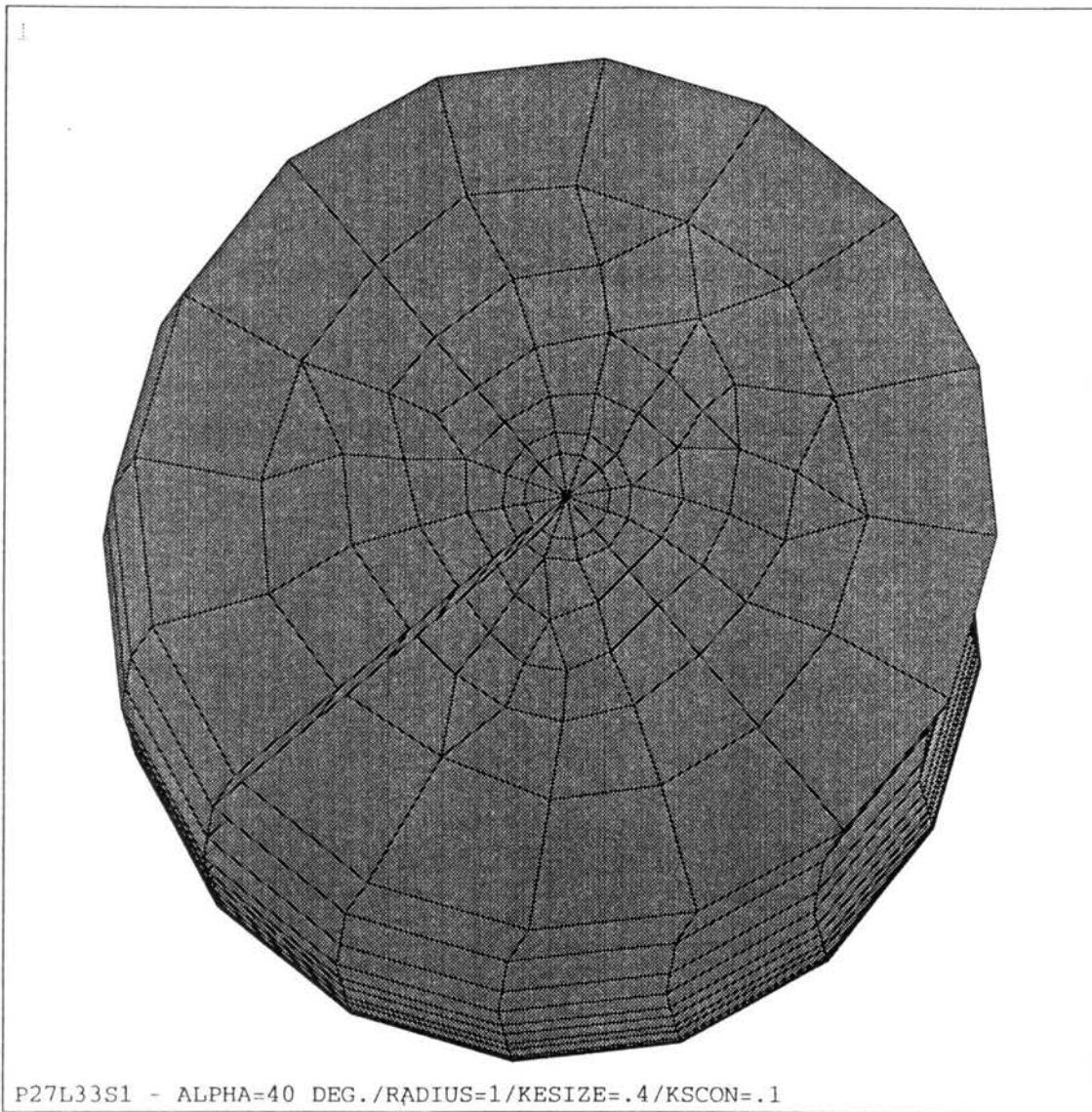


Figure 42. Submodel Generated by CURVECRK

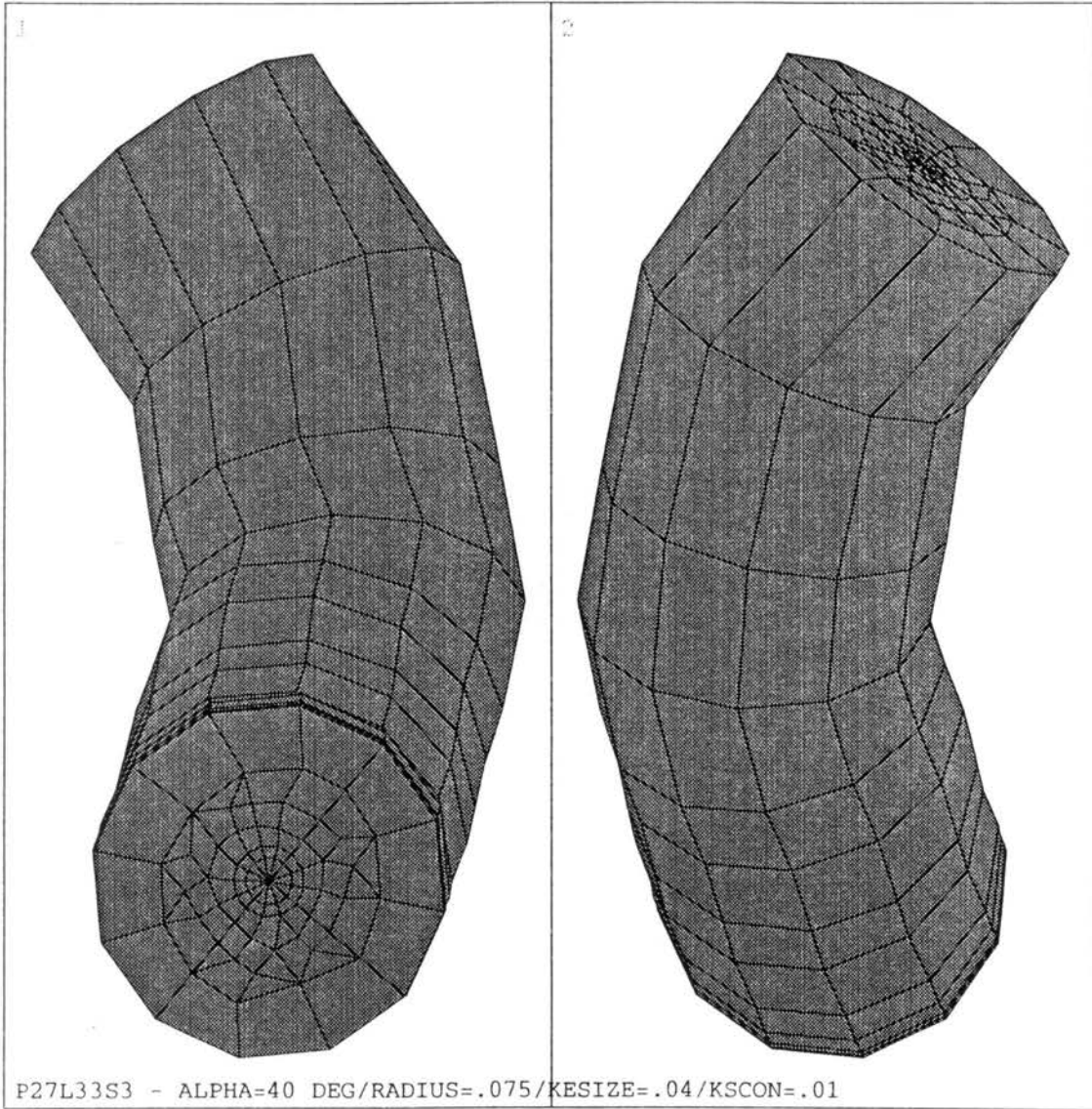


Figure 43. Submodel Generated by WARPCRKR

4.6 Mode I/Mode III Specimen

The above listed programs were not specifically written to handle the Mode I/Mode III specimen because of its asymmetric crack front shape. With a few changes it was possible to use these programs to model this specimen. It must be emphasized that these program modifications only allowed for a "rough" modeling of the Mode I/Mode III specimen. The main inaccuracy in the model was the element shapes and boundary conditions on the backside (left side) of the specimen. With a reasonable amount of work these programs could be modified to allow accurate modeling of this specimen.

Since the Mode I/Mode III specimen does not have a plane of symmetry the entire plate had to be modeled. This caused the ANSYS wavefront limit to be exceeded when the crack front submodels were constructed in the same manner as the Mode I/Mode II specimen. To resolve this problem larger element aspect ratios had to be used. Toward the end of the project the ANSYS software was upgraded to a wavefront limit of 3000. This allowed for another model to be created with the proper element aspect ratios which resulted in 22 layers of elements. The original model with the smaller wavefront had 12 layers of elements.

4.7 Observations on Modeling

Several attempts were made at building plates with cracks using SESAM which is a software distributed by Det Norske Veritas Industry, Inc. The preprocessor used is called PREFEM. PREFEM turned out to be a disappointment because of its crack modeling limitations. PREFEM cannot create through-cracks or edge-cracks. It only

allows for surface cracks. PREFEM does not have the flexibility or number of options as does PRETUBE which is a preprocessor for constructing tubular joint models. The impression is that unlike PRETUBE, PREFEM has not been upgraded through the years.

CHAPTER 5

RESULTS

5.1 Mode I/Mode II Specimen

Plots of normalized SIF values with respect to their location along the actual curved crack front are shown in Figures 44 and 45. These figures also show the normalized SIF's if the specimens are modeled assuming a straight crack front. It is interesting to note that for the actual specimens with curved crack fronts the K_{II} and K_{III} values are less than 5-6% of K_I except near the side groove and often they approach zero. For the specimens modeled with an assumed straight crack front the K_{II} value is considerably greater. As an example, for the plates with alpha angles of 30 and 40 degrees the K_{II} values are 23% and 31% of K_I , respectively. Figure 46 shows the normalized SIF's for the plate with alpha equal to zero degrees.

In Figures 44 through 46 the SIF values vary considerably near the side grooves. The reason for this variation at the side grooves can be explained as follows:

- 1) It was very difficult to accurately measure the crack front coordinates near the side groove because the crack front has an extremely steep slope at this location. There was a problem determining where to place the measuring probe on this steep slope. As a result, the measured crack "depths" at the second to last and third to last points could be inaccurate by as much as .040-.050 inches.

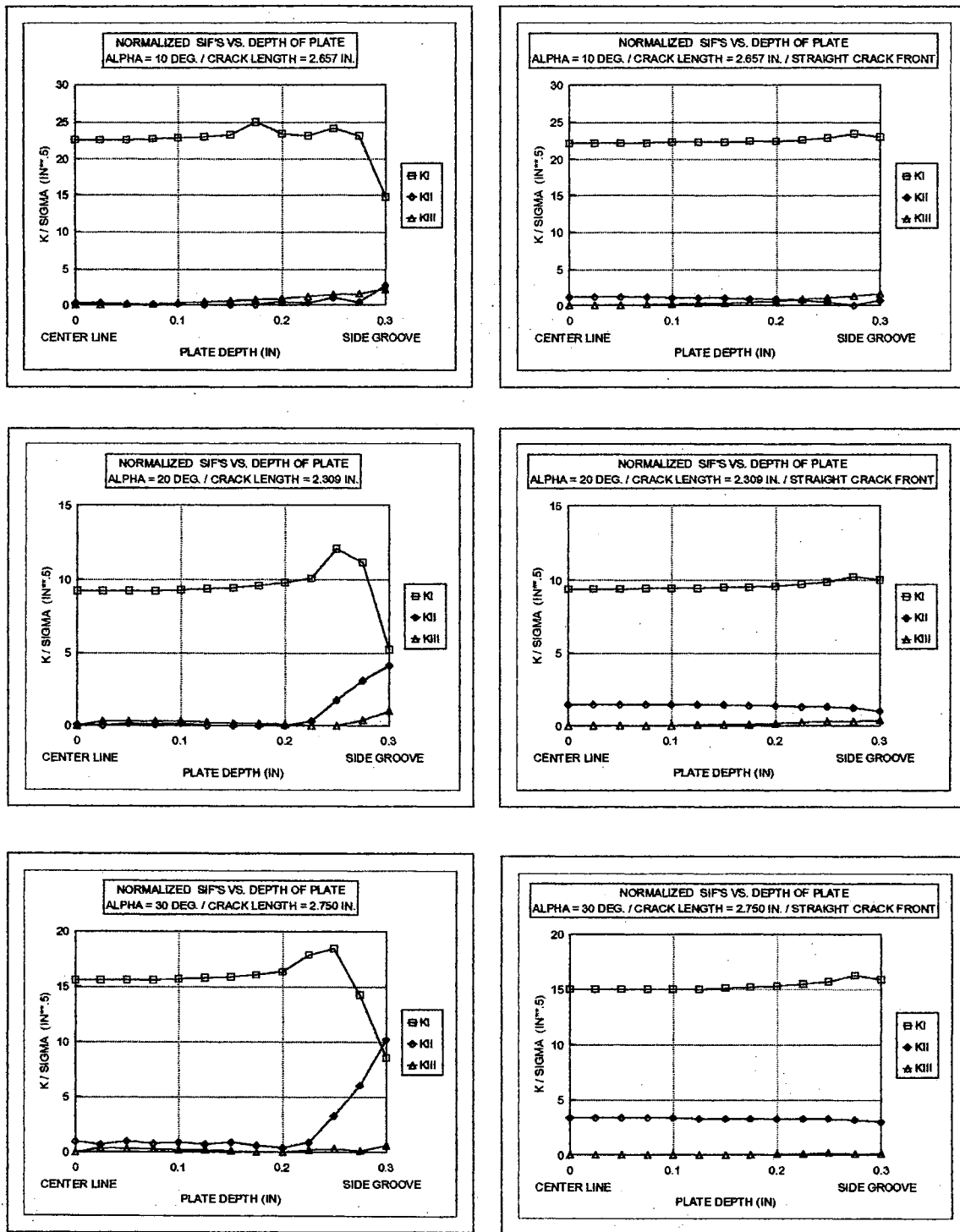


Figure 44. Plots of Normalized SIF's vs. Plate Depth for Alpha= 10-30 Degrees

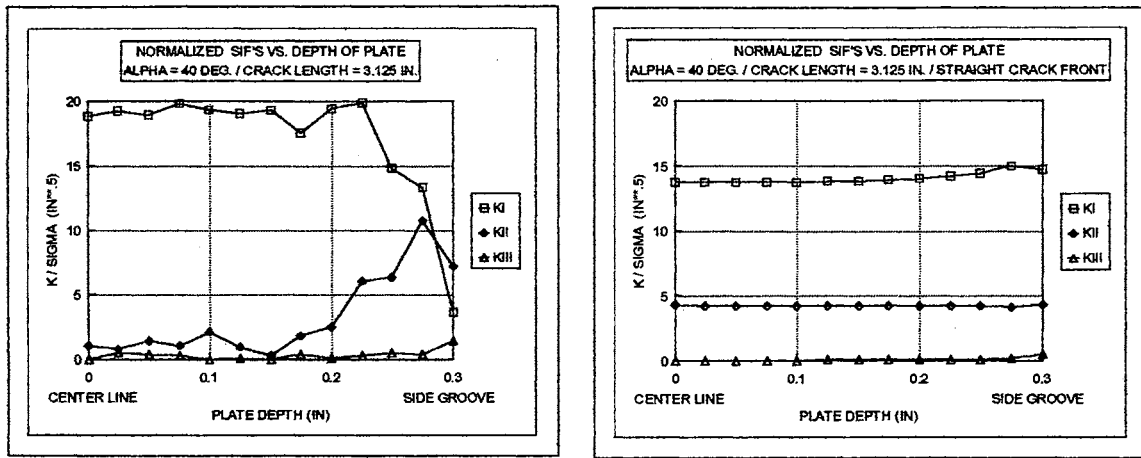


Figure 45. Plots of Normalized SIF's vs. Plate Depth for Alpha= 40 Degrees

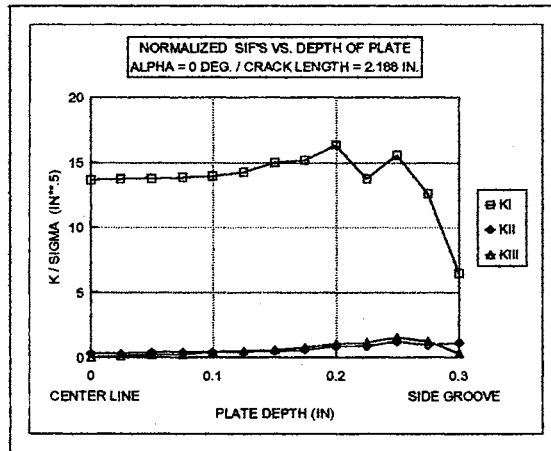


Figure 46. Plot of Normalized SIF's vs. Plate Depth for Alpha=0 Degrees

- 2) The forced displacements on the computer submodels were difficult to impose at the side groove corner. As a result, the stress concentration is not fully imposed at the last node on the side groove corner.
- 3) The extreme curvature of the crack front at the side grooves caused the elements at that location to have poor aspect ratios and extreme distortion.

4) ANSYS calculates the SIF's assuming plane strain which may not be the case at the side grooves.

The SIF's for all the plates modeled are in tabular form in Appendix B. There are also additional plots of the normalized SIF's in Appendix C.

Another interesting observation is that for each plate the computer model values for K_{II} and K_{III} tend to increase as a percentage of K_I as the crack becomes extremely long. It appears this is only true when the crack is very long and the remaining cross section is small. One possible explanation for this phenomenon is the plasticity effects in the remaining small cross section. The ANSYS computer model did not take into account the plastic deformation in our specimens. The specimens were modeled as behaving in a totally linear elastic manner. The plot in Figure 47 shows a stress contour of the maximum principal stress in the remaining ligament for the specimen with an alpha angle of 40 degrees. Notice that approximately two-thirds of the remaining material exceeds the nominal yield strength of the material.

Plots of the typical crack tip strain distribution are shown in Figures 48 and 49. These plots were created using the specimens' actual curved crack fronts. In comparison, Figure 50 shows a plot of the strain distribution for a specimen with an assumed straight crack front. It is interesting to note that the "dumbbell" shape is rotated and perpendicular to the crack faces for the actual curved crack fronts. The "dumbbell" remains parallel to the load and is not perpendicular to the crack faces for the specimen with an assumed straight crack front.

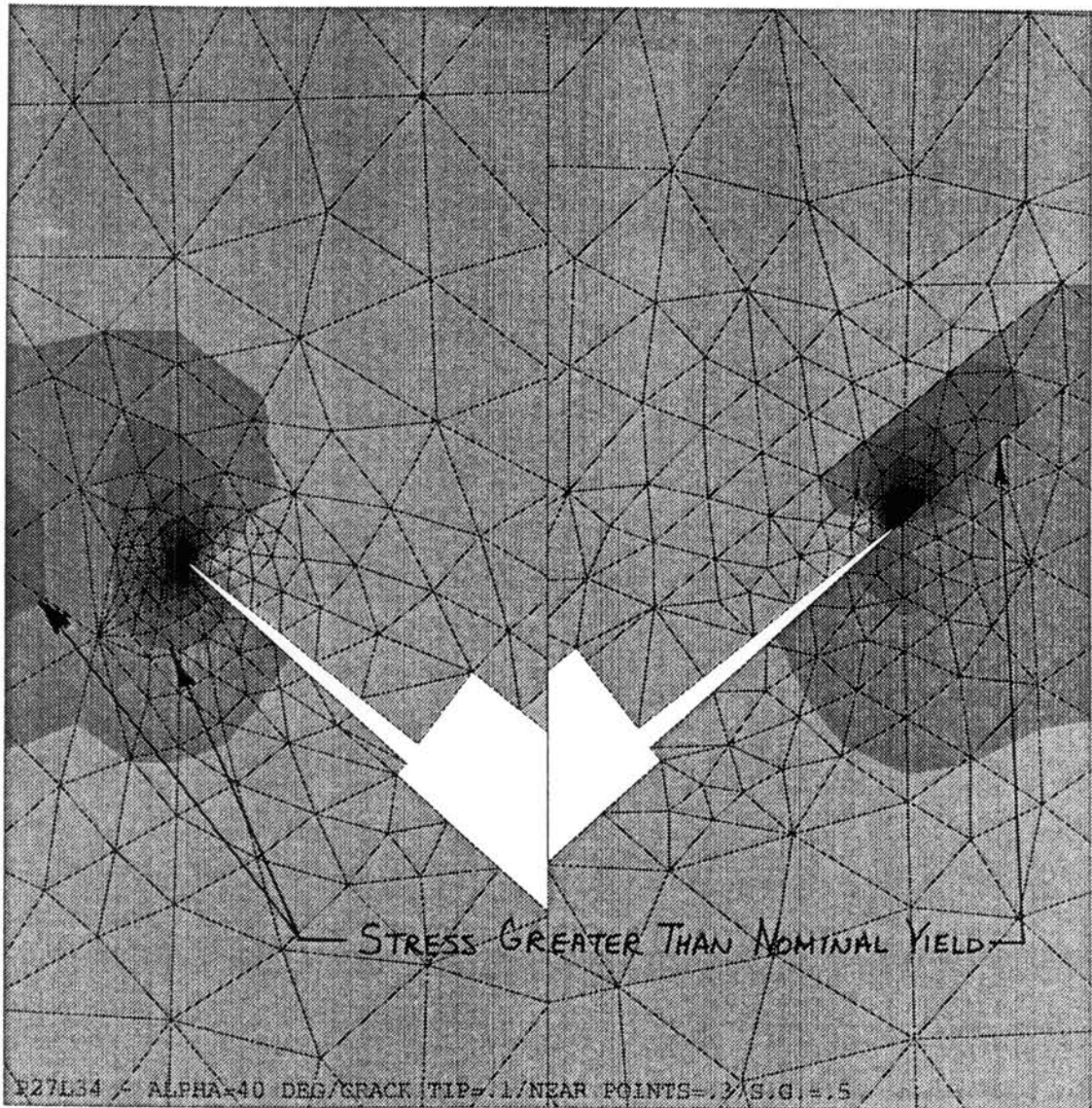


Figure 47. Contour of the Maximum Principal Stress in 40 Degree Plate

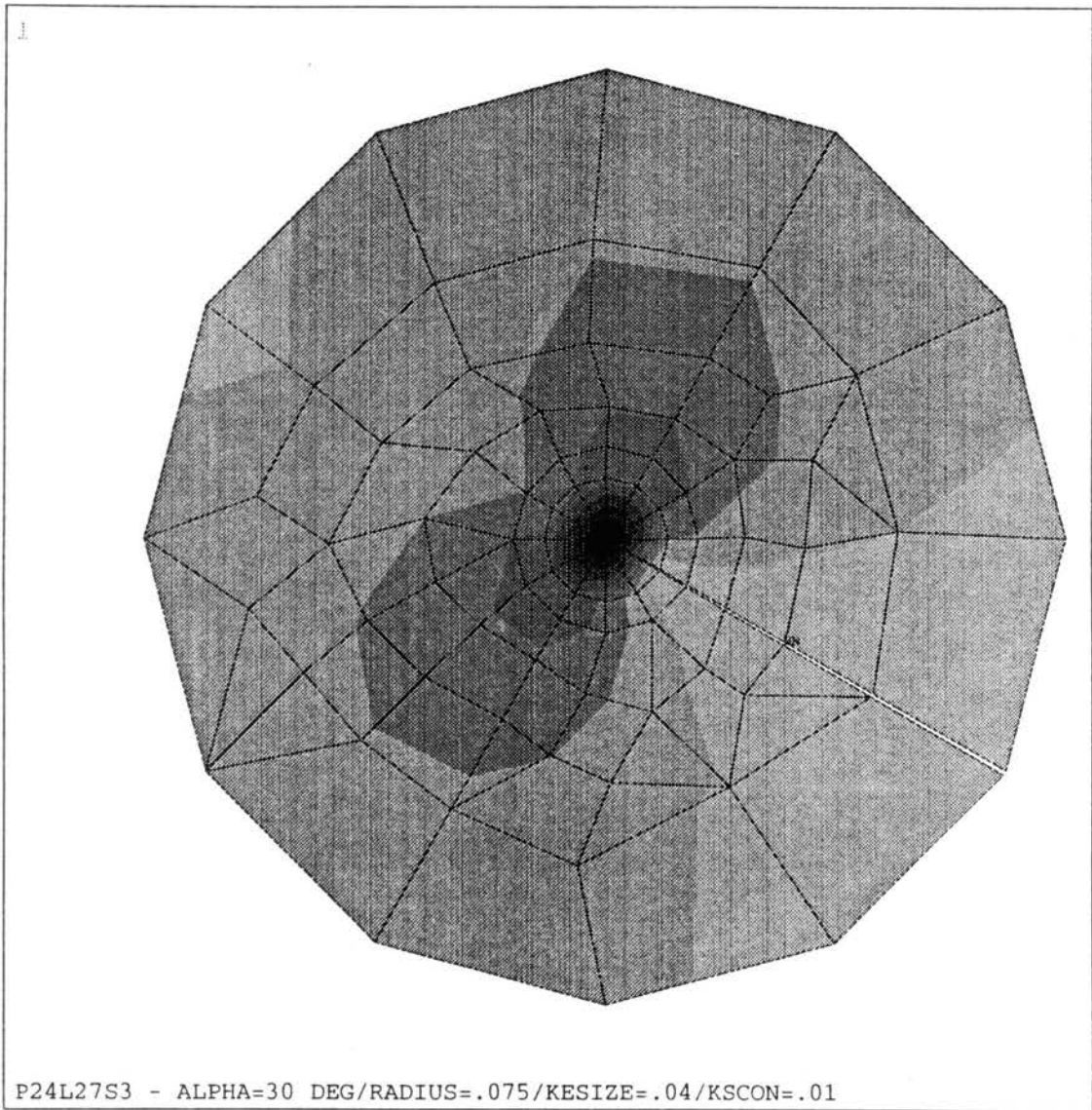


Figure 48. Strain Distribution Near Crack Tip for Curved Crack Front (Alpha= 30 Deg.)

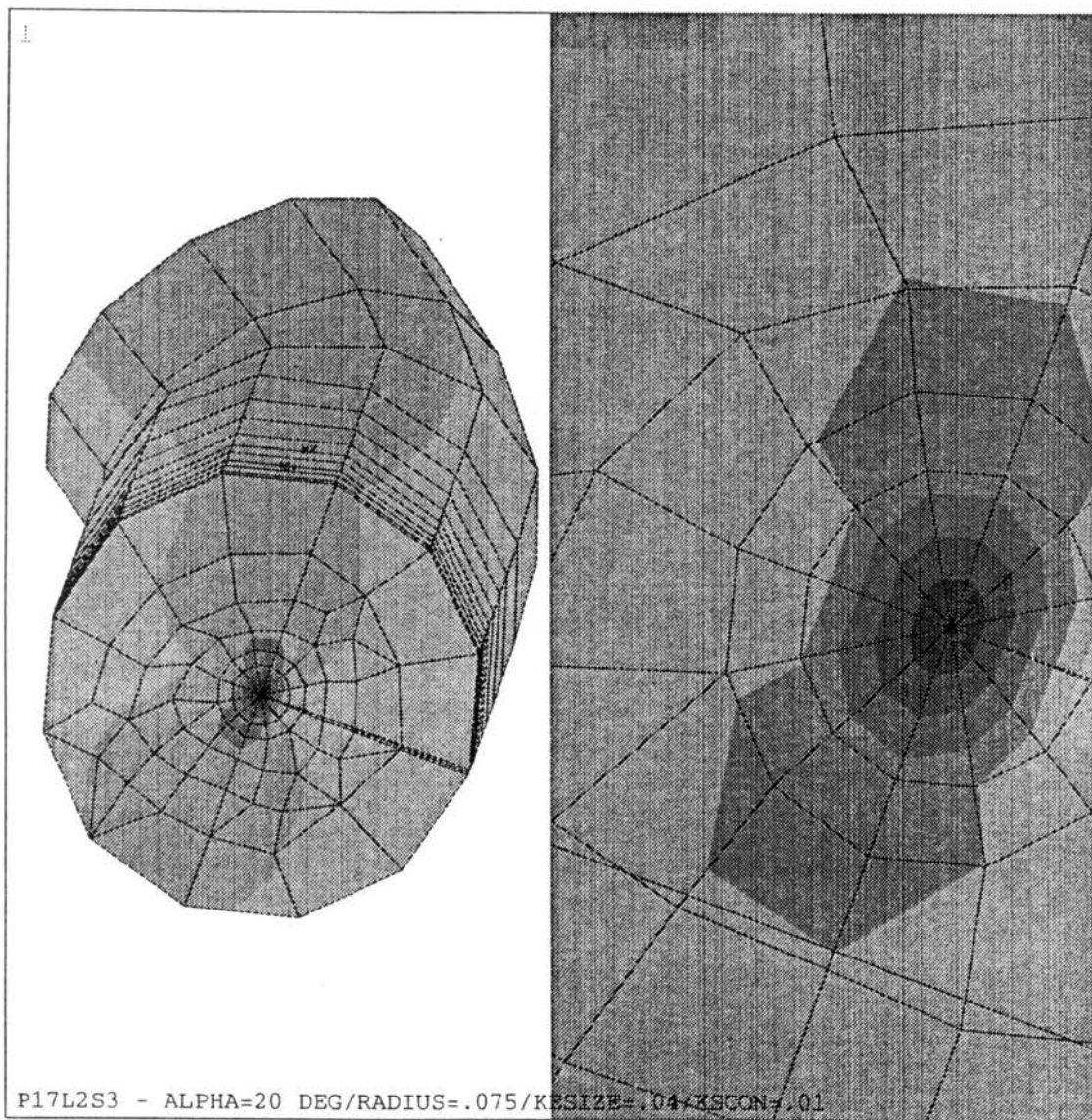


Figure 49. Strain Distribution Near Crack Tip for Curved Crack Front (Alpha= 20 Deg.)

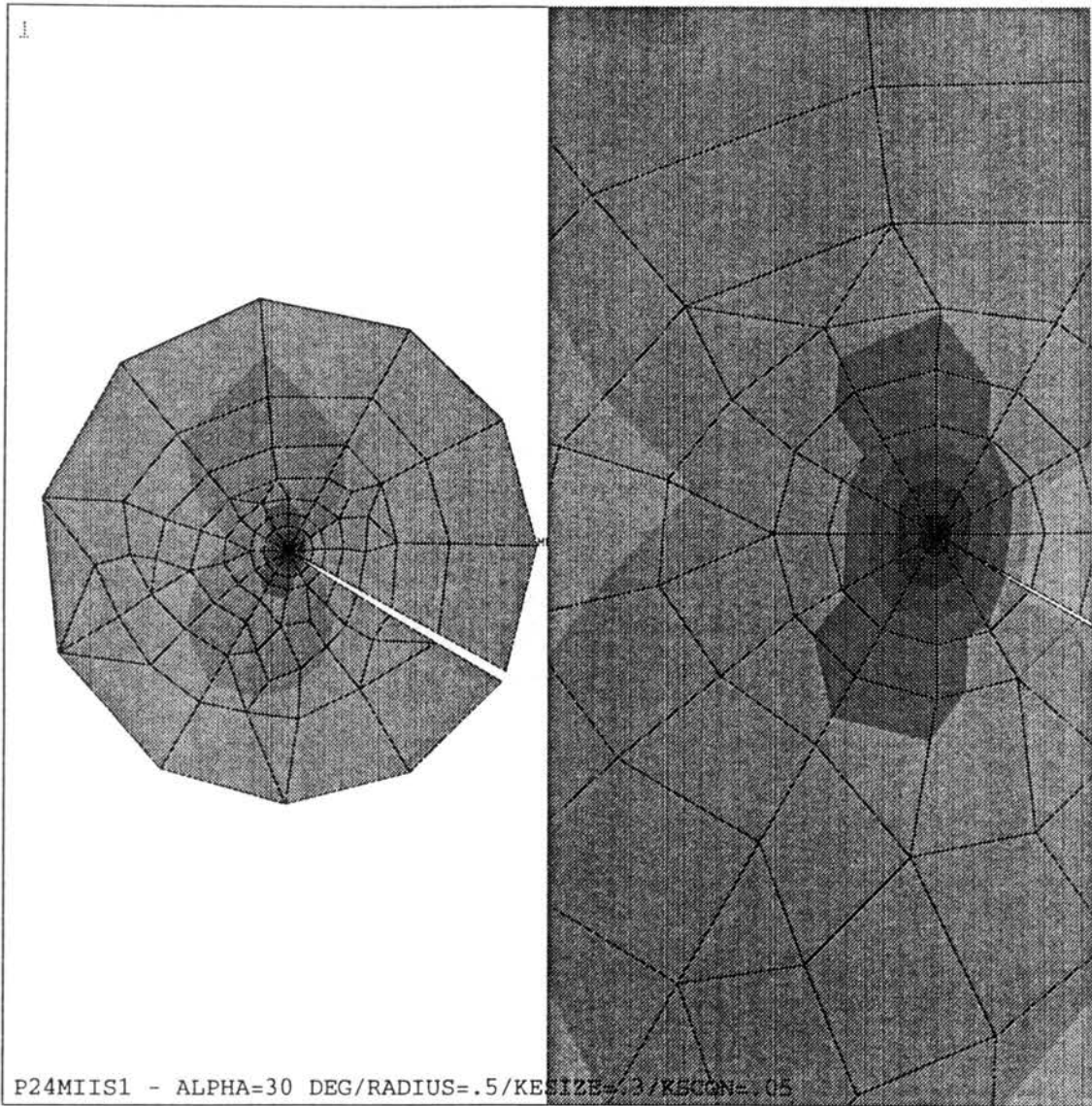


Figure 50. Strain Distribution Near Crack Tip for an Assumed Straight Crack Front

Figure 51 shows the direction of the maximum principal stress for the elements near the crack tip when modeled with the actual curved crack front. It is interesting to note that the maximum principal stress is perpendicular to the crack faces at the crack tip. Figure 52 shows the direction of the maximum principal stress for the elements near the crack tip when modeled with an assumed straight crack front. For the straight crack front the maximum principal stress basically remains parallel to the load and not perpendicular to the crack faces.

Appendix G contains a simple comparison of several actual Mode I/Mode II specimen stress intensity factors to the handbook solutions for a horizontal crack.

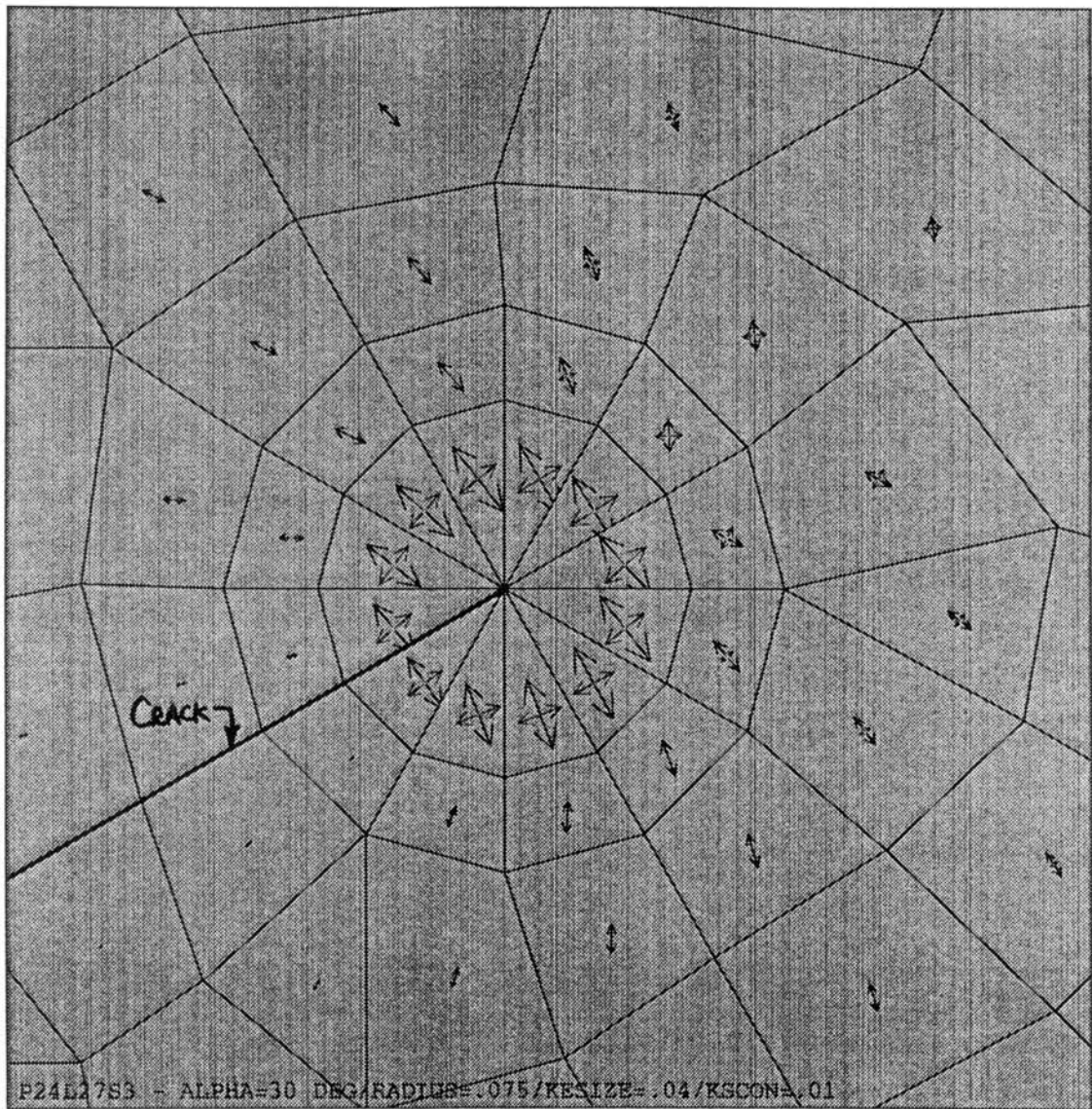


Figure 51. Maximum Principal Stress Direction for Actual Curved Crack Front

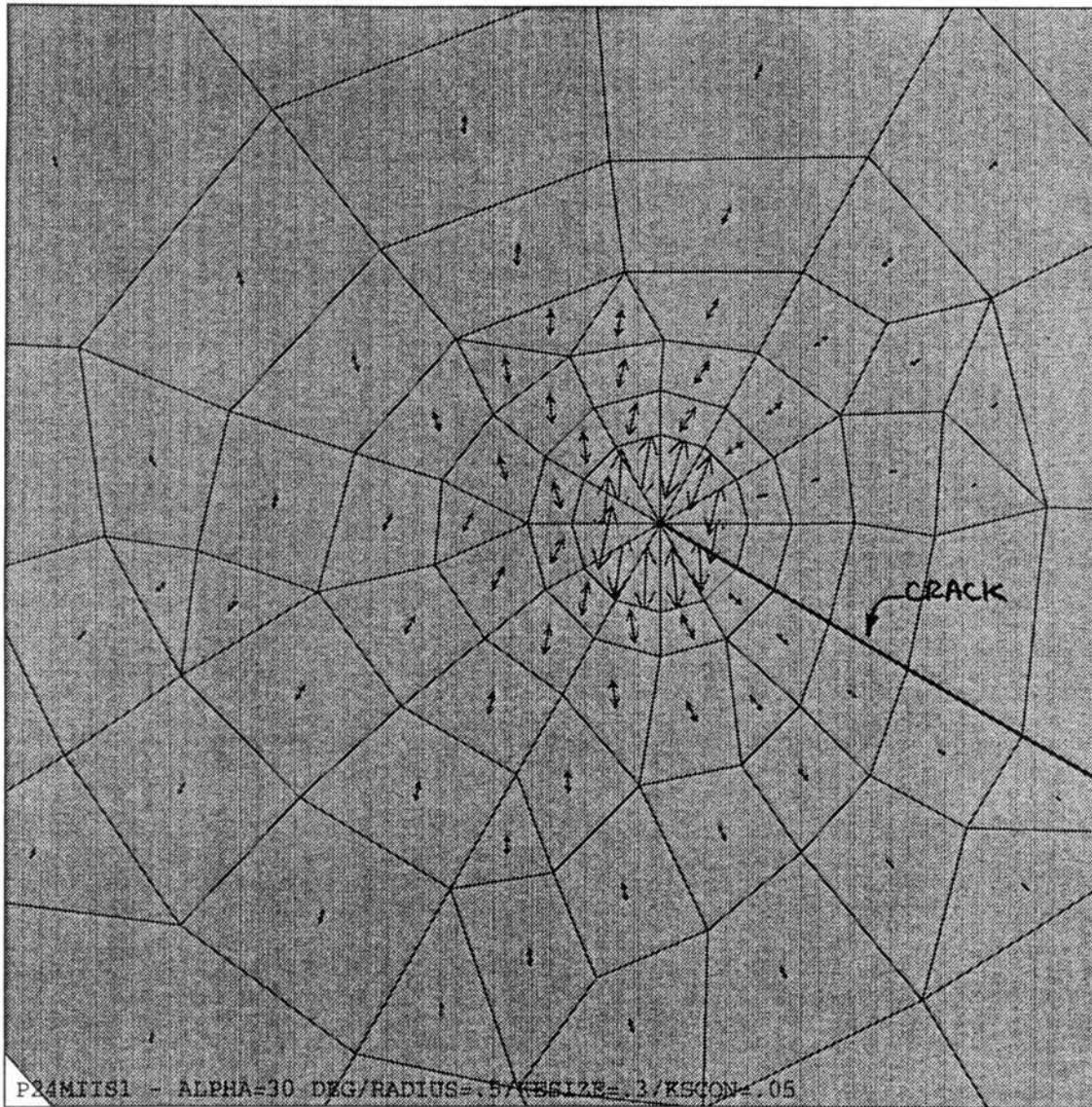


Figure 52. Maximum Principal Stress Direction for Assumed Straight Crack Front

5.2 Mode I/Mode III Specimen

Plots of the normalized SIF values with respect to their location along the actual curved crack front are shown in Figure 53. It is interesting to note that the K_{III} values are approximately 50% of K_I . It is also interesting to note that the SIF values are basically the same for both the 12 layer model and the 22 layer model.

The SIF values in Figure 53 vary considerably near the side grooves, especially the left side. The primary reason for this variation is the limitations of the computer model for the Mode I/Mode III specimen as explained in Chapter 4. Additional reasons for the variation in the SIF values at the side grooves are the same as for the Mode I/Mode II specimen. The values through the middle of the specimen should be fairly accurate.

The crack tip strain distribution at the middle of the specimen is shown in Figure 54 and the maximum principal stress direction at the crack tip in Figure 55.

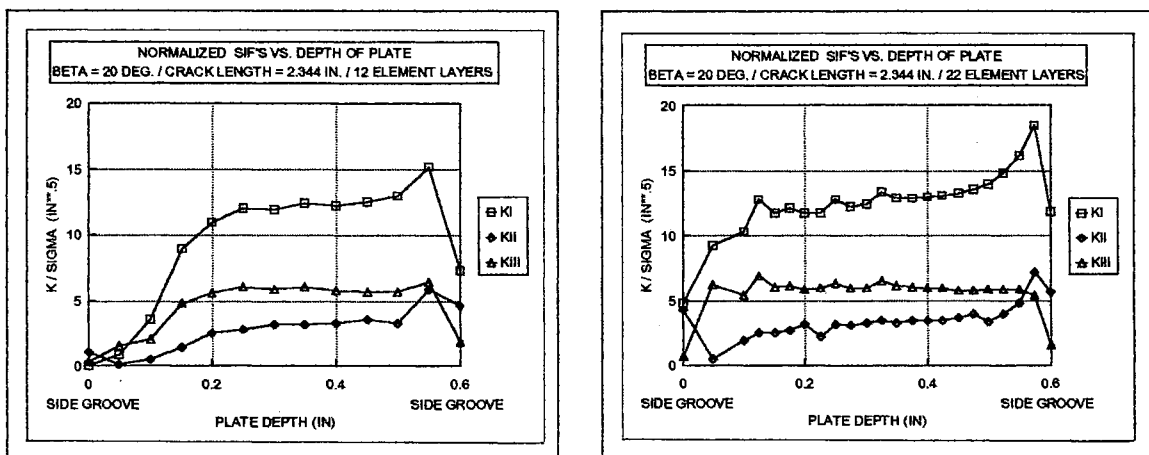


Figure 53. Plots of Normalized SIF's vs. Plate Depth for Beta= 20 Degrees

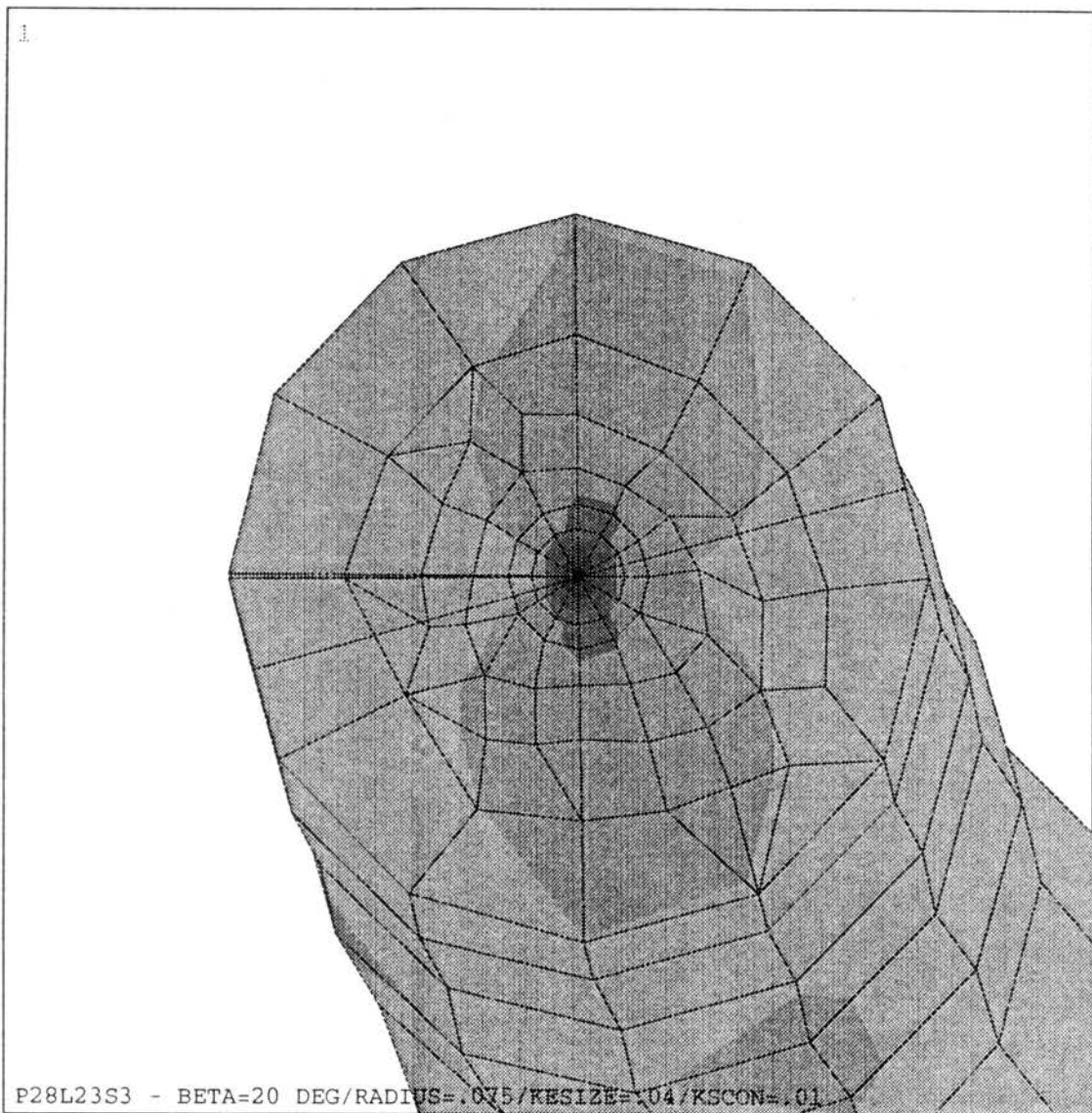


Figure 54. Strain Distribution Near Crack Tip for Curved Crack Front (Beta= 20 Deg.)

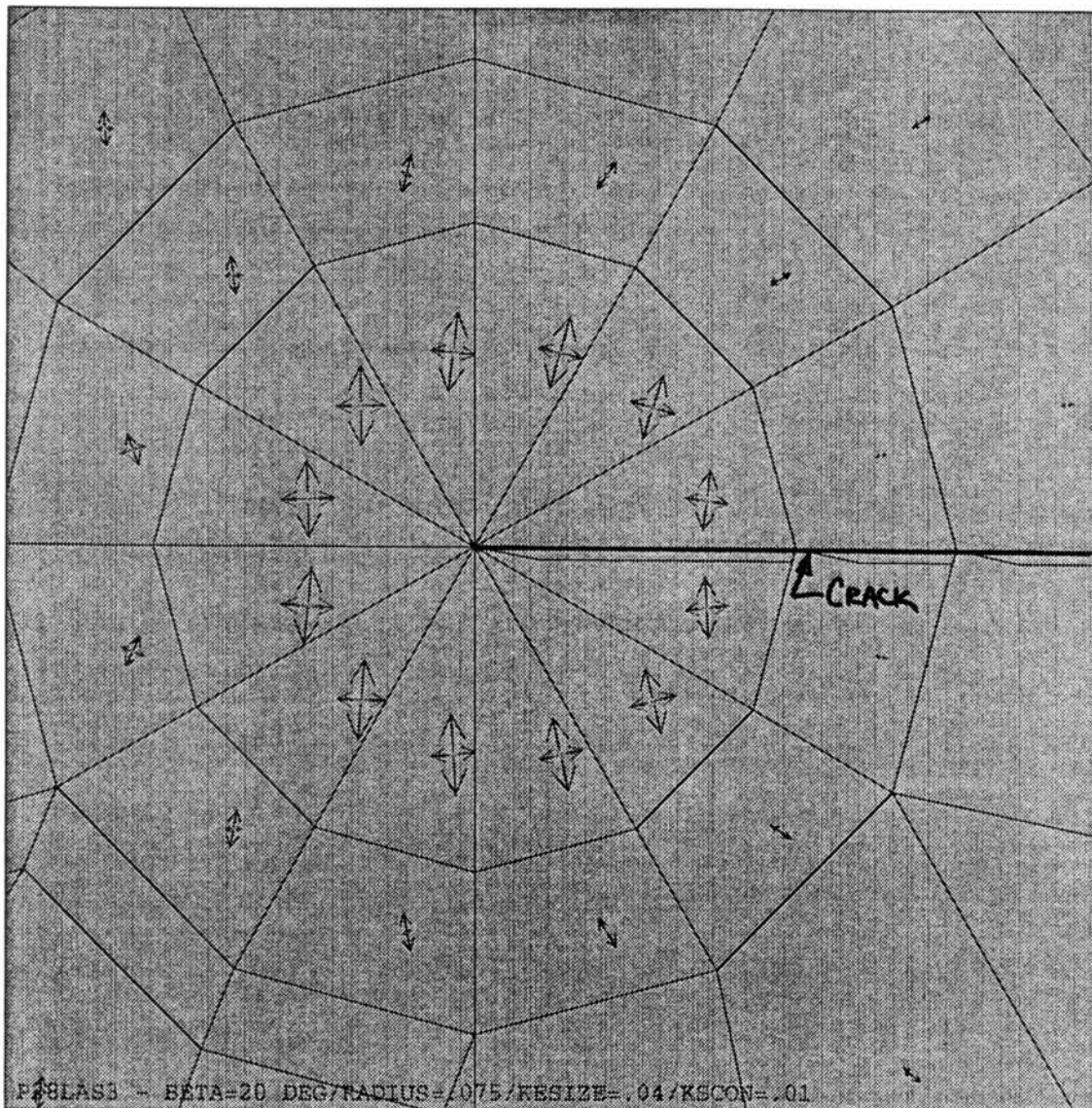


Figure 55. Maximum Principal Stress Direction for Mode I/Mode III Specimen

5.3 Crack Growth Rate Comparison

The crack growth data for two Mode I/Mode II specimens is shown in Figures 56 and 57. As can be seen, this crack growth data was smoothed with a third order parabola using MATLAB. This smoothed crack growth data was then used to calculate crack growth rates. Tabular listings of the data in Figures 56 and 57 and the crack growth rate data are in Appendix E.

A FORTRAN program was written to calculate the crack growth rates in Appendix E. The core statements for this program were obtained from ASTM Standard E647 [74]. This FORTRAN program is given in Appendix F.

SIF values were calculated at three locations on each plate. Using the crack growth rate data and the SIF values, the log-log plot in Figure 58 was developed. The straight line in this plot is the fatigue-crack growth rate relationship developed by Barsom [91]. This relationship is $\frac{da}{dN} = 3.6 \times 10^{-10} (\Delta K_I)^3$, which is applicable for ferrite-pearlite steels.

The following are possible reasons for the data not following a straight line or lying near the Barsom relationship line.

- 1) The two cracks propagated in different directions relative to the rolled grain of the material due to the alpha angles. The literature indicates that the rolled grain direction of the material does effect the crack growth rate [92,93].
- 2) It is difficult to establish any definite trends from just three data points for each specimen.

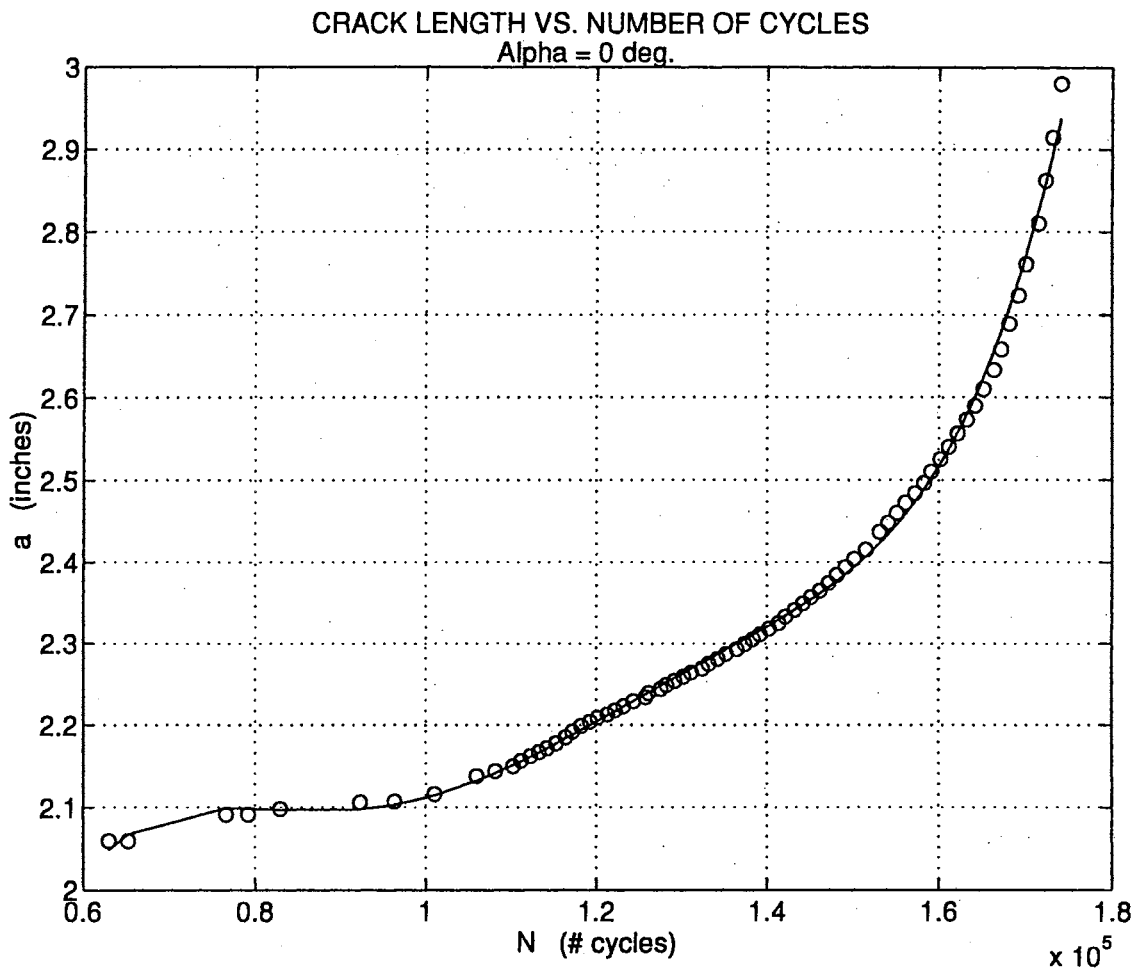


Figure 56. Crack Growth Data for The Specimen With Alpha=0 Degrees

- 3) The computer model values for K_I may be inaccurate for extremely long cracks where the cross section is small as discussed in Section 5.1.
- 4) The crack growth rate values may have small inaccuracies due to scatter in the measured crack growth data.

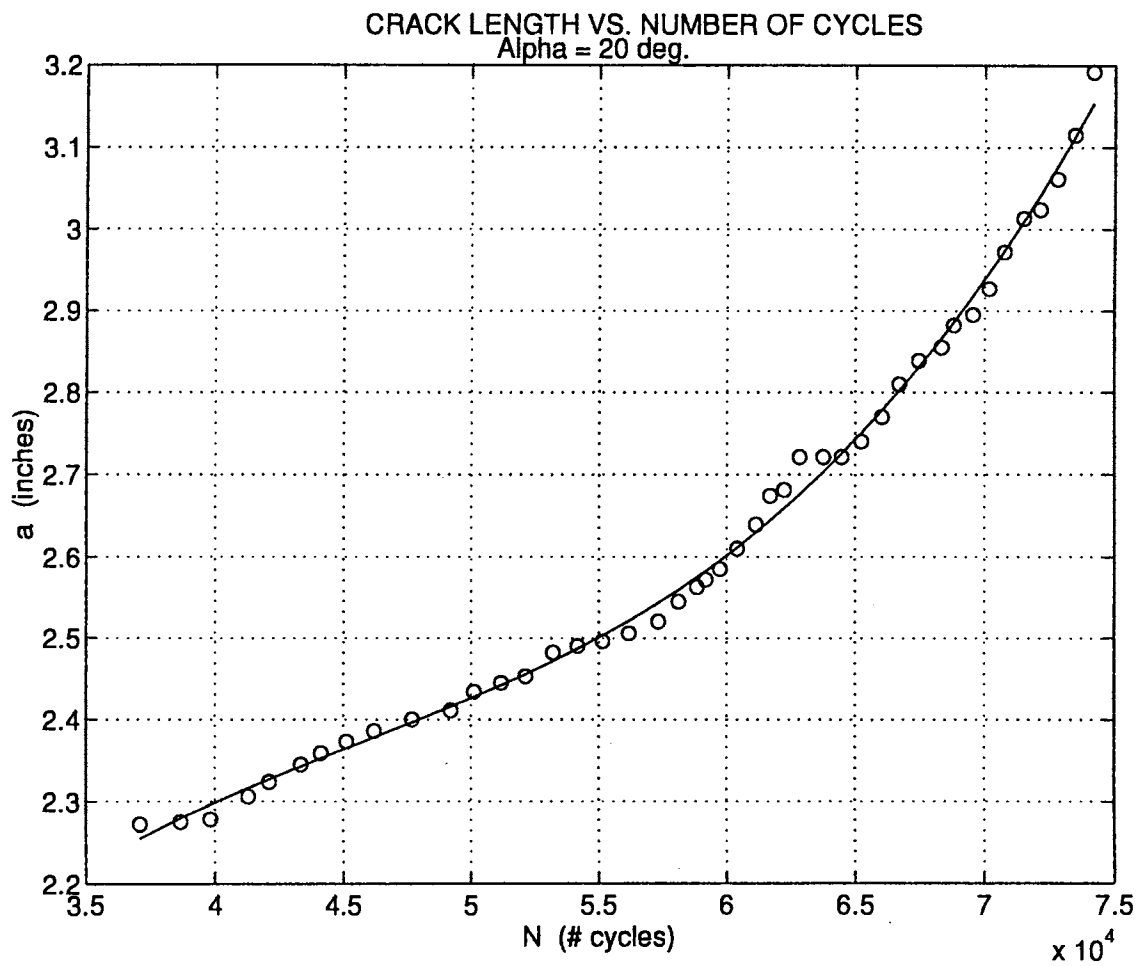


Figure 57. Crack Growth Data for The Specimen With Alpha=20 Degrees

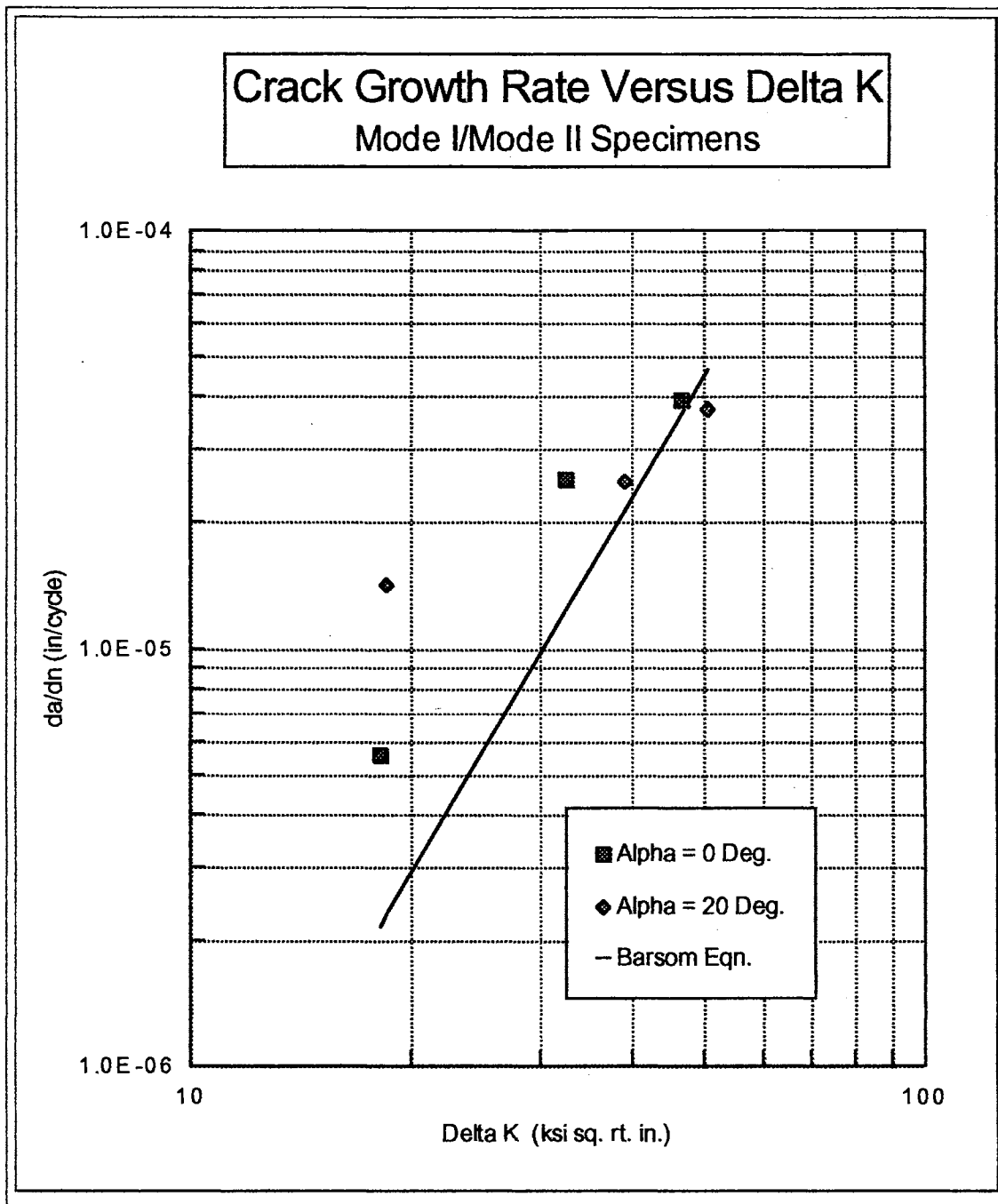


Figure 58. Crack Growth Rate Versus Delta K

CHAPTER 6

CONCLUSIONS

The following conclusions can be drawn from the results obtained:

- 1) A crack can be forced to grow other than perpendicular to the load with the specimens discussed herein.
- 2) The curved crack front developed in these specimens can be modeled with ANSYS using the custom programs discussed herein.
- 3) For the Mode I/Mode II specimens tested, the crack front does not remain straight and flat but curves until it stabilizes into a primarily mode I growth.
- 4) For the Mode I/Mode II specimens tested, the maximum principal stress is perpendicular to the crack faces at the crack tip.
- 5) From conclusions three and four above, it is reasonable to conclude that for the Mode I/Mode II specimens tested, the crack is controlled primarily by Mode I and is driven by the maximum principal stress. This is consistent with the results obtained by Bowness and Lee [89,90] which are discussed in Section 2.3.2.
- 6) For the Mode I/Mode II specimens tested, the mode I SIF's are approximately the same for both the actual curved crack front and the assumed straight crack front.
- 7) For the Mode I/Mode III specimen tested, the crack front does not remain straight and flat but stabilizes into a curved shape.

- 8) From the computer model of the Mode I/Mode III specimen it appears that the mode III SIF is not zero but is significantly large relative to the mode I SIF.
- 9) It is difficult to draw any definite conclusions from the crack growth rate data obtained.

CHAPTER 7

RECOMMENDATIONS FOR FUTURE RESEARCH

- 1) Investigate in more depth the contribution that mode III makes in fatigue crack growth. This could be accomplished by building and testing several Mode I/Mode III specimens, writing the appropriate finite element software, and calculating the SIF's.
- 2) Investigate the crack growth rates for different Mode I/Mode II and Mode I/Mode III specimens. SIF data for the Mode I/Mode II specimen is available from this project so it would be necessary only to measure crack growth data for additional specimens.
- 3) Develop and test a specimen that will sustain all three SIF modes during crack growth. From this it could be determined how the three modes interact.
- 4) Develop a completely different specimen that can sustain mixed mode crack growth and compare its results to this project.
- 5) Try different specimen materials and different rolled grain directions to determine their contributions in mixed loading.
- 6) Investigate the "tunneling" effect that occurs at slower growth rates on the Mode I/Mode II specimens.

BIBLIOGRAPHY

- [1] Rhee, H.C., and M.F. Kanninen, "Opportunities for Application of Fracture Mechanics for Offshore Structures," *Appl. Mech. Rev.* vol.41, no.2, Feb. 1988, pp.23-35.
- [2] Pook, L.P., J.C.P. Kam, and Y. Mshana, "On Mixed Mode Fatigue Crack Growth in Tubular Welded Joints," *Proceedings, International Conference on Offshore Mechanics and Arctic Engineering*, The Hague, Netherlands, Vol.III-B, 1992, pp. 251-256.
- [3] Broek, D., and R.C. Rice, "Fatigue Crack Growth Properties of Rail Steels," Battelle Report to DOT/TC, 1976.
- [4] Baloch, R.A., and M.W. Brown, "The Effect of Pre-Cracking History on Branch Crack Threshold Under Mixed Mode I/II Loading," *Fatigue Under Biaxial and Multiaxial Loading, ESIS10*, 1991, Mechanical Engineering Publications, London, pp. 179-197.
- [5] Zamrik, S.Y., A. Seibi, and D.C. Davis, "Fatigue Crack Initiation from an Induced Angled Surface Crack Under Biaxial Anticlastic Bending," *Fatigue Under Biaxial and Multiaxial Loading, ESIS10* (Edited by K. Dussmaul, D. McDiarmid, and D. Socie), 1991, Mechanical Engineering Publications, London, pp. 223-238.
- [6] Erdogan, F., and G.C. Sih, "On the Crack Extension in Plates Under Plane Loading and Transverse Shear," *Journal of Basic Engineering*, Transactions of the ASME, Dec 1963, pp. 519-527.
- [7] Ewing, P.D., and J.G. Williams, "The Fracture of Spherical Shells Under Pressure and Circular Tubes with Angled Cracks in Torsion," *International Journal of Fracture*, Vol. 10, No. 4, December 1974, pp. 537-543.
- [8] Hojfeldt, E., and C.B. Ostervig, "Fatigue Crack Propagation in Shafts with Shoulder Fillets," *Engineering Fracture Mechanics*, Vol. 25, No. 4, 1986, pp. 421-427.
- [9] Hua, G., "Mixed-Mode Fatigue Thresholds," *Fatigue of Engineering Materials and Structures*, Vol. 5, No. 1, 1982, pp. 1-17.

- [10] Iida, S., and A.S. Kobayashi, "Crack Propagation Rate in 7075-T6 Plates Under Cyclic Tensile and Transverse Shear Loadings," *Journal of Basic Engineering*, Transactions of the ASME, December 1969, pp. 764-769.
- [11] Linnig, W., H.A. Richard, and K. Henn, "Change in the Crack Growth Rates Under Mixed Mode Loading," *Fatigue 90*, Materials and Component Engineering Publications Ltd., Birmingham, 1990, pp. 573-579.
- [12] Miglin, M.T., I.H. Lin, J.P. Hirth, and A.R. Rosenfield, "Mixed Mode Crack Growth Using the Compact Specimen," *Fracture Mechanics: 14th Symposium - Volume II: Testing and Applications*, ASTM STP 791, American Society for Testing and Materials, 1983, pp. II353-II369.
- [13] Nunomura, S. and Y. Oda, "Cracked Ring Specimen for Environment Fatigue and Mixed Mode Fatigue Tests," *Fatigue 90*, Materials and Component Engineering Publications Ltd., Birmingham, 1990, pp. 589-595.
- [14] Pook, L.P., and D.G. Crawford, "The Fatigue Crack Direction and Threshold Behaviour of a Medium Strength Structural Steel Under Mixed Mode I and III Loading," *Fatigue Under Biaxial and Multiaxial Loading*, ESIS10, 1991, Mechanical Engineering Publications, London, pp. 199-211.
- [15] Pook, L.P., and D.G. Crawford, "Stress Intensity Factors for Twist Cracks," *International Journal of Fracture*, Vol. 42, 1990, pp. R27-R32.
- [16] Pook, L.P., "The Significance of Mode I Branch Cracks for Mixed Mode Fatigue Crack Growth Threshold Behaviour," *Biaxial and Multiaxial Fatigue*, EGF3, 1989, Mechanical Engineering Publications, London, pp. 247-263.
- [17] Pook, L.P., "Comments on Fatigue Crack Growth Under Mixed Modes I and III and Pure Mode III Loading," *Multiaxial Fatigue*, ASTM STP 853, American Society for Testing and Materials, Philadelphia, 1985, pp. 249-263.
- [18] Pook, L.P., "A Failure Mechanism Map for Mixed Mode I and II Fatigue Crack Growth Thresholds," *International Journal of Fracture*, Vol. 28, 1985, pp. R21-R23.
- [19] Pook, L.P., "The Fatigue Crack Direction and Threshold Behaviour of Mild Steel Under Mixed Mode I and III Loading," *International Journal of Fatigue*, Vol. 7, No. 1, 1985, pp. 21-30.
- [20] Pook, L.P., "The Effect of Crack Angle on Fracture Toughness," *Engineering Fracture Mechanics*, Vol. 3, 1971, pp. 205-218.

- [21] Richard, H.A., "Fracture Predictions for Cracks Exposed to Superimposed Normal and Shear Stresses," VDI-Forschungsheft 631, VDI-Verlag, Dusseldorf., 1985.
- [22] Sehitoglu, H., D.F. Socie, and D. Worthem, "Crack Growth Studies in Biaxial Fatigue," *Basic Questions in Fatigue: Volume I, ASTM STP 924*, J.T. Fong and R.J. Fields, Eds., American Society for Testing and Materials, Philadelphia, 1988, pp. 120-135.
- [23] Shah, R.C., "Fracture Under Combined Modes in 4340 Steel," *Fracture Analysis ASTM STP 560*, 1974, pp. 29-52.
- [24] Shields, E.B., T.S. Srivatsan, and J. Padovan, "Analytical Methods for Evaluation of Stress Intensity Factors and Fatigue Crack Growth", *Engineering Fracture Mechanics*, Vol.42, No.1, 1992, pp.1-26.
- [25] Tschegg, E.K., H.R. Mayer, M. Czegley, and S.E. Stanzl, "Influence of a Constant Mode III Load on Mode I Fatigue Crack Growth Thresholds," *Fatigue Under Biaxial and Multiaxial Loading, ESIS10*, Mechanical Engineering Publications, London, 1991, pp. 213-222.
- [26] Tschegg, E.K. and S.E. Stanzl, "Fatigue Crack Propagation Measurements under Rotating-Bending Loading," *Fatigue 90*, Materials and Component Engineering Publications Ltd., Birmingham, 1990, pp. 1217-1222.
- [27] Tschegg, E.K., and S.E. Stanzl, "The Significance of Sliding Mode Crack Closure on Mode III Fatigue Crack Growth," *Basic Questions in Fatigue: Volume I, ASTM STP 924*, J.T. Fong and R.J. Fields, Eds., American Society for Testing and Materials, Philadelphia, 1988, pp. 214-232.
- [28] Tschegg, E.K., "Mode III and Mode I Fatigue Crack Propagation Behaviour Under Torsional Loading," *Journal of Materials Science*, Vol. 18, 1983, pp. 1604-1614.
- [29] Tschegg, E.K., "The Influence of the Static I Load Mode and R Ratio on Mode III Fatigue Crack Growth Behaviour in Mild Steel," *Materials Science and Engineering*, Vol. 59, 1983, pp. 127-137.
- [30] Tschegg, E.K., "A Contribution to Mode III Fatigue Crack Propagation," *Materials Science and Engineering*, Vol. 54, 1982, pp. 127-136.
- [31] Abdel Mageed, A.M., and R.K. Pandey, "Mixed Mode Crack Growth Under Static and Cyclic Loading in Al-Alloy Sheets," *Engineering Fracture Mechanics*, Vol. 40, 1991, pp. 371-385.

- [32] Richard, H.A., and M. Kuna, "Theoretical and Experimental Study of Superimposed Fracture Modes I, II, and III," *Engineering Fracture Mechanics*, Vol. 35, 1990, pp.949-960.
- [33] Richard, H.A., "Specimens for Investigating Biaxial Fracture and Fatigue Processes", *Biaxial and Multiaxial Fatigue, EGF3*, 1989, Mechanical Engineering Publications, London, pp. 217-229.
- [34] Yishu, Z., "Elliptic Rule Criterion for Mixed Mode Crack Propagation," *Engineering Fracture Mechanics*, Vol. 37, 1990, pp. 283-292.
- [35] Yishu, Z., "Experimental Study of Mixed Mode Crack Propagation," *Engineering Fracture Mechanics*, Vol. 34, No. 4, 1989, pp. 891-899.
- [36] Rhee, H.C., and M.M. Salama, "On the Evaluation of Stress Intensity Factor for Tubular Joint Fatigue Study," OTC Paper 4998, *17th Annual Offshore Technology Conference*, Texas, May 1985.
- [37] Rhee, H.C., "The Behavior of Stress Intensity Factors of Weld Toe Surface Flaw of Tubular X-Joints," OTC Paper 5136, *18th Annual Offshore Technology Conference*, Texas, May 1986.
- [38] Rhee, H.C., and J.A. Tyson, "Fatigue Life Calculation for Offshore Structural Tubular Joint Using Fracture Mechanics Crack Growth Analysis," No. 5557, *Offshore Technology Conference*, 1987, pp. 65-75.
- [39] Rhee, H.C., "Fatigue Crack Growth Analyses of Offshore Structural Tubular Joint," *Journal of Offshore Mechanics and Arctic Engineering, transactions of the ASME*, Vol.111, Feb. 1989, pp.49-55.
- [40] Rhee, H.C., S. Han, and G.S. Gipson, "Reliability of Solution Method and Empirical Formulas of Stress Intensity Factors for Weld Toe Cracks of Tubular Joints," *Proceedings of the Conference on Offshore Mechanics and Arctic Engineering*, Vol. III-B, Materials Engineering, 1991, pp. 441-452.
- [41] Broek, D., *Elementary Engineering Fracture Mechanics*, 4th Ed., Martinus Nijhoff Publishers, 1987.
- [42] Rhee, H.C., and M.M Salama, "Mixed-Mode Stress-Intensity Factor Solutions for Offshore Structural Tubular Joints," *Fracture Mechanics: Nineteenth Symposium, ASTM STP 969*, T.A. Cruse, Ed., American Society for Testing and Materials, Philadelphia, 1988, pp. 669-676.

- [43] Freitas, M. de, and M.H. Carvalho, "Short Fatigue Crack Growth in Mixed Mode Conditions in AL-LI Alloy 2090," *Fatigue 90*, Materials and Component Engineering Publications Ltd., Birmingham, 1990, pp. 1061-1066.
- [44] Sih, G.C., and B.M. Barthelemy, "Mixed Mode Fatigue Crack Growth Predictions," *Engineering Fracture Mechanics*, Vol. 13, 1980, pp.439-451.
- [45] Badaliane, R., "Application of Strain Energy Density Factor to Fatigue Crack Growth Analysis," *Engineering Fracture Mechanics*, Vol. 13, 1980, pp. 657-666.
- [46] Tohgo, K., Otusks, A., Yoshida, M., "Fatigue Behaviour of a Surface Crack Under Mixed Mode Loading," *Fatigue 90*, Materials and Component Engineering Publications Ltd., Birmingham, 1990, pp. 567-572.
- [47] Roberts, R., and J.J. Kibler, "Mode II Fatigue Crack Propagation," *Journal of Basic Engineering*, December 1971, pp. 671-680.
- [48] Han, S., and F. Zwerneman, "Fracture Mechanics Investigation of Tubular Joint Weld Toe Cracks Through 3-D Finite Element Analysis," Phase I Report to Joint Industry Project, July 1993.
- [49] Chell, G.G., and E. Girvan, "An Experimental Technique For Fast Fracture Testing in Mixed Mode," *International Journal of Fracture*, Vol. 14, 1974, pp. R81-R84.
- [50] Found, M.S., U.S. Fernando, K.J. Miller, "Requirements of a New Multiaxial Fatigue Testing Facility," *Multiaxial Fatigue, ASTM STP 853*, American Society for Testing and Materials, Philadelphia, 1985, pp. 11-23.
- [51] Anderson, T.L., Fracture Mechanics: Fundamentals and Applications, CRC Press, 1991.
- [52] Ritter, M.A., and R.O. Ritchie, "On the Calibration, Optimization and Use of D.C. Electrical Potential Methods for Monitoring Mode III Crack Growth in Torsionally-Loaded Samples," *Fatigue of Engineering Materials and Structures*, Vol. 5, 1982, pp. 91-104.
- [53] Wei, R.P., and R.L. Brazill, "An Assessment of AC and DC Potential Systems for Monitoring Fatigue Crack Growth," *Fatigue Crack Growth Measurement and Data Analysis, ASTM STP 738*, American Society for Testing and Materials, 1981, pp. 103-119.

- [54] Wilkowski, G.M., and W.A. Maxey, "Review and Applications of the Electric Potential Method for Measuring Crack Growth in Specimens, Flawed Pipes, and Pressure Vessels," *Fracture Mechanics: Fourteenth Symposium-Volume II: Testing and Applications*, ASTM STP 791, ASTM, Philadelphia, 1983, pp. II-266-II-294.
- [55] Connolly, M.P., and R. Collins, "The Measurement and Analysis of Semi-Elliptical Surface Fatigue Crack Growth," *Engineering Fracture Mechanics*, Vol. 26, No. 6, 1987, pp. 897-911.
- [56] Deshayes, F.R., and W.H. Hartt, "Development of a Fatigue Crack Growth Rate Specimen Suitable for a Multiple-Specimen Test Configuration," *Fracture Mechanics: Twenty-Third Symposium, ASTM STP 1189*, American Society for Testing and Materials, 1993, pp. 598-618.
- [57] Ostergaard, D.F., J.R. Thomas, and B.M. Hillberry, "Effect of Delta-a Increment on Calculating da/dn from a versus N Data," *Fatigue Crack Growth Measurement and Data Analysis, ASTM STP 738*, American Society for Testing and Materials, 1981, pp. 194-204.
- [58] Marci, G., V. Bachmann, and K. Hartmann, "Experimental Determination of Delta K_{eff}," *Fatigue 90*, Materials and Component Engineering Publications Ltd., Birmingham, 1990, pp. 1277-1282.
- [59] Stanzl, S.E., M. Czegley, H.R. Mayer, and E.K. Tschegg, "Fatigue Crack Growth Under Combined Mode I and Mode III Loading," *Fracture Mechanics Perspectives and Directions*, ASTM STP 1020, ASTM, Philadelphia, 1989, pp. 479-496.
- [60] Stanzl, S.E., and E.K. Tschegg, "Fatigue Crack Growth and Threshold Behaviour at Ultrasonic Frequencies," *Fracture Mechanics: Fourteenth Symposium-Volume II: Testing and Applications*, ASTM STP 791, ASTM, Philadelphia, 1983.
- [61] Yazdan, N. and P. Albrecht, "Crack Growth Rates of Structural Steel in Air and Aqueous Environments," *Engineering Fracture Mechanics*, Vol. 32, 1989, pp. 997-1007.
- [62] Zhang, X.P. and Y.W. Shi, "Constraint of Side-Groove and Its Influence on Fracture Toughness Parameter in Charpy-Size Specimens," *Engineering Fracture Mechanics*, Vol. 43, No. 5, 1992, pp. 863-867.
- [63] Roberts, R., and F. Erdogan, "The Effect of Mean Stress on Fatigue Crack Propagation in Plates Under Extension and Bending," *Journal of Basic Engineering, Transactions of the ASME*, December 1967, pp. 885-892.

- [64] Ritchie, R.O., F.A. McClintock, E.K. Tschegg, and H. Nayeb-Hashemi, "Mode III Fatigue Crack Growth Under Combined Torsional and Axial Loading," *Multiaxial Fatigue, ASTM STP 853*, American Society for Testing and Materials, Philadelphia, 1985, pp. 203-227.
- [65] Ritchie, R.O., "A Comparison of Fatigue Crack Propagation in Modes I and III," *Fracture Mechanics: Eighteenth Symposium, ASTM STP 945*, American Society for Testing and Materials, Philadelphia, 1988, pp. 821-842.
- [66] Paris, P.C., "The Fracture Mechanics Approach to Fatigue," *Fatigue--An Interdisciplinary Approach*, Syracuse, N.Y., Syracuse University Press, 1964, pp. 107-130.
- [67] Otsuka, A., K. Mori, and K. Tohgo, "Mode II Fatigue Crack Growth in Aluminium Alloys," *Current Research on Fatigue Cracks*, The Society of Materials Science, Japan, Kyoto, 1985, pp. 127-155.
- [68] Larsen, J.M., J.R. Jira, and T. Weerasooriya, "Crack Opening Displacement Measurements on Small Cracks in Fatigue," *Fracture Mechanics: Eighteenth Symposium, ASTM STP 945*, American Society for Testing and Materials, Philadelphia, 1988, pp. 896-912.
- [69] Kim, S.C., and D.M. Kang, "Strain Hardening Exponent on Fatigue Crack Propagation," *Fatigue 90*, Materials and Component Engineering Publications Ltd., Birmingham, 1990, pp. 111-116.
- [70] Wright, R.P., and R.A. Queeney, "Mode III Fatigue Crack Propagation Rates in 6061-T6 Aluminium," *International Journal of Fatigue*, Vol. 4, No. 1, January 1982, pp.27-30.
- [71] Gillemot, F., I. Havas, and L. Szabo, "Experiences in the Comparison of Large and Small Fracture Mechanics Specimens," *ASTM STP 909*, American Society for Testing and Materials, Philadelphia, 1986, pp. 118-124.
- [72] Pook, L.P., "On Mode III Fatigue Crack Propagation Rates in 6061-T6 Aluminium," *International Journal of Fatigue*, Vol. 4, No. 3, July 1982, pp. 175-176.
- [73] Andrews, W.R., and C.F. Shih, "Thickness and Side-Groove Effects on J- and - Resistance Curves for A533-B Steel at 93 Deg. C," *ASTM STP 668*, ASTM, Philadelphia, 1979, pp. 426-450.
- [74] Annual Book of ASTM Standards 1992, Section 3, ASTM, Philadelphia, PA, 1992.
- [75] Munz, D., "The Size Effect of Fracture Toughness and the Irwin Beta IC Adjustment," *International Journal of Fracture*, Vol. 32, 1986, pp.R17-R19.

- [76] Doong, J., J. Hwang, K. Peng, and C. Wang, "Effect of Heat Treatment Processes on the Fatigue Crack Growth in AISI 4340 Steel," *Fatigue 90*, Materials and Component Engineering Publications Ltd., Birmingham, 1990, pp. 1235-1240.
- [77] Smith, M.C., and R.A. Smith, "Toward an Understanding of Mode II Fatigue Crack Growth," *Basic Questions in Fatigue: Volume I, ASTM STP 924*, J.T. Fong and R.J. Fields, Eds., American Society for Testing and Materials, Philadelphia, 1988, pp. 260-280.
- [78] Hutchinson, J.W., M.E. Mear, and J.R. Rice, "Crack Paralleling and Interface Between Dissimilar Materials," *Journal of Applied Mechanics*, Vol. 54, December 1987, pp. 828-832.
- [79] Shih, C.F., and R.J. Asaro, "Elastic-Plastic Analysis of Cracks on Bimaterial Interfaces: Part I - Small Scale Yielding," *Journal of Applied Mechanics*, June 1988, Vol. 55, pp. 299-316.
- [80] Toya, M., "On Mode I and Mode II Energy Release Rates of an Interface Crack," *International Journal of Fracture*, 56, 1992, pp. 345-352.
- [81] Rhee, H.C., "Stress Intensity Factor Evaluation From Displacements Along Arbitrary Crack Tip Radial Lines for Warped Surface Flaws," *Engineering Fracture Mechanics*, vol.32, no.5, 1989, pp.723-730.
- [82] Rhee, H.C., and M.M. Salama, "Mixed-Mode Stress Intensity Factor Solutions of a Warped Surface Flaw by Three-Dimensional Finite Element Analysis," *Engineering Fracture Mechanics*, vol.28, 1987, pp.203-209.
- [83] Ingraffea, A.R., and C. Manu, "Stress-Intensity Factor Computation in Three Dimensions with Quarter-Point Elements," *International Journal for Numerical Methods in Engineering*, Vol. 15, 1980, pp. 1427-1445.
- [84] Barsom, J.M. and S.T. Rolfe, Fracture & Fatigue Control in Structures: Applications of Fracture Mechanics, 2nd ed., Prentice-Hall, 1987.
- [85] Hertzberg, R.W., Deformation and Fracture Mechanics of Engineering Materials, 3rd ed., John Wiley, 1989.
- [86] ANSYS User's Manual Rev. 5.0, Swanson Analysis Systems, Inc., 1992.
- [87] SESAM User's Manual, Veritas, 1990.
- [88] NDE Centre News, University College London, Issue 5, May 1992.

- [89] Bowness, D., and Lee, M.M.K., "Crack Curvature Under the Weld Toe in a Tubular Joint: A Three-Dimensional Numerical Investigation," *Proceedings of the Fourth (1994) International Offshore and Polar Engineering Conference*, Osaka, Japan, Vol. IV, April 10-15, 1994, pp. 664-669.
- [90] Bowness, D., and Lee, M.M.K., "Fatigue Crack Curvature Under the Weld Toe in a Tubular Joint", University College of Swansea, Wales, UK., Presented To 6th Tubular Joint Conference, Melbourne, Australia, December 1994.
- [91] Barsom, J.M., "Fatigue-Crack Propagation in Steels of Various Yield Strengths," *Transactions of the ASME-Journal of Engineering for Industry*, November 1971, pp. 1190-1196.
- [92] Campbell, J.E., W.W. Gerberich, and J.H. Underwood, Application of Fracture Mechanics for Selection of Metallic Structural Materials, American Society for Metals, Metals Park, Ohio, 1982, pp. 73.
- [93] Wilson, A.D., "Fatigue Crack Propagation in A533B Steels," *Transactions of the ASME-Journal of Pressure Vessel Technology*, August 1977, pp. 459-469.
- [94] Tada, H., P. Paris, and G. Irwin, *The Stress Analysis of Cracks Handbook*, Del Research Corporation, Hellertown, 1973.
- [95] Suresh, S., Fatigue of Materials, Cambridge University Press, 1991.

APPENDICES

APPENDIX A--ANSYS SIF VERIFICATIONS

2-D COMPACT SPECIMEN

Handbook Solution[94]

$$a = 2 \text{ in.}$$

$$d = 2 \text{ in.}$$

$$P = 1000 \text{ lb.}$$

$$h/b = .5$$

$$b = 4 \text{ in.}$$

$$h = 2 \text{ in.}$$

$$a/b = .5$$

$$d/h = 1$$

$$F_2 = .79 \quad (\text{From Chart})$$

$$\sigma_N = \frac{2P(2b+a)}{(b-a)^2}$$

$$\sigma_N = \frac{2(1000)(2(4)+2)}{(4-2)^2}$$

$$\sigma_N = 5000 \frac{\text{lb}}{\text{in}^2}$$

$$K_I = \sigma_N \sqrt{b-a} F_2$$

$$K_I = (5000) \sqrt{4-2} (.79)$$

$$K_I = 5586 \text{ psi} \sqrt{\text{in}}$$

Computer Solution

$$K_I = 5603 \text{ psi} \sqrt{\text{in}}$$

Error

$$\% = \frac{5603-5586}{5603} \times 100$$

$$\% \text{error} = 0.3\%$$

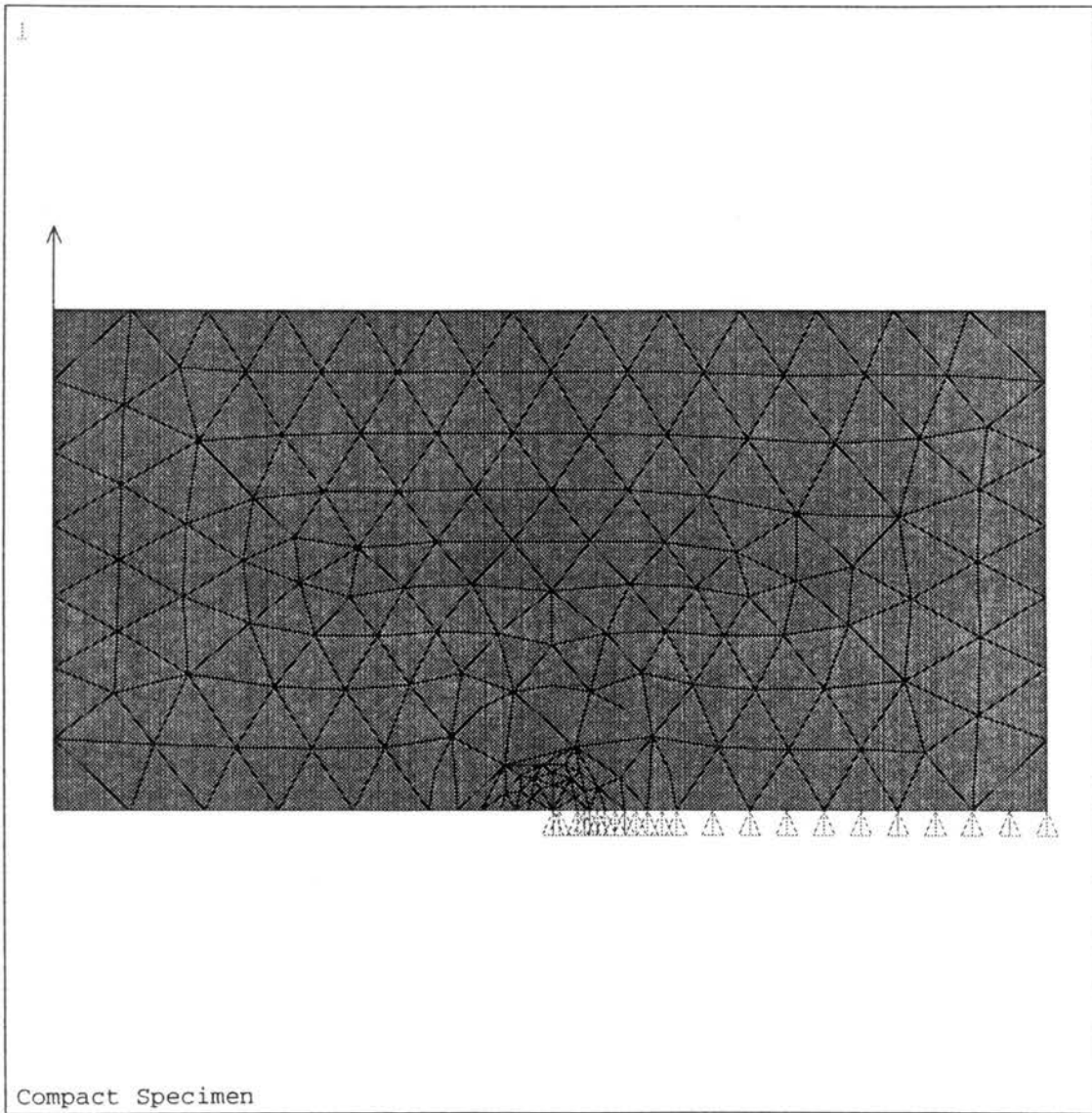


Figure 59. 2-D Compact Specimen

2-D PLATE WITH CENTER THROUGH CRACK

Handbook Solution[94]

$$a = .5 \text{ in.}$$

$$h = 5 \text{ in.}$$

$$\sigma = 1000 \text{ lb/in}^2$$

$$b = 3 \text{ in.}$$

$$a/b = .1667$$

$$F(a/b) = 1.0184 \quad (\text{From Chart})$$

$$K_I = \sigma \sqrt{\pi a} F(a/b)$$

$$K_I = (1000) \sqrt{\pi(.5)} (1.0184)$$

$$K_I = 1276 \text{ psi} \sqrt{\text{in}}$$

Computer Solution

$$K_I = 1281 \text{ psi} \sqrt{\text{in}}$$

Error

$$\% = \frac{1281 - 1276}{1281} \times 100$$

$$\% \text{error} = 0.4\%$$

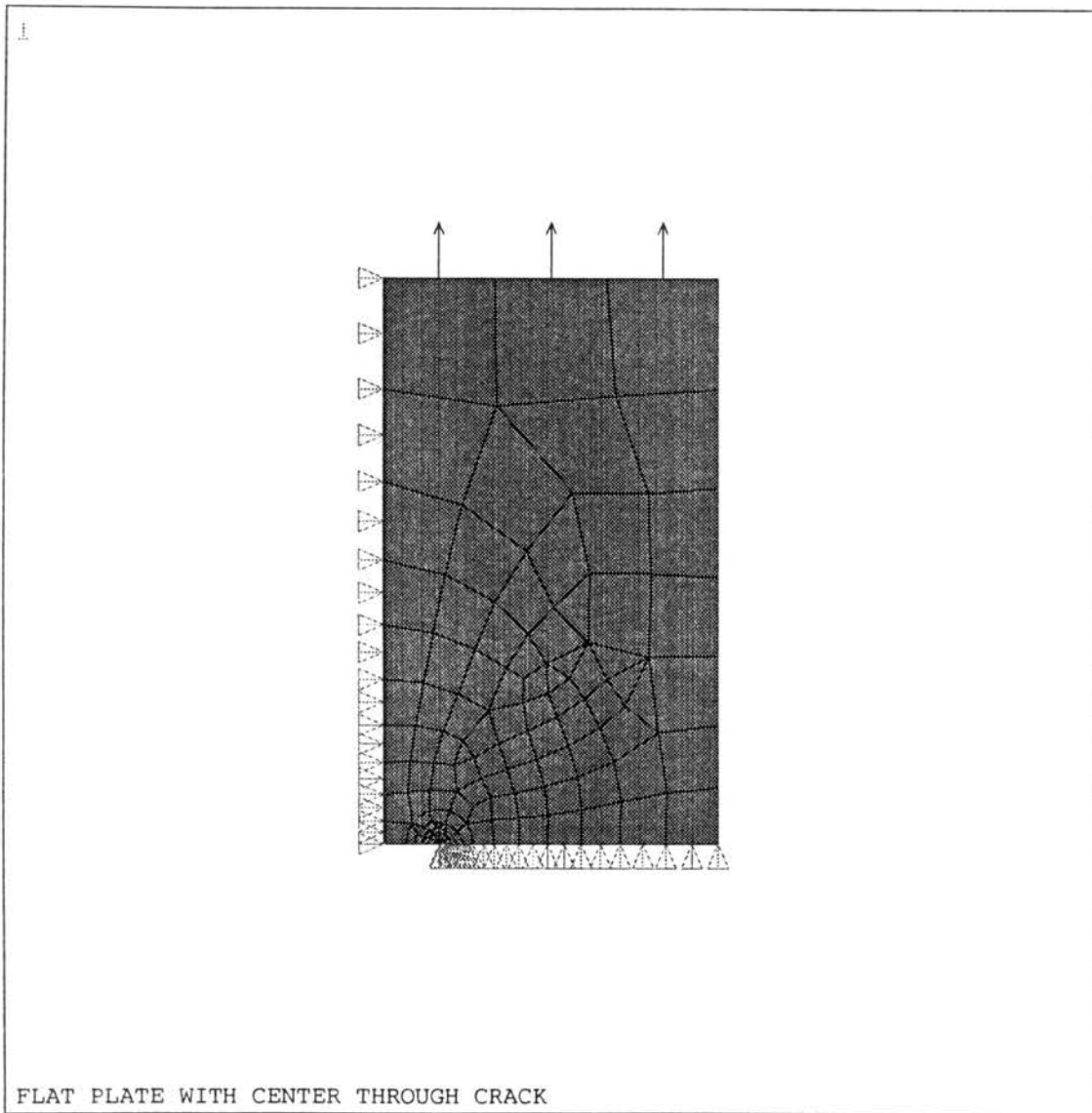


Figure 60. 2-D Plate With Center Through Crack

3-D PLATE WITH EDGE CRACK IN TENSION

Handbook Solution[94]

$$a = 2 \text{ in.}$$
$$W = 4 \text{ in.}$$

$$L = 21 \text{ in.}$$
$$a/w = .5$$

$$P = 2000 \text{ lb.}$$
$$t = .6 \text{ in.}$$

$$X_Crk = 2 \text{ in}$$
$$Y_Crk = 10.5 \text{ in}$$

$$\sigma = \frac{1000}{(.3 \times 4)}$$
$$\sigma = 833.33 \text{ psi}$$

$$\beta = 1.12 - 0.23(.5) + 10.6(.5)^2 - 21.7(.5)^3 + 30.4(.5)^4$$
$$\beta = 2.8425$$

$$K_I = \sigma \beta \sqrt{\pi a}$$
$$K_I = (833.33)(2.8425) \sqrt{\pi(2)}$$
$$K_I = 5938 \text{ psi} \sqrt{\text{in}}$$

Computer Solution

$$K_I = 5845 \text{ psi} \sqrt{\text{in}}$$

Error

$$\% = \frac{5938 - 5845}{5938} \times 100$$
$$\% \text{error} = 1.6\%$$

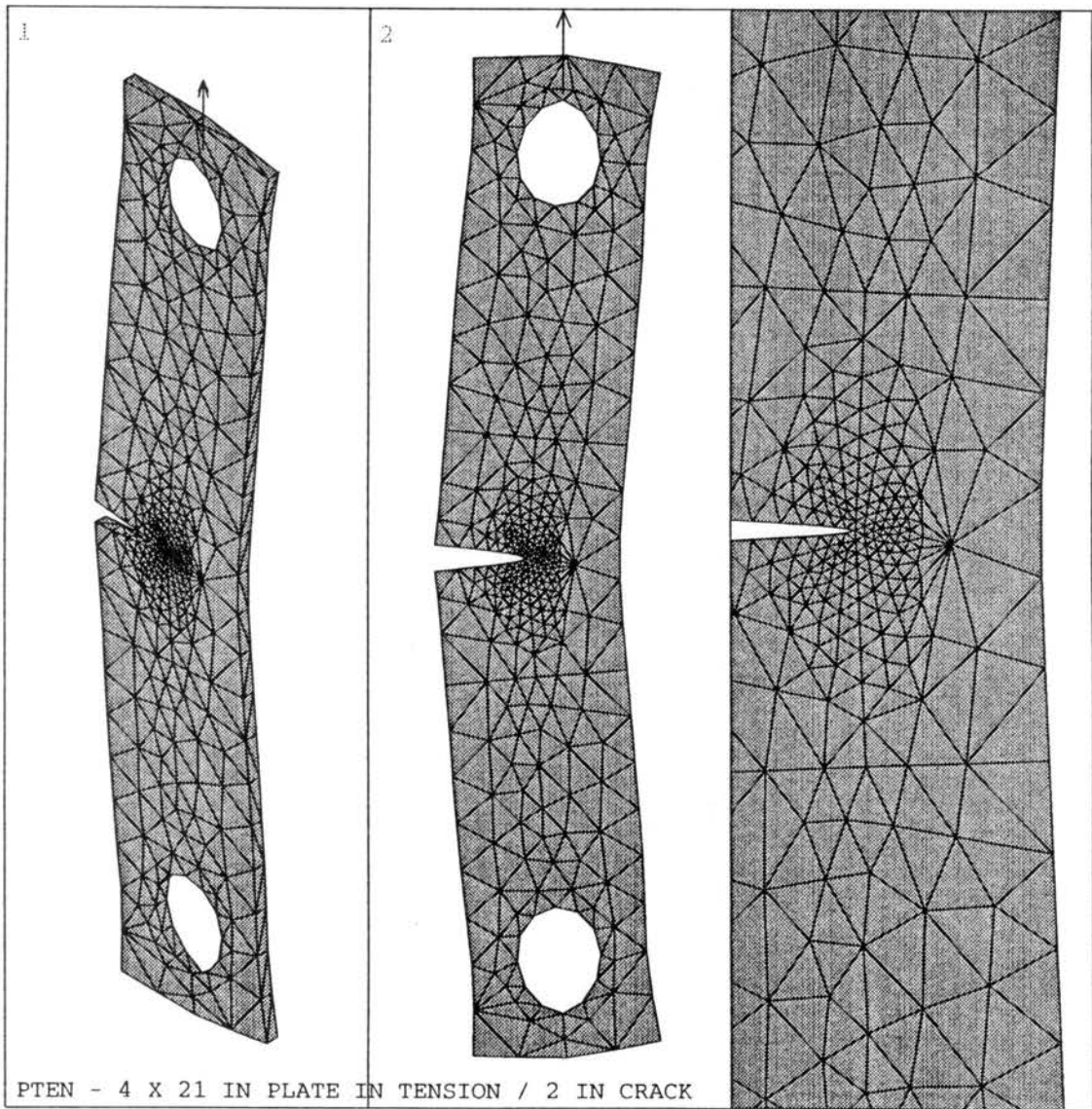


Figure 61. 3-D Plate With Edge Crack In Tension

2-D PLATE WITH EDGE CRACK IN MODE II SHEAR

Handbook Solution[94]

$$\begin{aligned} a &= 2 \text{ in.} & Q &= 1000 \text{ lb.} \\ b &= 4 \text{ in.} & a/b &= .5 \end{aligned}$$

$$F_{II} = \frac{1.30 - 0.65\left(\frac{a}{b}\right) + 0.37\left(\frac{a}{b}\right)^2 + 0.28\left(\frac{a}{b}\right)^3}{\sqrt{1 - \frac{a}{b}}}$$
$$F_{II} = \frac{1.30 - 0.65(.5) + 0.37(.5)^2 + 0.28(.5)^3}{\sqrt{1 - .5}}$$
$$F_{II} = 1.5592$$

$$K_{II} = \frac{2}{\sqrt{\pi a}} Q F_{II}$$
$$K_{II} = \frac{2}{\sqrt{\pi(2)}} (1000)(1.5592)$$
$$K_{II} = 1244 \text{ psi} \sqrt{\text{in}}$$

Computer Solution

$$K_{II} = 1195 \text{ psi} \sqrt{\text{in}}$$

Error

$$\% = \frac{1244 - 1195}{1244} \times 100$$
$$\% \text{error} = 3.9\%$$

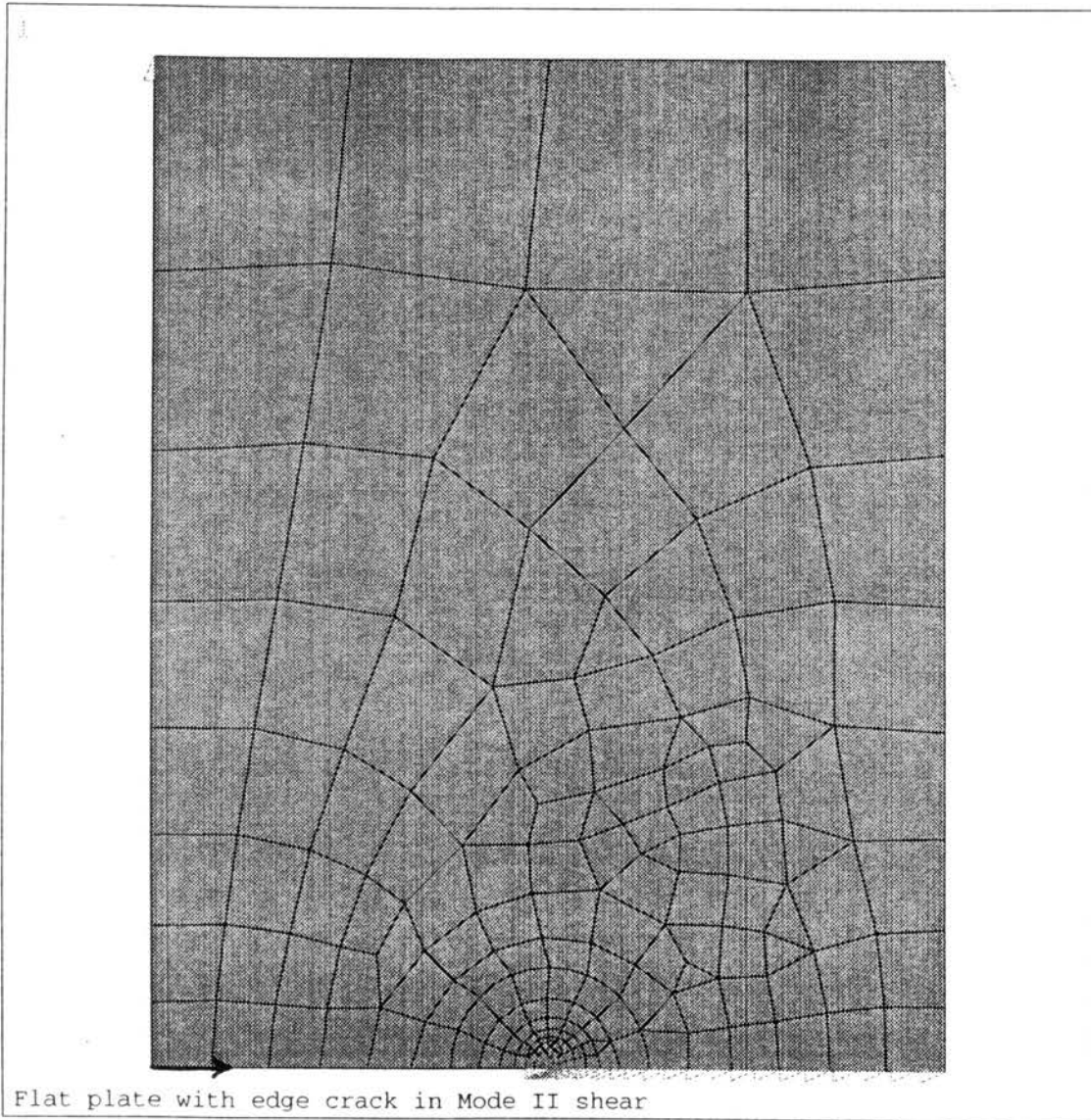


Figure 62. 2-D Plate With Edge Crack In Mode II Shear

**APPENDIX B--TABULAR VALUES OF PLATE
STRESS INTENSITY FACTORS**

TABLE I

STRESS INTENSITY FACTORS VERSUS PLATE DEPTH
Plate #25

Alpha= 0 deg.
Sigma= 510.72 psi
Crack Length= 2.188 in.

<u>Z(in)</u>	<u>K1</u>	<u>K1/Sigma</u>	<u>K2</u>	<u>K2/Sigma</u>	<u>K3</u>	<u>K3/Sigma</u>
0.000	7013	13.73159	182	0.35636	0	0
0.025	7020	13.7453	183	0.358318	43	0.084195
0.050	7042	13.78838	189	0.370066	88	0.172306
0.075	7082	13.8667	198	0.387688	135	0.264333
0.100	7157	14.01355	213	0.417058	187	0.36615
0.125	7273	14.24068	233	0.456219	245	0.479715
0.150	7678	15.03368	275	0.538456	329	0.644189
0.175	7793	15.25885	322	0.630482	418	0.818452
0.200	8368	16.38471	445	0.871319	565	1.106281
0.225	7018	13.74138	446	0.873277	582	1.139568
0.250	7953	15.57213	649	1.270755	793	1.55271
0.275	6460	12.64881	521	1.020128	657	1.286419
0.300	3331	6.522165	586	1.1474	154	0.301535

TABLE II

STRESS INTENSITY FACTORS VERSUS PLATE DEPTH
Plate #25

Alpha= 0 deg.
Sigma= 510.72 psi
Crack Length= 2.625 in.

<u>Z(in)</u>	<u>K1</u>	<u>K1/Sigma</u>	<u>K2</u>	<u>K2/Sigma</u>	<u>K3</u>	<u>K3/Sigma</u>
0.000	12607	24.68476	395	0.773418	0	0
0.025	12618	24.7063	398	0.779292	78	0.152726
0.050	12656	24.7807	407	0.796914	157	0.307409
0.075	12724	24.91385	424	0.830201	242	0.473841
0.100	12854	25.16839	450	0.881109	335	0.655937
0.125	13054	25.55999	487	0.953556	440	0.861529
0.150	13771	26.96389	564	1.104323	593	1.161106
0.175	13958	27.33004	650	1.272713	755	1.478305
0.200	14955	29.28219	876	1.715226	1029	2.014803
0.225	12494	24.4635	869	1.701519	1067	2.089207
0.250	14140	27.6864	1238	2.424029	1485	2.90766
0.275	11464	22.44674	905	1.772008	1254	2.455357
0.300	5783	11.32323	1038	2.032425	279	0.546288

TABLE III

STRESS INTENSITY FACTORS VERSUS PLATE DEPTH
Plate #25

Alpha= 0 deg.
Sigma= 510.72 psi
Crack Length= 2.850 in.

<u>Z(in)</u>	<u>K1</u>	<u>K1/Sigma</u>	<u>K2</u>	<u>K2/Sigma</u>	<u>K3</u>	<u>K3/Sigma</u>
0.000	18094	35.42841	625	1.223763	0	0
0.025	18109	35.45779	629	1.231595	111	0.21734
0.050	18161	35.5596	643	1.259007	226	0.442513
0.075	18256	35.74561	666	1.304041	347	0.679433
0.100	18438	36.10197	703	1.376488	481	0.941808
0.125	18721	36.65609	755	1.478305	632	1.237469
0.150	19740	38.65132	865	1.693687	854	1.672149
0.175	19991	39.14278	985	1.92865	1090	2.134242
0.200	21392	41.88596	1310	2.565006	1486	2.909618
0.225	17822	34.89583	1288	2.52193	1538	3.011435
0.250	20128	39.41103	1811	3.545974	2130	4.170583
0.275	16200	31.71992	1330	2.604167	1778	3.48136
0.300	8240	16.13409	1358	2.658991	414	0.81062

TABLE IV

STRESS INTENSITY FACTORS VERSUS PLATE DEPTH
Plate #20

Alpha= 5 deg.
 Sigma= 510.72 psi
 Crack Length= 2.317 in.

<u>Z(in)</u>	<u>K1</u>	<u>K1/Sigma</u>	<u>K2</u>	<u>K2/Sigma</u>	<u>K3</u>	<u>K3/Sigma</u>
0.000	7510	14.70473	299	0.585448	0	0
0.025	7513	14.7106	299	0.585448	39	0.076363
0.050	7523	14.73018	298	0.58349	80	0.156642
0.075	7539	14.76151	298	0.58349	124	0.242794
0.100	7565	14.81242	298	0.58349	173	0.338737
0.125	7603	14.88683	302	0.591322	230	0.450345
0.150	7663	15.00431	308	0.60307	302	0.591322
0.175	7747	15.16878	346	0.677475	387	0.757754
0.200	7932	15.53102	390	0.763628	538	1.053415
0.225	8075	15.81101	1073	2.100956	555	1.086701
0.250	9155	17.92567	472	0.924185	698	1.366698
0.275	7383	14.45606	1271	2.488643	554	1.084743
0.300	3982	7.796836	940	1.840539	125	0.244753

TABLE V

STRESS INTENSITY FACTORS VERSUS PLATE DEPTH
Plate #20

Alpha= 5 deg.
 Sigma= 510.72 psi
 Crack Length= 2.688 in.

<u>Z(in)</u>	<u>K1</u>	<u>K1/Sigma</u>	<u>K2</u>	<u>K2/Sigma</u>	<u>K3</u>	<u>K3/Sigma</u>
0.000	12667	24.80224	414	0.81062	0	0
0.025	12675	24.8179	414	0.81062	61	0.119439
0.050	12701	24.86881	413	0.808662	124	0.242794
0.075	12748	24.96084	411	0.804746	192	0.37594
0.100	12840	25.14098	410	0.802788	269	0.526707
0.125	12973	25.40139	412	0.806704	357	0.699013
0.150	13535	26.5018	423	0.828242	486	0.951598
0.175	13202	25.84978	440	0.861529	598	1.170896
0.200	13712	26.84837	546	1.069079	866	1.695645
0.225	13976	27.36529	1163	2.277177	964	1.887531
0.250	10460	20.48089	784	1.535088	547	1.071037
0.275	12510	24.49483	1663	3.256187	981	1.920818
0.300	7780	15.2334	2132	4.174499	588	1.151316

TABLE VI

STRESS INTENSITY FACTORS VERSUS PLATE DEPTH
Plate #21

Alpha= 10 deg.
Sigma= 514 psi
Crack Length= 2.657 in.

<u>Z(in)</u>	<u>K1</u>	<u>K1/Sigma</u>	<u>K2</u>	<u>K2/Sigma</u>	<u>K3</u>	<u>K3/Sigma</u>
0.000	11611	22.58949	140	0.272374	0	0
0.025	11617	22.60117	135	0.262646	36	0.070039
0.050	11634	22.63424	114	0.22179	74	0.143969
0.075	11668	22.70039	79	0.153696	107	0.208171
0.100	11720	22.80156	77	0.149805	169	0.328794
0.125	11834	23.02335	49	0.095331	237	0.461089
0.150	11986	23.31907	38	0.07393	285	0.554475
0.175	12849	24.99805	16	0.031128	364	0.708171
0.200	12007	23.35992	277	0.538911	432	0.840467
0.225	11930	23.21012	158	0.307393	623	1.212062
0.250	12408	24.14008	547	1.064202	790	1.536965
0.275	11880	23.11284	217	0.422179	868	1.688716
0.300	7581	14.74903	1397	2.717899	1103	2.145914

TABLE VII

STRESS INTENSITY FACTORS VERSUS PLATE DEPTH

Plate #21

(Assuming a Straight Crack Front)

Alpha= 10 deg.
 Sigma= 514 psi
 Crack Length= 2.657 in.

<u>Z(in)</u>	<u>K1</u>	<u>K1/Sigma</u>	<u>K2</u>	<u>K2/Sigma</u>	<u>K3</u>	<u>K3/Sigma</u>
0.000	11391	22.16148	592	1.151751	0	0
0.025	11393	22.16537	590	1.14786	27	0.052529
0.050	11397	22.17315	585	1.138132	56	0.108949
0.075	11405	22.18872	575	1.118677	86	0.167315
0.100	11416	22.21012	561	1.09144	120	0.233463
0.125	11432	22.24125	542	1.054475	159	0.309339
0.150	11454	22.28405	516	1.003891	205	0.398833
0.175	11487	22.34825	480	0.933852	262	0.509728
0.200	11536	22.44358	431	0.838521	335	0.651751
0.225	11619	22.60506	357	0.694553	427	0.830739
0.250	11733	22.82685	253	0.492218	559	1.087549
0.275	12076	23.49416	21	0.040856	667	1.297665
0.300	11790	22.93774	400	0.77821	869	1.690661

TABLE VIII

STRESS INTENSITY FACTORS VERSUS PLATE DEPTH
Plate #21

Alpha= 10 deg.
Sigma= 514 psi
Crack Length= 2.969 in.

Z(in)	K1	K1/Sigma	K2	K2/Sigma	K3	K3/Sigma
0.000	18969	36.90467	162	0.315175	0	0
0.025	18975	36.91634	172	0.33463	58	0.11284
0.050	18997	36.95914	211	0.410506	118	0.229572
0.075	19037	37.03696	279	0.542802	168	0.326848
0.100	19105	37.16926	563	1.095331	268	0.521401
0.125	19209	37.3716	390	0.758755	353	0.68677
0.150	19417	37.77626	776	1.509728	501	0.974708
0.175	19725	38.37549	57	0.110895	645	1.254864
0.200	21497	41.82296	262	0.509728	752	1.463035
0.225	20241	39.37938	603	1.173152	925	1.799611
0.250	19099	37.15759	201	0.391051	1119	2.177043
0.275	18233	35.47276	566	1.101167	1503	2.924125
0.300	12244	23.82101	3245	6.31323	1815	3.531128

TABLE IX

STRESS INTENSITY FACTORS VERSUS PLATE DEPTH
Plate #22

Alpha= 15 deg.
 Sigma= 518 psi
 Crack Length= 2.281 in.

<u>Z(in)</u>	<u>K1</u>	<u>K1/Sigma</u>	<u>K2</u>	<u>K2/Sigma</u>	<u>K3</u>	<u>K3/Sigma</u>
0.000	6634	12.80695	436	0.841699	0	0
0.025	6623	12.78571	340	0.656371	242	0.467181
0.050	6630	12.79923	166	0.320463	244	0.471042
0.075	6652	12.8417	268	0.517375	257	0.496139
0.100	6690	12.91506	465	0.897683	246	0.474903
0.125	6705	12.94402	642	1.239382	162	0.312741
0.150	6763	13.05598	3	0.005792	164	0.316602
0.175	6899	13.31853	404	0.779923	159	0.30695
0.200	7101	13.70849	60	0.11583	161	0.310811
0.225	8071	15.58108	319	0.61583	191	0.368726
0.250	7005	13.52317	721	1.391892	10	0.019305
0.275	6235	12.03668	1154	2.227799	141	0.272201
0.300	4463	8.61583	3154	6.088803	374	0.722008

TABLE X

STRESS INTENSITY FACTORS VERSUS PLATE DEPTH
Plate #22

Alpha= 15 deg.
Sigma= 518 psi
Crack Length= 2.594 in.

<u>Z(in)</u>	<u>K1</u>	<u>K1/Sigma</u>	<u>K2</u>	<u>K2/Sigma</u>	<u>K3</u>	<u>K3/Sigma</u>
0.000	9894	19.10039	832	1.606178	0	0
0.025	9885	19.08301	602	1.162162	234	0.451737
0.050	9899	19.11004	600	1.158301	238	0.459459
0.075	9929	19.16795	740	1.428571	220	0.42471
0.100	9966	19.23938	857	1.65444	169	0.326255
0.125	10009	19.32239	706	1.362934	120	0.23166
0.150	10100	19.49807	557	1.07529	119	0.22973
0.175	10275	19.83591	812	1.567568	78	0.150579
0.200	10507	20.28378	590	1.138996	38	0.073359
0.225	11996	23.1583	315	0.608108	40	0.07722
0.250	10351	19.98263	582	1.123552	186	0.359073
0.275	9363	18.07529	1388	2.679537	488	0.942085
0.300	6829	13.1834	4826	9.316602	619	1.194981

TABLE XI

STRESS INTENSITY FACTORS VERSUS PLATE DEPTH
Plate #17

Alpha= 20 deg.
Sigma= 4000 psi
Crack Length= 2.309 in.

<u>Z(in)</u>	<u>K1</u>	<u>K1/Sigma</u>	<u>K2</u>	<u>K2/Sigma</u>	<u>K3</u>	<u>K3/Sigma</u>
0.000	36654	9.1635	290	0.0725	0	0.0000
0.025	36622	9.1555	203	0.05075	1335	0.3338
0.050	36710	9.1775	759	0.18975	1292	0.3230
0.075	36841	9.2103	413	0.10325	1208	0.3020
0.100	37059	9.2648	729	0.18225	1140	0.2850
0.125	37333	9.3333	198	0.0495	1029	0.2573
0.150	37700	9.4250	196	0.049	784	0.1960
0.175	38230	9.5575	1	0.00025	600	0.1500
0.200	39160	9.7900	14	0.0035	338	0.0845
0.225	40329	10.0823	1207	0.30175	17	0.0043
0.250	48232	12.0580	7043	1.76075	111	0.0278
0.275	44668	11.1670	12522	3.1305	1504	0.3760
0.300	20943	5.2358	16502	4.1255	4196	1.0490

TABLE XII

STRESS INTENSITY FACTORS VERSUS PLATE DEPTH

Plate #17

(Assuming a Straight Crack Front)

Alpha= 20 deg.

Sigma= 4000 psi

Crack Length= 2.309 in.

<u>Z(in)</u>	<u>K1</u>	<u>K1/Sigma</u>	<u>K2</u>	<u>K2/Sigma</u>	<u>K3</u>	<u>K3/Sigma</u>
0.000	37395	9.3488	5940	1.485	0	0.0000
0.025	37404	9.3510	5934	1.4835	40	0.0100
0.050	37430	9.3575	5919	1.47975	82	0.0205
0.075	37475	9.3688	5892	1.473	130	0.0325
0.100	37543	9.3858	5852	1.463	188	0.0470
0.125	37640	9.4100	5799	1.44975	260	0.0650
0.150	37776	9.4440	5730	1.4325	352	0.0880
0.175	37969	9.4923	5644	1.411	474	0.1185
0.200	38248	9.5620	5540	1.385	641	0.1603
0.225	38691	9.6728	5408	1.352	860	0.2150
0.250	39358	9.8395	5311	1.32775	1192	0.2980
0.275	40837	10.2093	4946	1.2365	1244	0.3110
0.300	39952	9.9880	4205	1.05125	1412	0.3530

TABLE XIII

STRESS INTENSITY FACTORS VERSUS PLATE DEPTH
Plate #17

Alpha= 20 deg.
Sigma= 519 psi
Crack Length= 2.625 in.

<u>Z(in)</u>	<u>K1</u>	<u>K1/Sigma</u>	<u>K2</u>	<u>K2/Sigma</u>	<u>K3</u>	<u>K3/Sigma</u>
0.000	9651	18.5954	744	1.433526	0	0.0000
0.025	9622	18.5395	697	1.342967	481	0.9268
0.050	9630	18.5549	399	0.768786	453	0.8728
0.075	9666	18.6243	345	0.66474	465	0.8960
0.100	9712	18.7129	523	1.007707	433	0.8343
0.125	9770	18.8247	368	0.709056	385	0.7418
0.150	9877	19.0308	231	0.445087	383	0.7380
0.175	10072	19.4066	479	0.922929	362	0.6975
0.200	10205	19.6628	618	1.190751	245	0.4721
0.225	11413	21.9904	584	1.125241	228	0.4393
0.250	10455	20.1445	2240	4.315992	31	0.0597
0.275	11318	21.8073	3623	6.980732	135	0.2601
0.300	4816	9.2794	2933	5.651252	740	1.4258

TABLE XIV

STRESS INTENSITY FACTORS VERSUS PLATE DEPTH
Plate #17

Alpha= 20 deg.
 Sigma= 519 psi
 Crack Length= 2.813 in.

<u>Z(in)</u>	<u>K1</u>	<u>K1/Sigma</u>	<u>K2</u>	<u>K2/Sigma</u>	<u>K3</u>	<u>K3/Sigma</u>
0.000	12516	24.1156	970	1.868979	0	0.0000
0.025	12508	24.1002	685	1.319846	299	0.5761
0.050	12533	24.1484	812	1.564547	282	0.5434
0.075	12567	24.2139	806	1.552987	230	0.4432
0.100	12621	24.3179	790	1.522158	193	0.3719
0.125	12697	24.4644	857	1.651252	132	0.2543
0.150	12790	24.6435	633	1.219653	64	0.1233
0.175	13070	25.1830	408	0.786127	70	0.1349
0.200	13229	25.4894	1158	2.231214	65	0.1252
0.225	14998	28.8979	564	1.086705	119	0.2293
0.250	12456	24.0000	849	1.635838	288	0.5549
0.275	13827	26.6416	5373	10.3526	950	1.8304
0.300	6726	12.9595	3578	6.894027	918	1.7688

TABLE XV

STRESS INTENSITY FACTORS VERSUS PLATE DEPTH
Plate #23

Alpha= 25 deg.
Sigma= 519 psi
Crack Length= 2.938 in.

<u>Z(in)</u>	<u>K1</u>	<u>K1/Sigma</u>	<u>K2</u>	<u>K2/Sigma</u>	<u>K3</u>	<u>K3/Sigma</u>
0.000	13748	26.4894	322	0.620424	0	0.0000
0.025	13763	26.5183	372	0.716763	13	0.0250
0.050	13817	26.6224	740	1.425819	65	0.1252
0.075	13879	26.7418	832	1.603083	222	0.4277
0.100	14014	27.0019	16	0.030829	256	0.4933
0.125	14489	27.9171	398	0.766859	210	0.4046
0.150	14428	27.7996	766	1.475915	354	0.6821
0.175	15217	29.3198	160	0.308285	441	0.8497
0.200	15549	29.9595	133	0.256262	403	0.7765
0.225	16871	32.5067	628	1.210019	514	0.9904
0.250	14279	27.5125	2070	3.988439	882	1.6994
0.275	10713	20.6416	4481	8.633911	1005	1.9364
0.300	4937	9.5125	5634	10.85549	1539	2.9653

TABLE XVI

STRESS INTENSITY FACTORS VERSUS PLATE DEPTH
Plate #23

Alpha= 25 deg.
 Sigma= 519 psi
 Crack Length= 3.031 in.

<u>Z(in)</u>	<u>K1</u>	<u>K1/Sigma</u>	<u>K2</u>	<u>K2/Sigma</u>	<u>K3</u>	<u>K3/Sigma</u>
0.000	14435	27.8131	1304	2.512524	0	0.0000
0.025	14412	27.7688	449	0.865125	515	0.9923
0.050	14443	27.8285	707	1.362235	507	0.9769
0.075	14482	27.9037	268	0.516378	544	1.0482
0.100	14556	28.0462	1482	2.855491	441	0.8497
0.125	14666	28.2582	281	0.541426	437	0.8420
0.150	14761	28.4412	2016	3.884393	316	0.6089
0.175	14978	28.8593	80	0.154143	349	0.6724
0.200	15259	29.4008	1193	2.298651	435	0.8382
0.225	16627	32.0366	76	0.146435	335	0.6455
0.250	16159	31.1349	4419	8.514451	140	0.2697
0.275	9453	18.2139	3268	6.296724	273	0.5260
0.300	8303	15.9981	7480	14.41233	822	1.5838

TABLE XVII

STRESS INTENSITY FACTORS VERSUS PLATE DEPTH
Plate #24

Alpha= 30 deg.
Sigma= 519.21 psi
Crack Length= 2.750 in.

Z(in)	K1	K1/Sigma	K2	K2/Sigma	K3	K3/Sigma
0.000	8090	15.58136	520	1.001522	0	0
0.025	8086	15.57366	343	0.660619	204	0.392905
0.050	8099	15.5987	526	1.013078	186	0.358237
0.075	8117	15.63337	429	0.826255	153	0.294678
0.100	8143	15.68344	487	0.937963	125	0.24075
0.125	8188	15.77011	360	0.693361	102	0.196452
0.150	8249	15.8876	454	0.874405	71	0.136746
0.175	8358	16.09753	311	0.598987	38	0.073188
0.200	8503	16.3768	206	0.396757	14	0.026964
0.225	9303	17.91761	464	0.893665	106	0.204156
0.250	9599	18.4877	1737	3.345467	170	0.327421
0.275	7416	14.28324	3178	6.120837	49	0.094374
0.300	4480	8.628493	5328	10.26174	287	0.552763

TABLE XVIII

STRESS INTENSITY FACTORS VERSUS PLATE DEPTH

Plate #24

(Assuming a Straight Crack Front)

Alpha= 30 deg.
 Sigma= 519.21 psi
 Crack Length= 2.750 in.

<u>Z(in)</u>	<u>K1</u>	<u>K1/Sigma</u>	<u>K2</u>	<u>K2/Sigma</u>	<u>K3</u>	<u>K3/Sigma</u>
0.000	7788	14.99971	1749	3.368579	0	0
0.025	7790	15.00356	1748	3.366653	0	0
0.050	7795	15.01319	1746	3.362801	0	0
0.075	7803	15.0286	1743	3.357023	1	0.001926
0.100	7815	15.05171	1738	3.347393	3	0.005778
0.125	7833	15.08638	1731	3.333911	8	0.015408
0.150	7858	15.13453	1722	3.316577	16	0.030816
0.175	7896	15.20772	1712	3.297317	28	0.053928
0.200	7950	15.31172	1700	3.274205	47	0.090522
0.225	8037	15.47929	1687	3.249167	70	0.13482
0.250	8168	15.73159	1688	3.251093	111	0.213786
0.275	8447	16.26895	1668	3.212573	58	0.111708
0.300	8241	15.87219	1546	2.977601	41	0.078966

TABLE XIX

STRESS INTENSITY FACTORS VERSUS PLATE DEPTH
Plate #24

Alpha= 30 deg.
 Sigma= 519.21 psi
 Crack Length= 3.250 in.

<u>Z(in)</u>	<u>K1</u>	<u>K1/Sigma</u>	<u>K2</u>	<u>K2/Sigma</u>	<u>K3</u>	<u>K3/Sigma</u>
0.000	16420	31.62497	2953	5.687487	0	0
0.025	16348	31.4863	2049	3.94638	579	1.115156
0.050	16424	31.63267	2623	5.051906	568	1.09397
0.075	16468	31.71742	2789	5.371622	414	0.797365
0.100	16476	31.73282	2604	5.015312	276	0.531577
0.125	16515	31.80794	2129	4.10046	191	0.367867
0.150	16650	32.06795	1858	3.578514	129	0.248454
0.175	16777	32.31255	1537	2.960267	13	0.025038
0.200	17342	33.40074	37	0.071262	59	0.113634
0.225	19672	37.88833	522	1.005374	242	0.466093
0.250	19009	36.61139	2953	5.687487	166	0.319716
0.275	17433	33.57601	6620	12.75014	14	0.026964
0.300	5547	10.68354	8621	16.60407	1001	1.927929

TABLE XX

STRESS INTENSITY FACTORS VERSUS PLATE DEPTH
Plate #26

Alpha= 35 deg.
Sigma= 515.73 psi
Crack Length= 2.594 in.

<u>Z(in)</u>	<u>K1</u>	<u>K1/Sigma</u>	<u>K2</u>	<u>K2/Sigma</u>	<u>K3</u>	<u>K3/Sigma</u>
0.000	6318	12.2506	558	1.081961	0	0
0.025	6280	12.17691	656	1.271983	489	0.948171
0.050	6390	12.3902	363	0.703857	468	0.907452
0.075	6307	12.22927	279	0.540981	457	0.886123
0.100	6352	12.31652	283	0.548737	454	0.880306
0.125	6354	12.3204	433	0.839587	395	0.765905
0.150	6524	12.65003	193	0.374227	406	0.787234
0.175	7160	13.88323	334	0.647626	506	0.981134
0.200	7367	14.28461	1312	2.543967	525	1.017975
0.225	6882	13.34419	1817	3.523161	422	0.818258
0.250	5058	9.807457	1888	3.66083	205	0.397495
0.275	5515	10.69358	3862	7.488414	114	0.221046
0.300	2290	4.440308	2754	5.340003	507	0.983073

TABLE XXI

STRESS INTENSITY FACTORS VERSUS PLATE DEPTH
Plate #26

Alpha= 35 deg.
Sigma= 515.73 psi
Crack Length= 3.063 in.

Z(in)	K1	K1/Sigma	K2	K2/Sigma	K3	K3/Sigma
0.000	10661	20.67167	1253	2.429566	0	0
0.025	10662	20.67361	1042	2.020437	256	0.496384
0.050	10709	20.76474	1525	2.956974	167	0.323813
0.075	10746	20.83648	1125	2.181374	70	0.13573
0.100	10823	20.98579	1291	2.503248	16	0.031024
0.125	10950	21.23204	779	1.51048	76	0.147364
0.150	11353	22.01346	793	1.537626	108	0.209412
0.175	11568	22.43034	385	0.746515	171	0.331569
0.200	12800	24.81919	574	1.112985	65	0.126035
0.225	12342	23.93113	2376	4.607062	267	0.517713
0.250	7784	15.09317	1715	3.325383	530	1.02767
0.275	10442	20.24703	6303	12.22151	221	0.428519
0.300	2013	3.903205	4330	8.395866	917	1.778062

TABLE XXII

STRESS INTENSITY FACTORS VERSUS PLATE DEPTH
Plate #27

Alpha= 40 deg.
 Sigma= 516.26 psi
 Crack Length= 3.125 in.

Z(in)	K1	K1/Sigma	K2	K2/Sigma	K3	K3/Sigma
0.000	9766	18.91682	580	1.123465	0	0
0.025	9943	19.25968	390	0.755433	246	0.476504
0.050	9826	19.03305	744	1.441134	199	0.385465
0.075	10224	19.80397	539	1.044048	180	0.348662
0.100	10006	19.38171	1095	2.121024	34	0.065858
0.125	9837	19.05435	490	0.949134	84	0.162709
0.150	10021	19.41076	157	0.30411	39	0.075543
0.175	9101	17.62871	973	1.884709	205	0.397087
0.200	10060	19.48631	1329	2.574284	72	0.139465
0.225	10316	19.98218	3154	6.109325	149	0.288614
0.250	7659	14.83555	3289	6.370821	249	0.482315
0.275	6897	13.35955	5557	10.76396	211	0.408709
0.300	1890	3.660946	3741	7.246349	740	1.433386

TABLE XXIII

STRESS INTENSITY FACTORS VERSUS PLATE DEPTH

Plate #27

(Assuming a Straight Crack Front)

Alpha= 40 deg.

Sigma= 516.26 psi

Crack Length= 3.125 in.

Z(in)	K1	K1/Sigma	K2	K2/Sigma	K3	K3/Sigma
0.000	7113	13.77794	2224	4.307907	0	0
0.025	7115	13.78182	2223	4.30597	9	0.017433
0.050	7119	13.78956	2222	4.304033	19	0.036803
0.075	7127	13.80506	2220	4.300159	28	0.054236
0.100	7139	13.8283	2218	4.296285	36	0.069732
0.125	7157	13.86317	2215	4.290474	43	0.083291
0.150	7181	13.90966	2210	4.280789	49	0.094913
0.175	7216	13.97745	2205	4.271104	52	0.100724
0.200	7268	14.07818	2200	4.261419	53	0.102661
0.225	7350	14.23701	2192	4.245923	55	0.106535
0.250	7472	14.47333	2191	4.243986	50	0.09685
0.275	7751	15.01375	2150	4.164568	101	0.195638
0.300	7601	14.7232	2232	4.323403	257	0.497811

TABLE XXIV

STRESS INTENSITY FACTORS VERSUS PLATE DEPTH
Plate #27

Alpha= 40 deg.
 Sigma= 516.26 psi
 Crack Length= 3.347 in.

<u>Z(in)</u>	<u>K1</u>	<u>K1/Sigma</u>	<u>K2</u>	<u>K2/Sigma</u>	<u>K3</u>	<u>K3/Sigma</u>
0.000	19623	38.00992	1428	2.766048	0	0
0.025	19990	38.7208	1051	2.035796	368	0.712819
0.050	19775	38.30434	1748	3.385891	143	0.276992
0.075	20611	39.92368	1338	2.591717	58	0.112346
0.100	20229	39.18374	2456	4.757293	531	1.028552
0.125	19999	38.73823	803	1.555418	932	1.805292
0.150	20540	39.78615	135	0.261496	904	1.751056
0.175	18874	36.5591	1985	3.844962	1200	2.32441
0.200	21078	40.82826	2922	5.659939	864	1.673575
0.225	21937	42.49216	7371	14.27769	962	1.863402
0.250	16801	32.54368	8435	16.33867	1201	2.326347
0.275	15930	30.85655	15631	30.27738	840	1.627087
0.300	4957	9.601751	7156	13.86123	1328	2.572347

TABLE XXV

STRESS INTENSITY FACTORS VERSUS PLATE DEPTH

Plate #28

(12 Element Layers)

Beta= 20 deg.
 Alpha= 0 deg.
 Sigma= 258.4 psi
 Crack Length= 2.344 in.

<u>Z(in)</u>	<u>K1</u>	<u>K1/Sigma</u>	<u>K2</u>	<u>K2/Sigma</u>	<u>K3</u>	<u>K3/Sigma</u>
0.000	3	0.01161	274	1.060372	86	0.332817
0.050	225	0.870743	22	0.085139	402	1.555728
0.100	916	3.544892	128	0.495356	523	2.023994
0.150	2310	8.939628	378	1.462848	1257	4.864551
0.200	2841	10.99458	644	2.49226	1441	5.576625
0.250	3112	12.04334	725	2.805728	1561	6.041022
0.300	3092	11.96594	831	3.215944	1512	5.851393
0.350	3215	12.44195	822	3.181115	1572	6.083591
0.400	3165	12.24845	853	3.301084	1492	5.773994
0.450	3245	12.55805	920	3.560372	1469	5.684985
0.500	3367	13.03019	849	3.285604	1479	5.723684
0.550	3928	15.20124	1524	5.897833	1677	6.489938
0.600	1902	7.360681	1191	4.609133	491	1.900155

TABLE XXVI

STRESS INTENSITY FACTORS VERSUS PLATE DEPTH

Plate #28

(22 Element Layers)

Beta= 20 deg.

Alpha= 0 deg.

Sigma= 258.4 psi

Crack Length= 2.344 in.

<u>Z(in)</u>	<u>K1</u>	<u>K1/Sigma</u>	<u>K2</u>	<u>K2/Sigma</u>	<u>K3</u>	<u>K3/Sigma</u>
0.000	1262	4.883901	1124	4.349845	181	0.700464
0.050	2404	9.303406	122	0.472136	1632	6.315789
0.100	2679	10.36765	498	1.927245	1404	5.433437
0.125	3313	12.82121	660	2.55418	1791	6.931115
0.150	3029	11.72214	642	2.48452	1575	6.095201
0.175	3131	12.11687	696	2.693498	1605	6.2113
0.200	3038	11.75697	823	3.184985	1518	5.874613
0.225	3037	11.7531	588	2.275542	1544	5.975232
0.250	3323	12.85991	831	3.215944	1650	6.385449
0.275	3172	12.27554	802	3.103715	1550	5.998452
0.300	3214	12.43808	862	3.335913	1550	5.998452
0.325	3469	13.42492	914	3.537152	1689	6.536378
0.350	3340	12.9257	849	3.285604	1598	6.184211
0.375	3346	12.94892	895	3.463622	1564	6.052632
0.400	3362	13.01084	913	3.533282	1549	5.994582
0.425	3394	13.13467	894	3.459752	1540	5.959752
0.450	3442	13.32043	955	3.69582	1509	5.839783
0.475	3515	13.60294	1020	3.947368	1504	5.820433
0.500	3611	13.97446	885	3.424923	1534	5.936533
0.525	3844	14.87616	1020	3.947368	1515	5.863003
0.550	4179	16.1726	1240	4.798762	1522	5.890093
0.575	4788	18.52941	1873	7.248452	1412	5.464396
0.600	3065	11.86146	1479	5.723684	401	1.551858

**APPENDIX C--PLOTS OF PLATE
STRESS INTENSITY FACTORS**

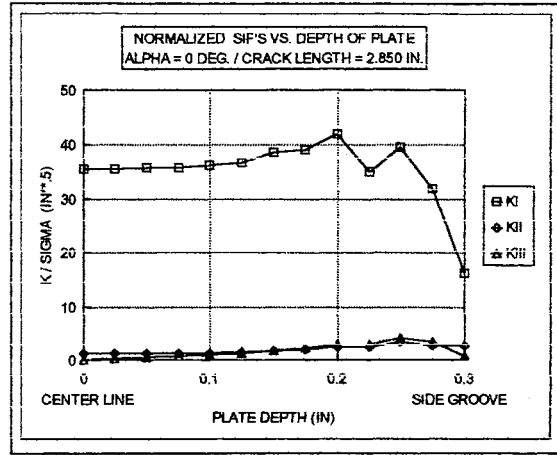
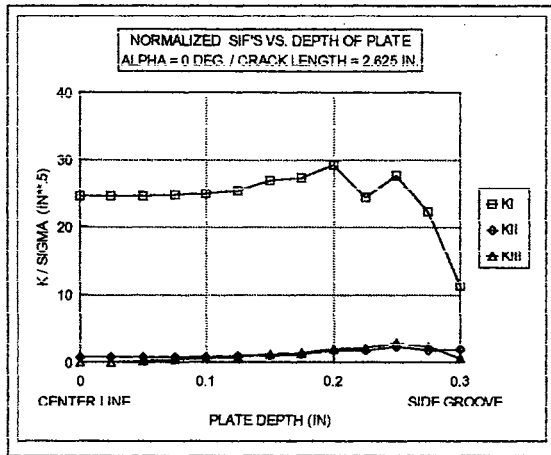


Figure 63. Normalized SIF's vs. Plate Depth for Alpha=0 Degrees

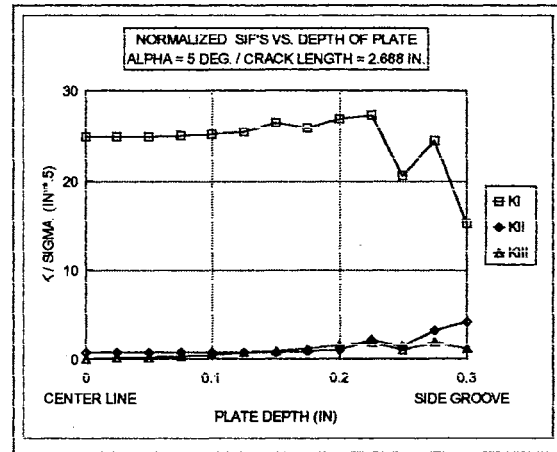
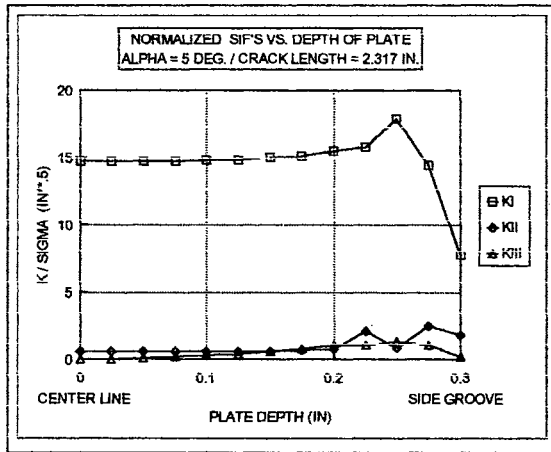


Figure 64. Normalized SIF's vs. Plate Depth for Alpha=5 Degrees

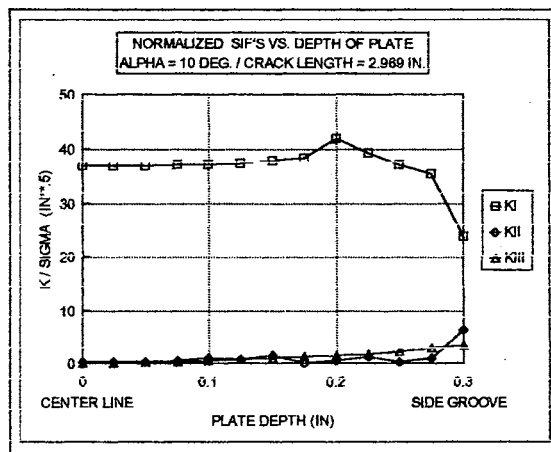


Figure 65. Normalized SIF's vs. Plate Depth for Alpha=10 Degrees

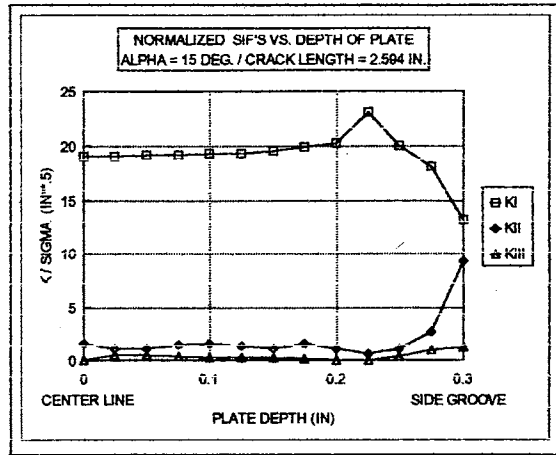
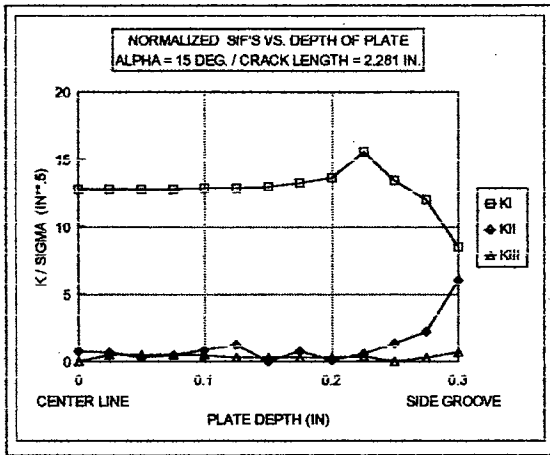


Figure 66. Normalized SIF's vs. Plate Depth for Alpha=15 Degrees

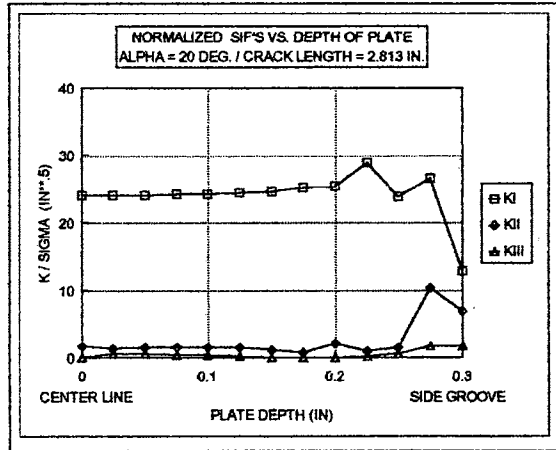
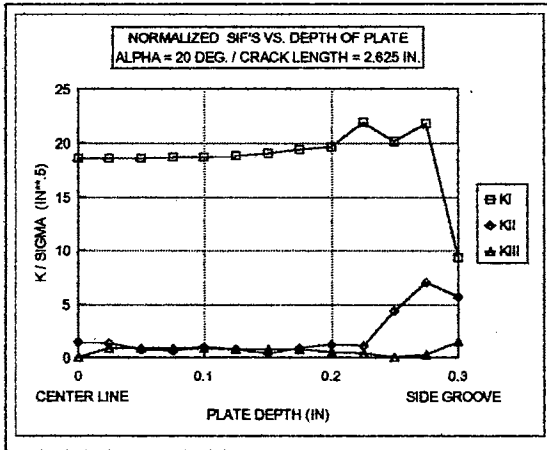


Figure 67. Normalized SIF's vs. Plate Depth for Alpha=20 Degrees

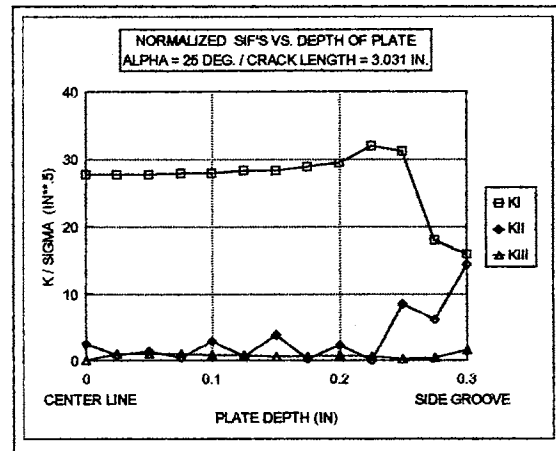
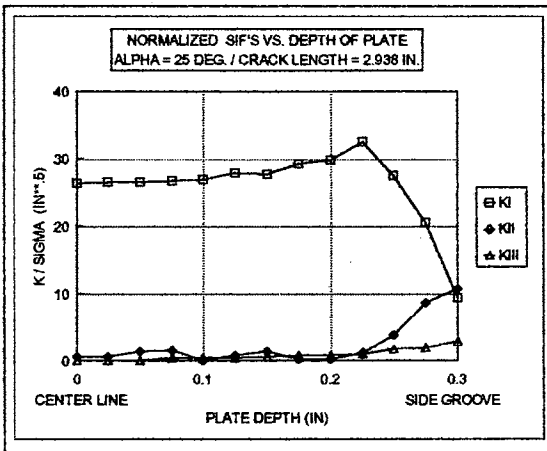


Figure 68. Normalized SIF's vs. Plate Depth for Alpha=25 Degrees

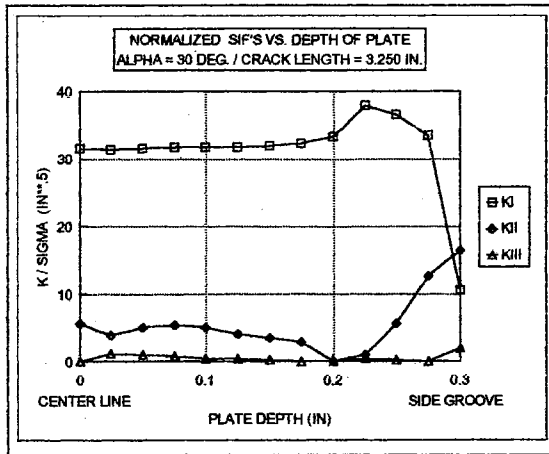


Figure 69. Normalized SIF's vs. Plate Depth for Alpha=30 Degrees

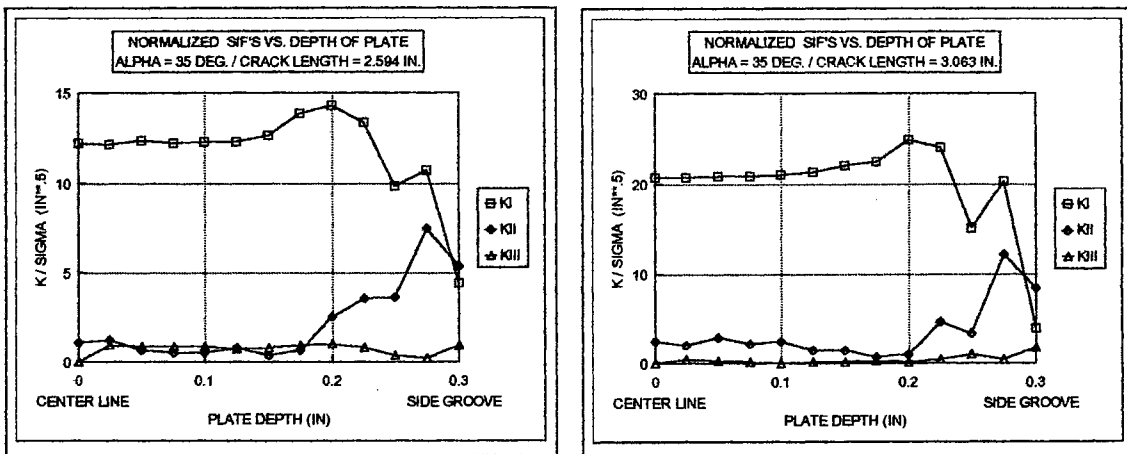


Figure 70. Normalized SIF's vs. Plate Depth for Alpha=35 Degrees

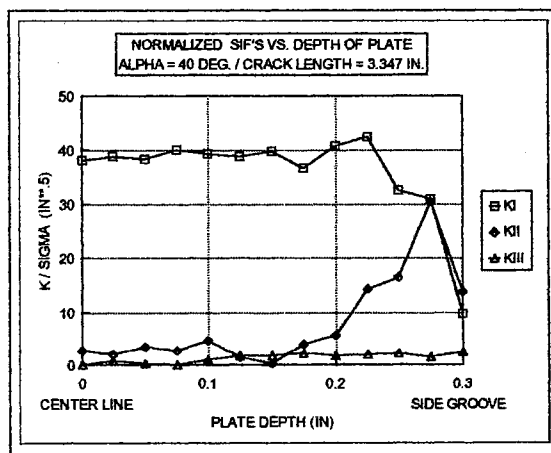


Figure 71. Normalized SIF's vs. Plate Depth for Alpha=40 Degrees

APPENDIX D—PROGRAMS FOR USE WITH ANSYS

: This Macro written by - Michael Magill, OSU
: 8/4/94
:

: **MACRO CURVECRK TO CONVERT 2-D SOLID ELEMENTS TO 3-D SOLID ELEMENTS AT**
: **A CRACK TIP AND MAKE A CURVED CRACK FRONT. THIS MACRO MUST BE RUN**
: **IN /PREP7!!**
:

: **NOTE:**
: **IT IS EXPECTED THAT THE USER READ AND UNDERSTAND THE**
: **FUNCTIONALITY OF THIS MACRO TO AVOID UNDESIRE RESULTS.**
: **THIS MACRO IS ESPECIALLY FOR EXTRUDING CRACK TIP ELEMENTS INTO**
: **3-D ELEMENTS TO MAKE A WARPED CRACK FRONT.**
:

: **USAGE:**
: ***USE,CURVECRK**
:

: *****
:

: **INPUT VALUES**
:

: *****
:

EL_TYPE=1 * ELEMENT TYPE TO BE CONVERTED.
NEW_STF=95 * NEW STIFFNESS NUMBER.
K_TRI=0 * 0 - 4 NODE ELEMENT TYPE BEING CONVERTED.
: * 1 - 6 NODE TRIANGULAR ELEMENT TYPE
: * (STIF 2,35,ETC.) BEING CONVERTED.
X_CRK=2.6395 * GLOBAL X-COORD. OF CRACK TIP
Y_CRK=10.5817 * GLOBAL Y-COORD. OF CRACK TIP
: * THE X,Y LOCATION OF THE CRACK TIP IS THE
: * LOCATION ON THE 2-D ELEMENTS.)
N_POINTS=13 * NUMBER OF POINTS ALONG CRACK FRONT
ALPHA=5 * ALPHA ANGLE OF CRACK OPENING
QPRAD=.0025 * RADIUS TO THE QUARTER-POINT NODES FROM CRACK TIP
*DIM,CRK_PNT,,N_POINTS,3 * DEFINES CRK_PNT ARRAY - DO NOT CHANGE!!
:

: * COORDINATES OF POINTS ALONG CRACK FRONT INCLUDING STARTING POINT
: * USE THE LOCAL COORDINATE SYSTEM THAT HAS ITS ORIGIN AT
: * (X_CRK,Y_CRK)
:

: * VERY IMPORTANT THE CRK_PNT VALUES MUST BE ENTERED BASED ON THE
: * ALPHA ANGLE BEING ZERO!! THEREFORE MEASURE CRACK FRONT POINTS WITH
: * THE SIDE GROOVE ON THE HORIZONTAL!!
:

CRK_PNT(1,1)=0 \$CRK_PNT(1,2)=0 CRK_PNT(1,3)=0
CRK_PNT(2,1)=0.000 \$CRK_PNT(2,2)=0.000 \$CRK_PNT(2,3)=0.025
CRK_PNT(3,1)=0.000 \$CRK_PNT(3,2)=0.000 \$CRK_PNT(3,3)=0.050

```

CRK_PNT(4,1)=0.000   $CRK_PNT(4,2)=0.000   $CRK_PNT(4,3)=0.075
CRK_PNT(5,1)=0.000   $CRK_PNT(5,2)=0.000   $CRK_PNT(5,3)=0.100
CRK_PNT(6,1)=0.000   $CRK_PNT(6,2)=0.000   $CRK_PNT(6,3)=0.125
CRK_PNT(7,1)=0.000   $CRK_PNT(7,2)=0.000   $CRK_PNT(7,3)=0.150
CRK_PNT(8,1)=0.002   $CRK_PNT(8,2)=0.000   $CRK_PNT(8,3)=0.175
CRK_PNT(9,1)=0.004   $CRK_PNT(9,2)=0.000   $CRK_PNT(9,3)=0.200
CRK_PNT(10,1)=0.008  $CRK_PNT(10,2)=0.000  $CRK_PNT(10,3)=0.225
CRK_PNT(11,1)=0.020  $CRK_PNT(11,2)=-0.010 $CRK_PNT(11,3)=-0.250
CRK_PNT(12,1)=0.025  $CRK_PNT(12,2)=-0.018 $CRK_PNT(12,3)=-0.275
CRK_PNT(13,1)=0.036  $CRK_PNT(13,2)=-0.022 $CRK_PNT(13,3)=-0.300

```

```

*****

```

```

END OF INPUT

```

```

*****

```

```

REMARKS:
THE CURRENT ELEMENT MATERIAL, REAL, AND ESYS ARE MAINTAINED.
IF THE ORIGINAL ELEMENT IS A MIDSIDE NODE ELEMENT, A 3-D MIDSIDE
NODE ELEMENT CAN BE CREATED. IF THE ORIGINAL ELEMENT IS MIDSIDE
NODE ELEMENT, A 3-D REGULAR ELEMENT CAN BE CREATED AS WELL.

```

```

NUMCMP,ELEM
NUMCMP,NODE
*GET,NMIN,NDMN      * CHECK FOR VALID NODE INCREMENT
*GET,NMAX,NDMX
*IF,NMIN+10000,GT,NMAX,GEN
/COM
/COM  NODE GENERATION NOT PERFORMED
/COM  NODAL OFFSET MAY REDEFINE NODES
/COM
*GO,:END
:GEN
MODM,DETA          * DETACH SOLID MODEL
ESEL,TYPE,EL_TYPE * SELECT ELEMENTS OF SPECIFIED TYPE
NSLE
*****
THIS IS WHERE THE CURVED CRACK FRONT IS DEFINED.
*****
LOCAL,20,0,X_CRK,Y_CRK,0,ALPHA,0,0,1
*DO,I,2,N_POINTS
NSLE
CSYS,20
DSYS,20

```

```

NGEN,2,10000*(I-1),ALL,,,CRK_PNT(I,1),CRK_PNT(I,2),CRK_PNT(I,3)
*ENDDO
: *****
:
:
:   END OF CRACK FRONT DEFINITION
:
: *****
:
CSYS,0
DSYS,0
NSEL,ALL
*GET,IEMX,ELMX           * GET MAX. ELEMENT NUMBER OF SELECTED SET
ET,EL_TYPE,NEW_STF      * REDEFINE ELEMENT TYPE
TYPE,EL_TYPE            * RESET TYPE FOR NEW ELEMENTS
IEL=1
LOCAL,18,1,X_CRK,Y_CRK,0,0,0,1
CSYS,18
DSYS,18
:TOP
*GET,IETY,TYPE,IEL       * GET ELEMENT TYPE FOR THIS ELEMENT
*IF,IETY,NE,EL_TYPE,:SK2 * CHECK TYPE
*GET,IERL,REAL,IEL       * GET MAT, REAL, AND ESYS
*GET,IEMT,MAT,IEL
*GET,IESY,ESYS,IEL
*GET,I1,EN1,IEL          * GET CORNER NODES OF ELEMENT
*GET,I2,EN2,IEL
*GET,I3,EN3,IEL
*GET,I4,EN4,IEL
*IF,K_TRI,NE,1,:NT2      * TRIANGULAR ELEMENT
I4=I3
:NT2
*IF,NX(I1),NE,0,:XEB1    * CHANGES ELEMENT NODES FOR CRACK TIP
I5=I1
I1=I2
I2=I3
I3=I5
I4=I5
:XEB1
*IF,NX(I2),NE,0,:XEB2
I5=I2
I2=I1
I1=I3
I3=I5
I4=I5
:XEB2
I1P=I1+10000             * ADD SPECIFIED NODE INCREMENT
I2P=I2+10000
I3P=I3+10000
I4P=I4+10000
MAT,IEMT                  * RESET MAT, REAL, AND ESYS
REAL,IERL
ESYS,IESY
EN,IEL,I1,I2,I3,I4,I1P,I2P,I3P,I4P * REDEFINE ELEMENT

```

```

:SK2
IEL=IEL+1                * INCREMENT LOOP COUNTER
*IF,IEL,LE,IEMX,:TOP    * LOOP BACK OR EXIT
CSYS,0
DSYS,0
:
:           PUTS MIDSIDE NODES IN ELEMENTS
:
EMDD=1
*IF,NEW_STF,GE,82,:NEXT
EMDD=0
:NEXT
*IF,EMDD,EQ,0,:NOM
EMID
:NOM
*IF,N_POINTS-1,EQ,1,:SK3    * THIS SECTION GENERATES THE EXTRA LAYERS IF
ESEL,TYPE,EL_TYPE          * REQUESTED
EGEN,N_POINTS-1,10000,ALL
:SK3
EALL
NELEM                    * THIS SECTION CLEARS THE EXTRA NODES FROM THE
NINV                    * NGEN OPERATION
:
:   ****WARNING: ALL NODES NOT ATTACHED TO AN ELEMENT WILL BE DELETED
:   AT THIS POINT
NDEL,ALL
NSEL,ALL
:   *****
:
:   MERGE NODES AT SAME LOCATION
:
:   *****
:   *****
:
:   CURVED CRACK FRONT DEFINED.
:
:   *****
CSYS,0
DSYS,0
*DO,I,2,N_POINTS
CSYS,20
DSYS,20
CLOCAL,19,1,CRK_PNT(I,1),CRK_PNT(I,2),CRK_PNT(I,3),0,0,0
CSYS,19
DSYS,19
:   *****
:
:   MERGE NODES
:
:   *****
NSEL,ALL
NSEL,S,LOC,Z,0,0
NSEL,R,LOC,Y,-20,175
NSEL,R,LOC,X,QPRAD,10

```

```
ESLN,S,0
NSLE,S
NUMMRG,NODE
ESEL,ALL
NSEL,ALL
NSEL,S,LOC,Z,0,0
NSEL,R,LOC,Y,185,380
NSEL,R,LOC,X,QPRAD,10
ESLN,S,0
NSLE,S
NUMMRG,NODE
CSYS,0
DSYS,0
ESEL,ALL
NSEL,ALL
*ENDDO
ESEL,ALL
NSEL,ALL
NUMCMP,ELEM
NUMCMP,NODE
/COM
/COM CURVECRK CONVERSION COMPLETE.
:END
```

```

:   This Macro written by - Michael Magill, OSU
:   8/4/94
:
:   MACRO CURVEQP TO MOVE MIDESIDE NODES TO THE QUARTER-POINT ON WEDGE
:   ELEMENTS FOR A CRACK THAT IS CURVED (IE CREATED WITH CURVECRK)
:   THIS MACRO MUST BE RUN IN /PREP7!!
:
:   NOTE:
:   IT IS EXPECTED THAT THE USER READ AND UNDERSTAND THE
:   FUNCTIONALITY OF THIS MACRO TO AVOID UNDESIRE RESULTS.
:
:   USAGE:
:   *USE,CURVEQP
:
:   *****
:
:   INPUT VALUES
:
:   *****
:
X_CRK=2.6395      * GLOBAL X-COORD. OF CRACK TIP
Y_CRK=10.5817    * GLOBAL Y-COORD. OF CRACK TIP
:               * THE X,Y LOCATION OF THE CRACK TIP IS THE
:               * LOCATION ON THE 2-D ELEMENTS.)
N_POINTS=13      * NUMBER OF POINTS ALONG CRACK FRONT
ALPHA=5          * ALPHA ANGLE OF CRACK OPENING
QPRAD=.0025     * RADIUS TO THE QUARTER-POINT NODES FROM CRACK TIP
*DIM,CRK_PNT,,N_POINTS,3 * DEFINES CRK_PNT ARRAY - DO NOT CHANGE!!
:
:   * COORDINATES OF POINTS ALONG CRACK FRONT INCLUDING STARTING POINT
:   * USE THE LOCAL COORDINATE SYSTEM THAT HAS ITS ORIGIN AT
:   * (X_CRK,Y_CRK)
:
CRK_PNT(1,1)=0   $CRK_PNT(1,2)=0   $CRK_PNT(1,3)=0
CRK_PNT(2,1)=0.000 $CRK_PNT(2,2)=0.000 $CRK_PNT(2,3)=0.025
CRK_PNT(3,1)=0.000 $CRK_PNT(3,2)=0.000 $CRK_PNT(3,3)=0.050
CRK_PNT(4,1)=0.000 $CRK_PNT(4,2)=0.000 $CRK_PNT(4,3)=0.075
CRK_PNT(5,1)=0.000 $CRK_PNT(5,2)=0.000 $CRK_PNT(5,3)=0.100
CRK_PNT(6,1)=0.000 $CRK_PNT(6,2)=0.000 $CRK_PNT(6,3)=0.125
CRK_PNT(7,1)=0.000 $CRK_PNT(7,2)=0.000 $CRK_PNT(7,3)=0.150
CRK_PNT(8,1)=0.002 $CRK_PNT(8,2)=0.000 $CRK_PNT(8,3)=0.175
CRK_PNT(9,1)=0.004 $CRK_PNT(9,2)=0.000 $CRK_PNT(9,3)=0.200
CRK_PNT(10,1)=0.008 $CRK_PNT(10,2)=0.000 $CRK_PNT(10,3)=0.225
CRK_PNT(11,1)=0.020 $CRK_PNT(11,2)=-0.010 $CRK_PNT(11,3)=0.250
CRK_PNT(12,1)=0.025 $CRK_PNT(12,2)=-0.018 $CRK_PNT(12,3)=0.275
CRK_PNT(13,1)=0.036 $CRK_PNT(13,2)=-0.022 $CRK_PNT(13,3)=0.300
:
:
:

```

```

*****
:
:
: END OF INPUT
:
:
: *****
:
: REMARKS:
: THE CURRENT ELEMENT MATERIAL, REAL, AND ESYS ARE MAINTAINED.
:
:
: MODM,DETA          * DETACH SOLID MODEL
: LOCAL,20,0,X_CRK,Y_CRK,0,ALPHA,0,0,1
: *****
:
: CURVED CRACK FRONT DEFINED.
:
: *****
: *DO,I,1,N_POINTS
: CSYS,20
: DSYS,20
: CLOCAL,19,1,CRK_PNT(1,1),CRK_PNT(1,2),CRK_PNT(1,3),0,0,0
: CSYS,19
: DSYS,19
: *****
:
: MID-SIDE NODES MOVED.
:
: *****
: NSEL,ALL
: NSEL,S,LOC,Z,0,0
: NSEL,R,LOC,X,QPRAD*2
: SHPP,OFF
: NMODIF,ALL,QPRAD
: SHPP,WARN
: CSYS,0
: DSYS,0
: NSEL,ALL
: *ENDDO

```

: This Macro written by - Michael Magill, OSU
: 8/4/94

: **MACRO CURVEBD TO FIND THE CUT BOUNDARY ON A CURVED CRACK FRONT.**
: **THIS MACRO MUST BE RUN IN /PREP7!!**

: **NOTE:**
: **IT IS EXPECTED THAT THE USER READ AND UNDERSTAND THE**
: **FUNCTIONALITY OF THIS MACRO TO AVOID UNDESIRE RESULTS.**
: **THIS MACRO IS ESPECIALLY FOR EXTRUDING CRACK TIP ELEMENTS INTO**
: **3-D ELEMENTS TO MAKE A WARPED CRACK FRONT.**

: **USAGE:**
: ***USE,CURVEBD**

: *****

: **INPUT VALUES**

: *****

: EL_TYPE=1 * ELEMENT TYPE TO BE CONVERTED.
: NEW_STF=95 * NEW STIFFNESS NUMBER.
: K_TR1=0 * 0 - 4 NODE ELEMENT TYPE BEING CONVERTED.
: * 1 - 6 NODE TRIANGULAR ELEMENT TYPE
: * (STIF 2,35,ETC.) BEING CONVERTED.
: X_CRK=2.6395 * GLOBAL X-COORD. OF CRACK TIP
: Y_CRK=10.5817 * GLOBAL Y-COORD. OF CRACK TIP
: * THE X,Y LOCATION OF THE CRACK TIP IS THE
: * LOCATION ON THE 2-D ELEMENTS.)
: SIDEGR=.5 * HEIGHT OF SIDE GROOVE
: RADIUS1=.060 * RADIUS AT OUTER BOUNDARY
: AN1=-170 * BEGINNING POINT FOR SWEEPING OUTER BOUNDARY
: AN2=170 * ENDING POINT FOR SWEEPING OUTER BOUNDARY
: N_POINTS=13 * NUMBER OF POINTS ALONG CRACK FRONT
: ALPHA=5 * ALPHA ANGLE OF CRACK OPENING
: QPRAD=.0025 * RADIUS TO THE QUARTER-POINT NODES FROM CRACK TIP
: *DIM,CRK_PNT,,N_POINTS,3 * DEFINES CRK_PNT ARRAY - DO NOT CHANGE!!
:
: * COORDINATES OF POINTS ALONG CRACK FRONT INCLUDING STARTING POINT
: * USE THE LOCAL COORDINATE SYSTEM THAT HAS ITS ORIGIN AT
: * (X_CRK,Y_CRK)
:
: * VERY IMPORTANT THE CRK_PNT VALUES MUST BE ENTERED BASED ON THE
: * ALPHA ANGLE BEING ZERO!! THEREFORE MEASURE CRACK FRONT POINTS WITH
: * THE SIDE GROOVE ON THE HORIZONTAL!!


```

CRK_PNT(1,1)=0      $CRK_PNT(1,2)=0      $CRK_PNT(1,3)=0
CRK_PNT(2,1)=0.000  $CRK_PNT(2,2)=0.000    $CRK_PNT(2,3)=0.025
CRK_PNT(3,1)=0.000  $CRK_PNT(3,2)=0.000    $CRK_PNT(3,3)=0.050
CRK_PNT(4,1)=0.000  $CRK_PNT(4,2)=0.000    $CRK_PNT(4,3)=0.075
CRK_PNT(5,1)=0.000  $CRK_PNT(5,2)=0.000    $CRK_PNT(5,3)=0.100
CRK_PNT(6,1)=0.000  $CRK_PNT(6,2)=0.000    $CRK_PNT(6,3)=0.125
CRK_PNT(7,1)=0.000  $CRK_PNT(7,2)=0.000    $CRK_PNT(7,3)=0.150
CRK_PNT(8,1)=0.002  $CRK_PNT(8,2)=0.000    $CRK_PNT(8,3)=0.175
CRK_PNT(9,1)=0.004  $CRK_PNT(9,2)=0.000    $CRK_PNT(9,3)=0.200
CRK_PNT(10,1)=0.008  $CRK_PNT(10,2)=0.000   $CRK_PNT(10,3)=0.225
CRK_PNT(11,1)=0.020  $CRK_PNT(11,2)=-0.010  $CRK_PNT(11,3)=0.250
CRK_PNT(12,1)=0.025  $CRK_PNT(12,2)=-0.018  $CRK_PNT(12,3)=0.275
CRK_PNT(13,1)=0.036  $CRK_PNT(13,2)=-0.022  $CRK_PNT(13,3)=0.300

```

```

:
:
: *****
:

```

```

: END OF INPUT
:

```

```

: *****
: LOCAL,20,0,X_CRK,Y_CRK,0,ALPHA,0,0,1
: CSYS,20
: DSYS,20
:

```

```

: FIRST ROW OF NODES
:

```

```

: *****
: CLOCAL,19,1,CRK_PNT(1,1),CRK_PNT(1,2),CRK_PNT(1,3),0,0,0
: CSYS,19
: DSYS,19
:

```

```

: SELECT NODES FOR FIRST ROW
:

```

```

: *****
: NSEL,ALL
: NSEL,S,LOC,Z,0,CRK_PNT(2,3)-CRK_PNT(1,3)
: NSEL,R,LOC,Y,AN1,AN2
: NSEL,R,LOC,X,RADIUS1,100
: NWRITE,,,0
:

```

```

: DEFINE CRACK FRONT
:

```

```

: *****
: CSYS,0
: DSYS,0
: NSEL,ALL
: *DO,I,2,N_POINTS
: CSYS,20

```

```

DSYS,20
CLOCAL,19,1,CRK_PNT(1,1),CRK_PNT(1,2),CRK_PNT(1,3),0,0,0
CSYS,19
DSYS,19
: *****
:
: SELECT NODES
:
: *****
NSEL,ALL
*IF,I,NE,N_POINTS,THEN
NSEL,S,LOC,Y,AN1,AN2
NSEL,R,LOC,Z,CRK_PNT(1-1,3)-CRK_PNT(1,3),CRK_PNT(1+1,3)-CRK_PNT(1,3)
NSEL,R,LOC,X,RADIUS1,100
*ENDIF
*IF,I,EQ,N_POINTS,THEN
NSEL,S,LOC,Y,AN1,AN2
NSEL,R,LOC,Z,0,0
NSEL,R,LOC,X,RADIUS1,100
NWRITE,,,,1
NSEL,ALL
NSEL,S,LOC,Y,AN1,0
NSEL,R,LOC,Z,-.005,.005
NSEL,R,LOC,X,QPRAD/2,100
NWRITE,,,,1
NSEL,ALL
CSYS,20
DSYS,20
CLOCAL,19,0,CRK_PNT(1,1),CRK_PNT(1,2),CRK_PNT(1,3),0,0,0
CSYS,19
DSYS,19
NSEL,S,LOC,Y,SIDEGR,1000
NSEL,R,LOC,Z,0,0
NSEL,R,LOC,X,-1000,1000
*ENDIF
NWRITE,,,,1
CSYS,0
DSYS,0
NSEL,ALL
*ENDDO
ESEL,ALL
NSEL,ALL

```

: This Macro written by - Michael Magill, OSU
: 8/4/94

: **MACRO CURVEK TO CALCULATE STRESS INTENSITY FACTORS (KI, KII, KIII)**
: **ALONG A CURVED CRACK FRONT (IE CREATED WITH CURVECRK)**
: **THIS MACRO MUST BE RUN IN /POST1!!**

: **NOTE:**
: **IT IS EXPECTED THAT THE USER READ AND UNDERSTAND THE**
: **FUNCTIONALITY OF THIS MACRO TO AVOID UNDESIRE RESULTS.**

: **USAGE:**
: ***USE,CURVEK**

: **INPUT VALUES**

X_CRK=2.6395 * GLOBAL X-COORD. OF CRACK TIP
Y_CRK=10.5817 * GLOBAL Y-COORD. OF CRACK TIP
: * THE X,Y LOCATION OF THE CRACK TIP IS THE
: * LOCATION ON THE 2-D ELEMENTS.)
N_POINTS=13 * NUMBER OF POINTS ALONG CRACK FRONT
ALPHA=5 * ALPHA ANGLE OF CRACK OPENING
QPRAD=.0025 * RADIUS TO THE QUARTER-POINT NODES FROM CRACK TIP
*DIM,CRK_PNT,,N_POINTS,3 * DEFINES CRK_PNT ARRAY - DO NOT CHANGE!!

: * COORDINATES OF POINTS ALONG CRACK FRONT INCLUDING STARTING POINT
: * USE THE LOCAL COORDINATE SYSTEM THAT HAS ITS ORIGIN AT
: * (X_CRK,Y_CRK)

CRK_PNT(1,1)=0	\$CRK_PNT(1,2)=0	\$CRK_PNT(1,3)=0
CRK_PNT(2,1)=0.000	\$CRK_PNT(2,2)=0.000	\$CRK_PNT(2,3)=0.025
CRK_PNT(3,1)=0.000	\$CRK_PNT(3,2)=0.000	\$CRK_PNT(3,3)=0.050
CRK_PNT(4,1)=0.000	\$CRK_PNT(4,2)=0.000	\$CRK_PNT(4,3)=0.075
CRK_PNT(5,1)=0.000	\$CRK_PNT(5,2)=0.000	\$CRK_PNT(5,3)=0.100
CRK_PNT(6,1)=0.000	\$CRK_PNT(6,2)=0.000	\$CRK_PNT(6,3)=0.125
CRK_PNT(7,1)=0.000	\$CRK_PNT(7,2)=0.000	\$CRK_PNT(7,3)=0.150
CRK_PNT(8,1)=0.002	\$CRK_PNT(8,2)=0.000	\$CRK_PNT(8,3)=0.175
CRK_PNT(9,1)=0.004	\$CRK_PNT(9,2)=0.000	\$CRK_PNT(9,3)=0.200
CRK_PNT(10,1)=0.008	\$CRK_PNT(10,2)=0.000	\$CRK_PNT(10,3)=0.225
CRK_PNT(11,1)=0.020	\$CRK_PNT(11,2)=-0.010	\$CRK_PNT(11,3)=0.250
CRK_PNT(12,1)=0.025	\$CRK_PNT(12,2)=-0.018	\$CRK_PNT(12,3)=0.275
CRK_PNT(13,1)=0.036	\$CRK_PNT(13,2)=-0.022	\$CRK_PNT(13,3)=0.300

```

:
:
:   END OF INPUT
:
:
: *****
:
: REMARKS:
: THE CURRENT ELEMENT MATERIAL, REAL, AND ESYS ARE MAINTAINED.
:
:
:
: *DIM,KONE,,N_POINTS
: *DIM,KTWO,,N_POINTS
: *DIM,KTHREE,,N_POINTS
: *DIM,POINT1,,N_POINTS
: *DIM,POINT2,,N_POINTS
: *DIM,POINT3,,N_POINTS
: *DIM,POINT4,,N_POINTS
: *DIM,POINT5,,N_POINTS
: *DIM,ELEMENTH,,N_POINTS
: *DIM,ELEMENTL,,N_POINTS
: *****
:
:   FIND THE FIVE NODES FOR CALCULATING STRESS INTENSITY FACTORS
:   AT CRK_PNT(1)
:
: *****
: LOCAL,20,0,X_CRK,Y_CRK,0,ALPHA,0,0,1
: CSYS,20
: DSYS,20
: CLOCAL,19,1,CRK_PNT(1,1),CRK_PNT(1,2),CRK_PNT(1,3),0,0,0
: CSYS,19
: DSYS,19
: *****
:   POINT 1
: *****
: NSEL,ALL
: NSEL,S,LOC,Z,-.0001,.0001
: NSEL,R,LOC,X,-.0001,.0001
: *GET,POINT1(1),NODE,,NUM,MAX
: *****
:   FIND WEDGE ELEMENTS AT CRACK TIP
: *****
: NSEL,ALL
: NSEL,S,LOC,Y,178,182
: NSEL,R,LOC,Z,-.0001,.0001
: NSEL,R,LOC,X,QPRAD,QPRAD
: ESLN,S,0
: *GET,ELEMENTH(1),ELEM,,NUM,MAX
: *GET,ELEMENTL(1),ELEM,,NUM,MIN
: *****
:   POINT 2
: *****

```

```

NSEL,ALL
ESEL,ALL
ESEL,R,ELEM,,ELEMENTH(1)
NSLE,S
NSEL,R,LOC,Y,178,182
NSEL,R,LOC,Z,-.0001,.0001
NSEL,R,LOC,X,QPRAD
*GET,POINT2(1),NODE,,NUM,MAX
: *****
: POINT 3
: *****
NSEL,ALL
ESEL,ALL
ESEL,R,ELEM,,ELEMENTH(1)
NSLE,S
NSEL,R,LOC,Y,178,182
NSEL,R,LOC,Z,-.0001,.0001
NSEL,R,LOC,X,QPRAD*4
*GET,POINT3(1),NODE,,NUM,MAX
: *****
: POINT 4
: *****
NSEL,ALL
ESEL,ALL
ESEL,R,ELEM,,ELEMENTL(1)
NSLE,S
NSEL,R,LOC,Y,178,182
NSEL,R,LOC,Z,-.0001,.0001
NSEL,R,LOC,X,QPRAD
*GET,POINT4(1),NODE,,NUM,MAX
: *****
: POINT 5
: *****
NSEL,ALL
ESEL,ALL
ESEL,R,ELEM,,ELEMENTL(1)
NSLE,S
NSEL,R,LOC,Y,178,182
NSEL,R,LOC,Z,-.0001,.0001
NSEL,R,LOC,X,QPRAD*4
*GET,POINT5(1),NODE,,NUM,MAX
: *****
:
: DEFINE CRACK PATH
:
: *****
CSYS,20
DSYS,20
CLOCAL,19,0,CRK_PNT(1,1),CRK_PNT(1,2),CRK_PNT(1,3),0,0,0
CSYS,19
DSYS,19
RSYS,19
LPATH,POINT1(1),POINT2(1),POINT3(1),POINT4(1),POINT5(1)
: *****

```

```

::
:   STRESS INTENSITY FACTORS CALCULATED
:
:   *****
KCALC,0,1,3,0
*GET,KONE(1),KCALC,,K,1
*GET,KTWO(1),KCALC,,K,2
*GET,KTHREE(1),KCALC,,K,3
CSYS,0
DSYS,0
RSYS,0
:   *****
:
:   WARPED CRACK FRONT IS DEFINED.
:
:   *****
*DO,I,2,N_POINTS
CSYS,20
DSYS,20
CLOCAL,19,1,CRK_PNT(1,1),CRK_PNT(1,2),CRK_PNT(1,3),0,0,0
CSYS,19
DSYS,19
:   *****
:
:   FIND THE FIVE NODES FOR CALCULATING STRESS INTENSITY FACTORS
:
:   *****
:   POINT 1
:   *****
NSEL,ALL
NSEL,S,LOC,Z,-.0001,.0001
NSEL,R,LOC,X,0,0
*GET,POINT1(I),NODE,,NUM,MAX
:   *****
:   FIND WEDGE ELEMENTS AT CRACK TIP
:   *****
NSEL,ALL
NSEL,S,LOC,Y,178,182
NSEL,R,LOC,Z,-.0001,.0001
NSEL,R,LOC,X,QPRAD,QPRAD
ESLN,S,0
*GET,ELEMENTH(I),ELEM,,NUM,MAX
*GET,ELEMENTL(I),ELEM,,NUM,MIN
:   *****
:   POINT 2
:   *****
NSEL,ALL
ESEL,ALL
ESEL,R,ELEM,,ELEMENTH(I)
NSLE,S
NSEL,R,LOC,Y,178,182
NSEL,R,LOC,Z,-.0001,.0001
NSEL,R,LOC,X,QPRAD
*GET,POINT2(I),NODE,,NUM,MAX

```

```

: *****
: POINT 3
: *****
NSEL,ALL
ESEL,ALL
ESEL,R,ELEM,,ELEMENTH(I)
NSLE,S
NSEL,R,LOC,Y,178,182
NSEL,R,LOC,Z,-.0001,.0001
NSEL,R,LOC,X,QPRAD*4
*GET,POINT3(I),NODE,,NUM,MAX
: *****
: POINT 4
: *****
NSEL,ALL
ESEL,ALL
ESEL,R,ELEM,,ELEMENTL(I)
NSLE,S
NSEL,R,LOC,Y,178,182
NSEL,R,LOC,Z,-.0001,.0001
NSEL,R,LOC,X,QPRAD
*GET,POINT4(I),NODE,,NUM,MAX
: *****
: POINT 5
: *****
NSEL,ALL
ESEL,ALL
ESEL,R,ELEM,,ELEMENTL(I)
NSLE,S
NSEL,R,LOC,Y,178,182
NSEL,R,LOC,Z,-.0001,.0001
NSEL,R,LOC,X,QPRAD*4
*GET,POINT5(I),NODE,,NUM,MAX
: *****
:
: DEFINE CRACK PATH
:
: *****
CSYS,20
DSYS,20
CLOCAL,19,0,CRK_PNT(I,1),CRK_PNT(I,2),CRK_PNT(I,3),0,0,0
CSYS,19
DSYS,19
RSYS,19
LPATH,POINT1(I),POINT2(I),POINT3(I),POINT4(I),POINT5(I)
: *****
::
: STRESS INTENSITY FACTORS CALCULATED
:
: *****
KCALC,0,1,3,0
*GET,KONE(I),KCALC,,K,1
*GET,KTWO(I),KCALC,,K,2
*GET,KTHREE(I),KCALC,,K,3

```

CSYS,0
DSYS,0
NSEL,ALL
*ENDDO
CSYS,0
DSYS,0
RSYS,0
NSEL,ALL
ESEL,ALL
PARSAV,ALL

: This Macro written by - Michael Magill, OSU
: 8/18/94
:

: MACRO **WARPCRKR** TO CONVERT 2-D SOLID ELEMENTS TO 3-D SOLID ELEMENTS AT
: A CRACK TIP AND MAKE A WARPED CRACK FRONT WITH TWO POSSIBLE ROTATIONS.
: THIS MACRO MUST BE RUN IN /PREP7!!
:

: NOTE:
: IT IS EXPECTED THAT THE USER READ AND UNDERSTAND THE
: FUNCTIONALITY OF THIS MACRO TO AVOID UNDESIRE RESULTS.
: THIS MACRO IS ESPECIALLY FOR EXTRUDING CRACK TIP ELEMENTS INTO
: 3-D ELEMENTS TO MAKE A WARPED CRACK FRONT.
:

: USAGE:
: *USE,WARPCRKR
:

: *****
:

: INPUT VALUES
:

: *****
:

EL_TYPE=1 * ELEMENT TYPE TO BE CONVERTED.
NEW_STF=95 * NEW STIFFNESS NUMBER.
K_TRI=0 * 0 - 4 NODE ELEMENT TYPE BEING CONVERTED.
: * 1 - 6 NODE TRIANGULAR ELEMENT TYPE
: * (STIF 2,35,ETC.) BEING CONVERTED.
X_CRK=2.4960 * GLOBAL X-COORD. OF CRACK TIP
Y_CRK=10.5488 * GLOBAL Y-COORD. OF CRACK TIP
: * THE X,Y LOCATION OF THE CRACK TIP IS THE
: * LOCATION ON THE 2-D ELEMENTS.)
N_POINTS=13 * NUMBER OF POINTS ALONG CRACK FRONT
ALPHA=15 * ALPHA ANGLE OF CRACK OPENING
QPRAD=.0025 * RADIUS TO THE QUARTER-POINT NODES FROM CRACK TIP
*DIM,CRK_PNT,,N_POINTS,3 * DEFINES CRK_PNT ARRAY - DO NOT CHANGE!!
:

: * COORDINATES OF POINTS ALONG CRACK FRONT INCLUDING STARTING POINT
: * USE THE LOCAL COORDINATE SYSTEM THAT HAS ITS ORIGIN AT
: * (X_CRK,Y_CRK)
:

: * VERY IMPORTANT THE CRK_PNT VALUES MUST BE ENTERED BASED ON THE
: * ALPHA ANGLE BEING ZERO!! THEREFORE MEASURE CRACK FRONT POINTS WITH
: * THE SIDE GROOVE ON THE HORIZONTAL!!
:

CRK_PNT(1,1)=0 \$CRK_PNT(1,2)=0 \$CRK_PNT(1,3)=0
CRK_PNT(2,1)=0.000 \$CRK_PNT(2,2)=0.001 \$CRK_PNT(2,3)=0.025
CRK_PNT(3,1)=0.000 \$CRK_PNT(3,2)=0.002 \$CRK_PNT(3,3)=0.050


```

*ENDIF
*IF,I,NE,N_POINTS,THEN
M=-(CRK_PNT(I+1,2)-CRK_PNT(I-1,2))/(CRK_PNT(I+1,3)-CRK_PNT(I-1,3))
*ENDIF
*IF,M,EQ,0,THEN
M=-.0000001
*ENDIF
B=CRK_PNT(I,3)-M*CRK_PNT(I,2)
YO=-(B/M)
R=((CRK_PNT(I,3))**2+(YO-CRK_PNT(I,2))**2)**(.5)
*AFUN,DEG
THETA=ASIN(CRK_PNT(I,3)/R)
NSLE
CSYS,20
DSYS,20
CLOCAL,19,1,0,YO,0,-90,90,0
CSYS,19
DSYS,19
NGEN,2,10000*(I-1),ALL,,,R-YO,THETA,-CRK_PNT(I,1)
*IF,I,NE,N_POINTS,THEN
X2=(CRK_PNT(I+1,1)-CRK_PNT(I-1,1))**2
Y2=(CRK_PNT(I+1,2)-CRK_PNT(I-1,2))**2
Z2=(CRK_PNT(I+1,3)-CRK_PNT(I-1,3))**2
DELTAL=(X2+Y2+Z2)**(.5)
DELTAX=CRK_PNT(I+1,1)-CRK_PNT(I-1,1)
*ENDIF
*IF,I,EQ,N_POINTS,THEN
X2=(CRK_PNT(I,1)-CRK_PNT(I-1,1))**2
Y2=(CRK_PNT(I,2)-CRK_PNT(I-1,2))**2
Z2=(CRK_PNT(I,3)-CRK_PNT(I-1,3))**2
DELTAL=(X2+Y2+Z2)**(.5)
DELTAX=CRK_PNT(I,1)-CRK_PNT(I-1,1)
*ENDIF
THETA1=ASIN(DELTAX/DELTAL)
CSYS,20
DSYS,20
CLOCAL,17,1,CRK_PNT(I,1),CRK_PNT(I,2),CRK_PNT(I,3),0,90-THETA,0
CSYS,17
DSYS,17
NSEL,ALL
NSEL,S,NODE,,10000*(I-1),10000*(I-1)+9999,1
NSEL,R,LOC,Y,178,182,,0
NMODIF,ALL,,180-THETA1
NSEL,ALL
NSEL,S,NODE,,10000*(I-1),10000*(I-1)+9999,1
NSEL,R,LOC,Y,-2,2,,0
NMODIF,ALL,-,THETA1
CSYS,0
DSYS,0
NSEL,ALL
*ENDDO
: *****
:
:

```

```

:   END OF CRACK FRONT DEFINITION
:
:
: *****
CSYS,0
DSYS,0
NSEL,ALL
*GET,IEMX,ELMX           * GET MAX. ELEMENT NUMBER OF SELECTED SET
ET,EL_TYPE,NEW_STF     * REDEFINE ELEMENT TYPE
TYPE,EL_TYPE           * RESET TYPE FOR NEW ELEMENTS
IEL=1
LOCAL,18,1,X_CRK,Y_CRK,0,0,0,1
CSYS,18
DSYS,18
:TOP
*GET,IETY,TYPE,IEL      * GET ELEMENT TYPE FOR THIS ELEMENT
*IF,IETY,NE,EL_TYPE,:SK2 * CHECK TYPE
*GET,IERL,REAL,IEL      * GET MAT, REAL, AND ESYS
*GET,IEMT,MAT,IEL
*GET,IESY,ESYS,IEL
*GET,I1,EN1,IEL        * GET CORNER NODES OF ELEMENT
*GET,I2,EN2,IEL
*GET,I3,EN3,IEL
*GET,I4,EN4,IEL
*IF,K_TRI,NE,1,:NT2    * TRIANGULAR ELEMENT
I4=I3
:NT2
*IF,NX(I1),NE,0,:XEB1  * CHANGES ELEMENT NODES FOR CRACK TIP
I5=I1
I1=I2
I2=I3
I3=I5
I4=I5
:XEB1
*IF,NX(I2),NE,0,:XEB2
I5=I2
I2=I1
I1=I3
I3=I5
I4=I5
:XEB2
I1P=I1+10000           * ADD SPECIFIED NODE INCREMENT
I2P=I2+10000
I3P=I3+10000
I4P=I4+10000
MAT,IEMT               * RESET MAT, REAL, AND ESYS
REAL,IERL
ESYS,IESY
EN,IEL,I1,I2,I3,I4,I1P,I2P,I3P,I4P * REDEFINE ELEMENT
:SK2
IEL=IEL+1              * INCREMENT LOOP COUNTER
*IF,IEL,LE,IEMX,:TOP   * LOOP BACK OR EXIT
CSYS,0
DSYS,0

```

```

:
:           PUTS MIDSIDE NODES IN ELEMENTS
:
EMDD=1
*IF,NEW_STF,GE,82,:NEXT
EMDD=0
:NEXT
*IF,EMDD,EQ,0,:NOM
EMID
:NOM
*IF,N_POINTS-1,EQ,1,:SK3      * THIS SECTION GENERATES THE EXTRA LAYERS IF
ESEL,TYPE,EL_TYPE           * REQUESTED
EGEN,N_POINTS-1,10000,ALL
:SK3
EALL
NELEM                        * THIS SECTION CLEARS THE EXTRA NODES FROM THE
NINV                          * NGEN OPERATION
:
:     ****WARNING: ALL NODES NOT ATTACHED TO AN ELEMENT WILL BE DELETED
:     AT THIS POINT
:
NDEL,ALL
NSEL,ALL
:
:     *****
:
:     MERGE NODES AT SAME LOCATION
:
:     *****
:     *****
:
:     WARPED CRACK FRONT DEFINED.
:
:     *****
:
CSYS,0
DSYS,0
*DO,I,2,N_POINTS
*IF,I,EQ,N_POINTS,THEN
M=-(CRK_PNT(I,2)-CRK_PNT(I-1,2))/(CRK_PNT(I,3)-CRK_PNT(I-1,3))
*ENDIF
*IF,I,NE,N_POINTS,THEN
M=-(CRK_PNT(I+1,2)-CRK_PNT(I-1,2))/(CRK_PNT(I+1,3)-CRK_PNT(I-1,3))
*ENDIF
*IF,M,EQ,0,THEN
M=-.0000001
*ENDIF
B=CRK_PNT(I,3)-M*CRK_PNT(I,2)
YO=-(B/M)
R=((CRK_PNT(I,3))**2+(YO-CRK_PNT(I,2))**2)**(.5)
*AFUN,DEG
THETA=ASIN(CRK_PNT(I,3)/R)
*IF,I,NE,N_POINTS,THEN
X2=(CRK_PNT(I+1,1)-CRK_PNT(I-1,1))**2
Y2=(CRK_PNT(I+1,2)-CRK_PNT(I-1,2))**2
Z2=(CRK_PNT(I+1,3)-CRK_PNT(I-1,3))**2
DELTA=(X2+Y2+Z2)**(.5)

```

```

DELTA1=CRK_PNT(I+1,1)-CRK_PNT(I-1,1)
*ENDIF
*IF,I,EQ,N_POINTS,THEN
X2=(CRK_PNT(I,1)-CRK_PNT(I-1,1))**2
Y2=(CRK_PNT(I,2)-CRK_PNT(I-1,2))**2
Z2=(CRK_PNT(I,3)-CRK_PNT(I-1,3))**2
DELTAL=(X2+Y2+Z2)**(.5)
DELTA1=CRK_PNT(I,1)-CRK_PNT(I-1,1)
*ENDIF
THETA1=ASIN(DELTA1/DELTAL)
CSYS,20
DSYS,20
CLOCAL,16,1,CRK_PNT(I,1),CRK_PNT(I,2),CRK_PNT(I,3),0,-THETA,THETA1
CSYS,16
DSYS,16
: *****
:
: MERGE NODES
:
: *****
NSEL,ALL
NSEL,S,LOC,Z,0,0
NSEL,R,LOC,Y,-20,175
NSEL,R,LOC,X,QPRAD,10
ESLN,S,0
NSLE,S
NUMMRG,NODE
ESEL,ALL
NSEL,ALL
NSEL,S,LOC,Z,0,0
NSEL,R,LOC,Y,185,380
NSEL,R,LOC,X,QPRAD,10
ESLN,S,0
NSLE,S
NUMMRG,NODE
CSYS,0
DSYS,0
ESEL,ALL
NSEL,ALL
*ENDDO
ESEL,ALL
NSEL,ALL
NUMCMP,ELEM
NUMCMP,NODE
/COM
/COM WARPCRKR CONVERSION COMPLETE.
:END

```

: This Macro written by - Michael Magill, OSU
: 8/18/94
:

: MACRO **WARPOPR** TO MOVE MIDESIDE NODES TO THE QUARTER-POINT ON WEDGE
: ELEMENTS FOR A CRACK THAT IS WARPED WITH TWO ROTATIONS (IE CREATED
: WITH WARPCRKR)
: THIS MACRO MUST BE RUN IN /PREP7!! -
:

: NOTE:
: IT IS EXPECTED THAT THE USER READ AND UNDERSTAND THE
: FUNCTIONALITY OF THIS MACRO TO AVOID UNDESIRE RESULTS.
:

: USAGE:
: *USE,WARPOPR
:

: *****
:

: INPUT VALUES
:

: *****
:

X_CRK=2.4960 * GLOBAL X-COORD. OF CRACK TIP
Y_CRK=10.5488 * GLOBAL Y-COORD. OF CRACK TIP
: * THE X,Y LOCATION OF THE CRACK TIP IS THE
: * LOCATION ON THE 2-D ELEMENTS.)
N_POINTS=13 * NUMBER OF POINTS ALONG CRACK FRONT
ALPHA=15 * ALPHA ANGLE OF CRACK OPENING
QPRAD=.0025 * RADIUS TO THE QUARTER-POINT NODES FROM CRACK TIP
*DIM,CRK_PNT,,N_POINTS,3 * DEFINES CRK_PNT ARRAY - DO NOT CHANGE!!
:

: * COORDINATES OF POINTS ALONG CRACK FRONT INCLUDING STARTING POINT
: * USE THE LOCAL COORDINATE SYSTEM THAT HAS ITS ORIGIN AT
: * (X_CRK,Y_CRK)
:

CRK_PNT(1,1)=0	\$CRK_PNT(1,2)=0	\$CRK_PNT(1,3)=0
CRK_PNT(2,1)=0.000	\$CRK_PNT(2,2)=0.001	\$CRK_PNT(2,3)=0.025
CRK_PNT(3,1)=0.000	\$CRK_PNT(3,2)=0.002	\$CRK_PNT(3,3)=0.050
CRK_PNT(4,1)=0.000	\$CRK_PNT(4,2)=0.003	\$CRK_PNT(4,3)=0.075
CRK_PNT(5,1)=0.000	\$CRK_PNT(5,2)=0.005	\$CRK_PNT(5,3)=0.100
CRK_PNT(6,1)=0.000	\$CRK_PNT(6,2)=0.009	\$CRK_PNT(6,3)=0.125
CRK_PNT(7,1)=0.000	\$CRK_PNT(7,2)=0.014	\$CRK_PNT(7,3)=0.150
CRK_PNT(8,1)=0.000	\$CRK_PNT(8,2)=0.019	\$CRK_PNT(8,3)=0.175
CRK_PNT(9,1)=0.000	\$CRK_PNT(9,2)=0.027	\$CRK_PNT(9,3)=0.200
CRK_PNT(10,1)=0.000	\$CRK_PNT(10,2)=0.037	\$CRK_PNT(10,3)=0.225
CRK_PNT(11,1)=0.010	\$CRK_PNT(11,2)=0.052	\$CRK_PNT(11,3)=0.250
CRK_PNT(12,1)=0.024	\$CRK_PNT(12,2)=0.072	\$CRK_PNT(12,3)=0.275
CRK_PNT(13,1)=0.036	\$CRK_PNT(13,2)=0.098	\$CRK_PNT(13,3)=0.300

:
:
:

```

: *****
:
:
: END OF INPUT
:
: *****
:
: REMARKS:
: THE CURRENT ELEMENT MATERIAL, REAL, AND ESYS ARE MAINTAINED.
:
:
: MODM,DETA          * DETACH SOLID MODEL
: *****
:
: MID-SIDE NODES AT CRK_PNT(1) MOVED
:
: *****
LOCAL,20,0,X_CRK,Y_CRK,0,ALPHA,0,0,1
CSYS,20
DSYS,20
CLOCAL,19,1,CRK_PNT(1,1),CRK_PNT(1,2),CRK_PNT(1,3),0,0,0
CSYS,19
DSYS,19
NSEL,ALL
NSEL,S,LOC,Z,0,0
NSEL,R,LOC,X,QPRAD*2
SHPP,OFF
NMODIF,ALL,QPRAD
SHPP,WARN
CSYS,0
DSYS,0
NSEL,ALL
: *****
:
: WARPED CRACK FRONT DEFINED.
:
: *****
*DO,I,2,N_POINTS
*IF,I,EQ,N_POINTS,THEN
M=-(CRK_PNT(I,2)-CRK_PNT(I-1,2))/(CRK_PNT(I,3)-CRK_PNT(I-1,3))
*ENDIF
*IF,I,NE,N_POINTS,THEN
M=-(CRK_PNT(I+1,2)-CRK_PNT(I-1,2))/(CRK_PNT(I+1,3)-CRK_PNT(I-1,3))
*ENDIF
*IF,M,EQ,0,THEN
M=-.0000001
*ENDIF
B=CRK_PNT(I,3)-M*CRK_PNT(I,2)
YO=-(B/M)
R=((CRK_PNT(I,3))**2+(YO-CRK_PNT(I,2))**2)**(.5)
*AFUN,DEG
THETA=ASIN(CRK_PNT(I,3)/R)

```



```

*IF,LINE,N_POINTS,THEN
X2=(CRK_PNT(I+1,1)-CRK_PNT(I-1,1))**2
Y2=(CRK_PNT(I+1,2)-CRK_PNT(I-1,2))**2
Z2=(CRK_PNT(I+1,3)-CRK_PNT(I-1,3))**2
DELTAL=(X2+Y2+Z2)**(.5)
DELTAX=CRK_PNT(I+1,1)-CRK_PNT(I-1,1)
*ENDIF
*IF,I,LEQ,N_POINTS,THEN
X2=(CRK_PNT(I,1)-CRK_PNT(I-1,1))**2
Y2=(CRK_PNT(I,2)-CRK_PNT(I-1,2))**2
Z2=(CRK_PNT(I,3)-CRK_PNT(I-1,3))**2
DELTAL=(X2+Y2+Z2)**(.5)
DELTAX=CRK_PNT(I,1)-CRK_PNT(I-1,1)
*ENDIF
THETA1=ASIN(DELTAX/DELTAL)
CSYS,20
DSYS,20
CLOCAL,19,1,CRK_PNT(I,1),CRK_PNT(I,2),CRK_PNT(I,3),0,-THETA,THETA1
CSYS,19
DSYS,19
: *****
:
:
:   MID-SIDE NODES MOVED.
:
: *****
NSEL,ALL
NSEL,S,LOC,Z,0,0
NSEL,R,LOC,X,QPRAD*2
SHPP,OFF
NMODIF,ALL,QPRAD
SHPP,WARN
CSYS,0
DSYS,0
NSEL,ALL
*ENDDO

```

: This Macro written by - Michael Magill, OSU
: 8/18/94

: **MACRO WARPBDR TO FIND THE CUT BOUNDARY ON A WARPED CRACK FRONT WITH**
: **TWO POSSIBLE ROTATIONS.**
: **THIS MACRO MUST BE RUN IN /PREP7!!**

: **NOTE:**
: **IT IS EXPECTED THAT THE USER READ AND UNDERSTAND THE**
: **FUNCTIONALITY OF THIS MACRO TO AVOID UNDESIRE RESULTS.**
: **THIS MACRO IS ESPECIALLY FOR EXTRUDING CRACK TIP ELEMENTS INTO**
: **3-D ELEMENTS TO MAKE A WARPED CRACK FRONT.**

: **USAGE:**
: ***USE,WARPBDR**

: *****

: **INPUT VALUES**

: *****

EL_TYPE=1 * ELEMENT TYPE TO BE CONVERTED.
NEW_STF=95 * NEW STIFFNESS NUMBER.
K_TRI=0 * 0 - 4 NODE ELEMENT TYPE BEING CONVERTED.
: * 1 - 6 NODE TRIANGULAR ELEMENT TYPE
: * (STIF 2,35,ETC.) BEING CONVERTED.
X_CRK=2.4960 * GLOBAL X-COORD. OF CRACK TIP
Y_CRK=10.5488 * GLOBAL Y-COORD. OF CRACK TIP
: * THE X,Y LOCATION OF THE CRACK TIP IS THE
: * LOCATION ON THE 2-D ELEMENTS.)
SGEND=-.010 * Z DISTANCE FOR SELECTING END NODES
SIDEGR=.5 * HEIGHT OF SIDE GROOVE
RADIUS1=.060 * RADIUS AT OUTER BOUNDARY
AN1=-172 * BEGINNING POINT FOR SWEEPING OUTER BOUNDARY
AN2=170 * ENDING POINT FOR SWEEPING OUTER BOUNDARY
N_POINTS=13 * NUMBER OF POINTS ALONG CRACK FRONT
ALPHA=15 * ALPHA ANGLE OF CRACK OPENING
QPRAD=.0025 * RADIUS TO THE QUARTER-POINT NODES FROM CRACK TIP
*DIM,CRK_PNT,,N_POINTS,3 * DEFINES CRK_PNT ARRAY - DO NOT CHANGE!!

: * COORDINATES OF POINTS ALONG CRACK FRONT INCLUDING STARTING POINT
: * USE THE LOCAL COORDINATE SYSTEM THAT HAS ITS ORIGIN AT
: * (X_CRK,Y_CRK)

: * VERY IMPORTANT THE CRK_PNT VALUES MUST BE ENTERED BASED ON THE
: * ALPHA ANGLE BEING ZERO!! THEREFORE MEASURE CRACK FRONT POINTS WITH
: * THE SIDE GROOVE ON THE HORIZONTAL!!

```

CRK_PNT(1,1)=0      $CRK_PNT(1,2)=0      $CRK_PNT(1,3)=0
CRK_PNT(2,1)=0.000  $CRK_PNT(2,2)=0.001  $CRK_PNT(2,3)=0.025
CRK_PNT(3,1)=0.000  $CRK_PNT(3,2)=0.002  $CRK_PNT(3,3)=0.050
CRK_PNT(4,1)=0.000  $CRK_PNT(4,2)=0.003  $CRK_PNT(4,3)=0.075
CRK_PNT(5,1)=0.000  $CRK_PNT(5,2)=0.005  $CRK_PNT(5,3)=0.100
CRK_PNT(6,1)=0.000  $CRK_PNT(6,2)=0.009  $CRK_PNT(6,3)=0.125
CRK_PNT(7,1)=0.000  $CRK_PNT(7,2)=0.014  $CRK_PNT(7,3)=0.150
CRK_PNT(8,1)=0.000  $CRK_PNT(8,2)=0.019  $CRK_PNT(8,3)=0.175
CRK_PNT(9,1)=0.000  $CRK_PNT(9,2)=0.027  $CRK_PNT(9,3)=0.200
CRK_PNT(10,1)=0.000 $CRK_PNT(10,2)=0.037  $CRK_PNT(10,3)=0.225
CRK_PNT(11,1)=0.010 $CRK_PNT(11,2)=0.052  $CRK_PNT(11,3)=0.250
CRK_PNT(12,1)=0.024 $CRK_PNT(12,2)=0.072  $CRK_PNT(12,3)=0.275
CRK_PNT(13,1)=0.036 $CRK_PNT(13,2)=0.098  $CRK_PNT(13,3)=0.300

```

```

*****

```

```

END OF INPUT

```

```

*****

```

```

LOCAL,20,0,X_CRK,Y_CRK,0,ALPHA,0,0,1
CSYS,20
DSYS,20

```

```

*****

```

```

FIRST ROW OF NODES

```

```

*****

```

```

CLOCAL,19,1,CRK_PNT(1,1),CRK_PNT(1,2),CRK_PNT(1,3),0,0,0
CSYS,19
DSYS,19

```

```

*****

```

```

SELECT NODES FOR FIRST ROW

```

```

*****

```

```

NSEL,ALL
NSEL,S,LOC,Z,0,CRK_PNT(2,3)-CRK_PNT(1,3)
NSEL,R,LOC,Y,AN1,AN2
NSEL,R,LOC,X,RADIUS1,100
NWRITE,,,0

```

```

*****

```

```

DEFINE CRACK FRONT

```

```

*****

```

```

CSYS,0
DSYS,0
NSEL,ALL*DO,I,2,N_POINTS

```

```

*IF,I,EQ,N_POINTS,THEN
M=-(CRK_PNT(I,2)-CRK_PNT(I-1,2))/(CRK_PNT(I,3)-CRK_PNT(I-1,3))
*ENDIF
*IF,I,NE,N_POINTS,THEN
M=-(CRK_PNT(I+1,2)-CRK_PNT(I-1,2))/(CRK_PNT(I+1,3)-CRK_PNT(I-1,3))
*ENDIF
*IF,M,EQ,0,THEN
M=-.0000001
*ENDIF
B=CRK_PNT(I,3)-M*CRK_PNT(I,2)
YO=-(B/M)
R=((CRK_PNT(I,3))**2+(YO-CRK_PNT(I,2))**2)**(.5)
*AFUN,DEG
THETA=ASIN(CRK_PNT(I,3)/R)
*IF,I,NE,N_POINTS,THEN
X2=(CRK_PNT(I+1,1)-CRK_PNT(I-1,1))**2
Y2=(CRK_PNT(I+1,2)-CRK_PNT(I-1,2))**2
Z2=(CRK_PNT(I+1,3)-CRK_PNT(I-1,3))**2
DELTAL=(X2+Y2+Z2)**(.5)
DELTAX=CRK_PNT(I+1,1)-CRK_PNT(I-1,1)
*ENDIF
*IF,I,EQ,N_POINTS,THEN
X2=(CRK_PNT(I,1)-CRK_PNT(I-1,1))**2
Y2=(CRK_PNT(I,2)-CRK_PNT(I-1,2))**2
Z2=(CRK_PNT(I,3)-CRK_PNT(I-1,3))**2
DELTAL=(X2+Y2+Z2)**(.5)
DELTAX=CRK_PNT(I,1)-CRK_PNT(I-1,1)
*ENDIF
THETA1=ASIN(DELTAX/DELTAL)
CSYS,20
DSYS,20
CLOCAL,19,1,CRK_PNT(I,1),CRK_PNT(I,2),CRK_PNT(I,3),0,-THETA,THETA1
CSYS,19
DSYS,19
: *****
:
:   SELECT NODES
:
: *****
NSEL,ALL
NSEL,S,LOC,Y,AN1,AN2
: *****
:
:   MIDDLE SECTION
:
: *****
*IF,I,NE,N_POINTS,THEN
NSEL,R,LOC,Z,CRK_PNT(I-1,3)-CRK_PNT(I,3),CRK_PNT(I+1,3)-CRK_PNT(I,3)
NSEL,R,LOC,X,RADIUS1,100
CSYS,20
DSYS,20
CLOCAL,19,0,CRK_PNT(N_POINTS,1),CRK_PNT(N_POINTS,2),CRK_PNT(N_POINTS,3),0,0,0
CSYS,19
DSYS,19

```

```

NSEL,R,LOC,Z,-10,0
NWRITE,,,,,1
: *****
:
: INTERNAL END NODES
:
: *****
CSYS,20
DSYS,20
CLOCAL,19,1,CRK_PNT(1,1),CRK_PNT(1,2),CRK_PNT(1,3),0,-THETA,THETA1
CSYS,19
DSYS,19
NSEL,ALL
NSEL,S,LOC,Y,AN1,AN2
NSEL,R,LOC,Z,0,0
NSEL,R,LOC,X,QPRAD/2,100
CSYS,20
DSYS,20
CLOCAL,19,0,CRK_PNT(N_POINTS,1),CRK_PNT(N_POINTS,2),CRK_PNT(N_POINTS,3),0,0,0
CSYS,19
DSYS,19
NSEL,R,LOC,Z,SGEND,0
*ENDIF
: *****
:
: SIDE GROOVE END
:
: *****
*IF,I,EQ,N_POINTS,THEN
NSEL,R,LOC,Z,0,0
NSEL,R,LOC,X,QPRAD/2,100
CSYS,20
DSYS,20
CLOCAL,19,0,CRK_PNT(N_POINTS,1),CRK_PNT(N_POINTS,2),CRK_PNT(N_POINTS,3),0,0,0
CSYS,19
DSYS,19
NSEL,R,LOC,Z,-10,0
*ENDIF
NWRITE,,,,,1
CSYS,0
DSYS,0
NSEL,ALL
*ENDDO
ESEL,ALL
NSEL,ALL

```

: This Macro written by - Michael Magill, OSU
: 8/18/94
:

: **MACRO WARPKR TO CALCULATE STRESS INTENSITY FACTORS (KI, KII, KIII)**
: **ALONG A WARPED CRACK FRONT WITH TWO ROTATIONS (IE CREATED WITH**
: **WARPCRKR)**
: **THIS MACRO MUST BE RUN IN /POST!!!**
:

: **NOTE:**
: **IT IS EXPECTED THAT THE USER READ AND UNDERSTAND THE**
: **FUNCTIONALITY OF THIS MACRO TO AVOID UNDESIRE RESULTS.**
:

: **USAGE:**
: ***USE,WARPKR**
:

: *****
:

: **INPUT VALUES**
:

: *****
:

X_CRK=2.4960 * GLOBAL X-COORD. OF CRACK TIP
Y_CRK=10.5488 * GLOBAL Y-COORD. OF CRACK TIP
: * THE X,Y LOCATION OF THE CRACK TIP IS THE
: * LOCATION ON THE 2-D ELEMENTS.)
N_POINTS=13 * NUMBER OF POINTS ALONG CRACK FRONT
ALPHA=15 * ALPHA ANGLE OF CRACK OPENING
QPRAD=.0025 * RADIUS TO THE QUARTER-POINT NODES FROM CRACK TIP
*DIM,CRK_PNT,,N_POINTS,3 * DEFINES CRK_PNT ARRAY - DO NOT CHANGE!!
:

: * COORDINATES OF POINTS ALONG CRACK FRONT INCLUDING STARTING POINT
: * USE THE LOCAL COORDINATE SYSTEM THAT HAS ITS ORIGIN AT
: * (X_CRK,Y_CRK)
:

CRK_PNT(1,1)=0	\$CRK_PNT(1,2)=0	\$CRK_PNT(1,3)=0
CRK_PNT(2,1)=0.000	\$CRK_PNT(2,2)=0.001	\$CRK_PNT(2,3)=0.025
CRK_PNT(3,1)=0.000	\$CRK_PNT(3,2)=0.002	\$CRK_PNT(3,3)=0.050
CRK_PNT(4,1)=0.000	\$CRK_PNT(4,2)=0.003	\$CRK_PNT(4,3)=0.075
CRK_PNT(5,1)=0.000	\$CRK_PNT(5,2)=0.005	\$CRK_PNT(5,3)=0.100
CRK_PNT(6,1)=0.000	\$CRK_PNT(6,2)=0.009	\$CRK_PNT(6,3)=0.125
CRK_PNT(7,1)=0.000	\$CRK_PNT(7,2)=0.014	\$CRK_PNT(7,3)=0.150
CRK_PNT(8,1)=0.000	\$CRK_PNT(8,2)=0.019	\$CRK_PNT(8,3)=0.175
CRK_PNT(9,1)=0.000	\$CRK_PNT(9,2)=0.027	\$CRK_PNT(9,3)=0.200
CRK_PNT(10,1)=0.000	\$CRK_PNT(10,2)=0.037	\$CRK_PNT(10,3)=0.225
CRK_PNT(11,1)=0.010	\$CRK_PNT(11,2)=0.052	\$CRK_PNT(11,3)=0.250
CRK_PNT(12,1)=0.024	\$CRK_PNT(12,2)=0.072	\$CRK_PNT(12,3)=0.275
CRK_PNT(13,1)=0.036	\$CRK_PNT(13,2)=0.098	\$CRK_PNT(13,3)=0.300

:
:
:

```

: *****
:
:
: END OF INPUT
:
: *****
:
: REMARKS:
: THE CURRENT ELEMENT MATERIAL, REAL, AND ESYS ARE MAINTAINED.
:
:
: *DIM,KONE,,N_POINTS
: *DIM,KTWO,,N_POINTS
: *DIM,KTHREE,,N_POINTS
: *DIM,POINT1,,N_POINTS
: *DIM,POINT2,,N_POINTS
: *DIM,POINT3,,N_POINTS
: *DIM,POINT4,,N_POINTS
: *DIM,POINT5,,N_POINTS
: *DIM,ELEMENTH,,N_POINTS
: *DIM,ELEMENTL,,N_POINTS
: *****
:
: FIND THE FIVE NODES FOR CALCULATING STRESS INTENSITY FACTORS
: AT CRK_PNT(1)
:
: *****
LOCAL,20,0,X_CRK,Y_CRK,0,ALPHA,0,0,1
CSYS,20
DSYS,20
CLOCAL,19,1,CRK_PNT(1,1),CRK_PNT(1,2),CRK_PNT(1,3),0,0,0
CSYS,19
DSYS,19
: *****
: POINT 1
: *****
NSEL,ALL
NSEL,S,LOC,Z,-.0001,.0001
NSEL,R,LOC,X,-.0001,.0001
*GET,POINT1(1),NODE,,NUM,MAX
: *****
: FIND WEDGE ELEMENTS AT CRACK TIP
: *****
NSEL,ALL
NSEL,S,LOC,Y,178,182
NSEL,R,LOC,Z,-.0001,.0001
NSEL,R,LOC,X,QPRAD,QPRAD
ESLN,S,0
*GET,ELEMENTH(1),ELEM,,NUM,MAX
*GET,ELEMENTL(1),ELEM,,NUM,MIN
: *****
: POINT 2

```

```

: *****
NSEL,ALL
ESEL,ALL
ESEL,R,ELEM,,ELEMENTH(1)
NSLE,S
NSEL,R,LOC,Y,178,182
NSEL,R,LOC,Z,-.0001,.0001
NSEL,R,LOC,X,QPRAD
*GET,POINT2(1),NODE,,NUM,MAX
: *****
: POINT 3
: *****
NSEL,ALL
ESEL,ALL
ESEL,R,ELEM,,ELEMENTH(1)
NSLE,S
NSEL,R,LOC,Y,178,182
NSEL,R,LOC,Z,-.0001,.0001
NSEL,R,LOC,X,QPRAD*4
*GET,POINT3(1),NODE,,NUM,MAX
: *****
: POINT 4
: *****
NSEL,ALL
ESEL,ALL
ESEL,R,ELEM,,ELEMENTL(1)
NSLE,S
NSEL,R,LOC,Y,178,182
NSEL,R,LOC,Z,-.0001,.0001
NSEL,R,LOC,X,QPRAD
*GET,POINT4(1),NODE,,NUM,MAX
: *****
: POINT 5
: *****
NSEL,ALL
ESEL,ALL
ESEL,R,ELEM,,ELEMENTL(1)
NSLE,S
NSEL,R,LOC,Y,178,182
NSEL,R,LOC,Z,-.0001,.0001
NSEL,R,LOC,X,QPRAD*4
*GET,POINT5(1),NODE,,NUM,MAX
: *****
:
: DEFINE CRACK PATH
:
: *****
CSYS,20
DSYS,20
CLOCAL,19,0,CRK_PNT(1,1),CRK_PNT(1,2),CRK_PNT(1,3),0,0,0
CSYS,19
DSYS,19
RSYS,19
LPATH,POINT1(1),POINT2(1),POINT3(1),POINT4(1),POINT5(1)

```



```

: *****
:
: STRESS INTENSITY FACTORS CALCULATED
:
: *****
KCALC,0,1,3,0
*GET,KONE(1),KCALC,,K,1
*GET,KTWO(1),KCALC,,K,2
*GET,KTHREE(1),KCALC,,K,3
CSYS,0
DSYS,0
RSYS,0
: *****
:
: WARPED CRACK FRONT IS DEFINED.
:
: *****
*DO,I,2,N_POINTS
*IF,I,EQ,N_POINTS,THEN
M=- (CRK_PNT(I,2)-CRK_PNT(I-1,2))/(CRK_PNT(I,3)-CRK_PNT(I-1,3))
*ENDIF
*IF,I,NE,N_POINTS,THEN
M=- (CRK_PNT(I+1,2)-CRK_PNT(I-1,2))/(CRK_PNT(I+1,3)-CRK_PNT(I-1,3))
*ENDIF
*IF,M,EQ,0,THEN
M=-.000001
*ENDIF
B=CRK_PNT(I,3)-M*CRK_PNT(I,2)
YO=- (B/M)
R= ((CRK_PNT(I,3))**2+(YO-CRK_PNT(I,2))**2)**(.5)
*AFUN,DEG
THETA=ASIN(CRK_PNT(I,3)/R)
*IF,I,NE,N_POINTS,THEN
X2=(CRK_PNT(I+1,1)-CRK_PNT(I-1,1))**2
Y2=(CRK_PNT(I+1,2)-CRK_PNT(I-1,2))**2
Z2=(CRK_PNT(I+1,3)-CRK_PNT(I-1,3))**2
DELTAL=(X2+Y2+Z2)**(.5)
DELTAX=CRK_PNT(I+1,1)-CRK_PNT(I-1,1)
*ENDIF
*IF,I,EQ,N_POINTS,THEN
X2=(CRK_PNT(I,1)-CRK_PNT(I-1,1))**2
Y2=(CRK_PNT(I,2)-CRK_PNT(I-1,2))**2
Z2=(CRK_PNT(I,3)-CRK_PNT(I-1,3))**2
DELTAL=(X2+Y2+Z2)**(.5)
DELTAX=CRK_PNT(I,1)-CRK_PNT(I-1,1)
*ENDIF
THETA1=ASIN(DELTAX/DELTAL)
CSYS,20
DSYS,20
CLOCAL,19,1,CRK_PNT(I,1),CRK_PNT(I,2),CRK_PNT(I,3),0,-THETA,THETA1
CSYS,19
DSYS,19
: *****
:

```

```

:   FIND THE FIVE NODES FOR CALCULATING STRESS INTENSITY FACTORS
:
:   *****
:   POINT 1
:   *****
NSEL,ALL
NSEL,S,LOC,Z,-.0001,.0001
NSEL,R,LOC,X,-.0001,.0001
*GET,POINT1(I),NODE,,NUM,MAX
:   *****
:   FIND WEDGE ELEMENTS AT CRACK TIP
:   *****
NSEL,ALL
NSEL,S,LOC,Y,178,182
NSEL,R,LOC,Z,-.0001,.0001
NSEL,R,LOC,X,QPRAD,QPRAD
ESLN,S,0
*GET,ELEMENTH(I),ELEM,,NUM,MAX
*GET,ELEMENTL(I),ELEM,,NUM,MIN
:   *****
:   POINT 2
:   *****
NSEL,ALL
ESEL,ALL
ESEL,R,ELEM,,ELEMENTH(I)
NSLE,S
NSEL,R,LOC,Y,178,182
NSEL,R,LOC,Z,-.0001,.0001
NSEL,R,LOC,X,QPRAD
*GET,POINT2(I),NODE,,NUM,MAX
:   *****
:   POINT 3
:   *****
NSEL,ALL
ESEL,ALL
ESEL,R,ELEM,,ELEMENTH(I)
NSLE,S
NSEL,R,LOC,Y,178,182
NSEL,R,LOC,Z,-.0001,.0001
NSEL,R,LOC,X,QPRAD*4
*GET,POINT3(I),NODE,,NUM,MAX
:   *****
:   POINT 4
:   *****
NSEL,ALL
ESEL,ALL
ESEL,R,ELEM,,ELEMENTL(I)
NSLE,S
NSEL,R,LOC,Y,178,182
NSEL,R,LOC,Z,-.0001,.0001
NSEL,R,LOC,X,QPRAD
*GET,POINT4(I),NODE,,NUM,MAX
:   *****
:   POINT 5

```

```

: *****
NSEL,ALL
ESEL,ALL
ESEL,R,ELEM,,ELEMENTL(I)
NSLE,S
NSEL,R,LOC,Y,178,182
NSEL,R,LOC,Z,-.0001,.0001
NSEL,R,LOC,X,QPRAD*4
*GET,POINT5(I),NODE,,NUM,MAX
: *****
:
:   DEFINE CRACK PATH
:
: *****
CSYS,20
DSYS,20
CLOCAL,19,0,CRK_PNT(I,1),CRK_PNT(I,2),CRK_PNT(I,3),0,-THETA,THETA1
CSYS,19
DSYS,19
RSYS,19
LPATH,POINT1(I),POINT2(I),POINT3(I),POINT4(I),POINT5(I)
: *****
:
:   STRESS INTENSITY FACTORS CALCULATED
:
: *****
KCALC,0,1,3,0
*GET,KONE(I),KCALC,,K,1
*GET,KTWO(I),KCALC,,K,2
*GET,KTHREE(I),KCALC,,K,3
CSYS,0
DSYS,0
NSEL,ALL
*ENDDO
CSYS,0
DSYS,0
RSYS,0
NSEL,ALL
ESEL,ALL
PARSAV,ALL

```

APPENDIX E--CRACK GROWTH RATE DATA

TABLE XXVII
 CRACK LENGTH VERSUS NUMBER OF CYCLES
 ALPHA = 0 DEGREES

N (Cycles)	A (Inches)	Calculated A (Inches)	Error (Inches)
63014	2.059	2.0479685	0.011031521
65274	2.059	2.0671364	-0.00813641
76617	2.091	2.0988992	-0.007899204
79198	2.091	2.0984791	-0.007479113
82939	2.098	2.0967586	0.001241415
92275	2.106	2.0974435	0.0085565447
96296	2.107	2.1030118	0.003988245
101008	2.116	2.1145481	0.0014518684
105989	2.138	2.1323903	0.005609699
108157	2.144	2.1417556	0.0022443501
110249	2.15	2.1515753	-0.001575316
111175	2.157	2.1561397	0.000860326
112273	2.162	2.1617068	0.000293233
113276	2.167	2.1669261	0.0000739155
114221	2.172	2.171949	0.0000509614
115308	2.178	2.1778395	0.0001604504
116445	2.185	2.1841139	0.0008861213
117213	2.192	2.1884085	0.0035914705
118237	2.199	2.1941953	0.0048047201
119257	2.204	2.2000173	0.0039827369
120167	2.209	2.2052508	0.0037491726
121331	2.213	2.2119868	0.0010131682
122210	2.218	2.2170962	0.0009037654
123210	2.223	2.2229245	0.0000754745
124358	2.229	2.2296263	-0.000626315
125790	2.234	2.2379881	-0.003988093
126138	2.239	2.2400189	-0.001018863
127546	2.244	2.2482249	-0.004224867
128232	2.249	2.2522153	-0.003215279
129209	2.254	2.2578884	-0.003888437
130234	2.259	2.2638277	-0.004827713
131132	2.264	2.2690217	-0.005021699
132460	2.269	2.2766919	-0.007691899
133197	2.275	2.2809468	-0.005946826
134236	2.281	2.2869498	-0.005949751
135234	2.287	2.2927292	-0.005729188
136486	2.293	2.3000153	-0.007015323
137428	2.299	2.3055385	-0.006538464
138355	2.305	2.3110224	-0.006022403
139173	2.311	2.3159133	-0.004913348
140243	2.318	2.3224039	-0.004403923
141374	2.325	2.329408	-0.004408019
142166	2.333	2.3344201	-0.001420113
143260	2.341	2.3415185	-0.000518536
144241	2.349	2.3480872	0.0009127757

TABLE XXVII (Continued)
 CRACK LENGTH VERSUS NUMBER OF CYCLES
 ALPHA = 0 DEGREES

<u>N</u> <u>(Cycles)</u>	<u>A</u> <u>(Inches)</u>	<u>Calculated A</u> <u>(Inches)</u>	<u>Error</u> <u>(Inches)</u>
145144	2.357	2.3543327	0.0026673109
146172	2.365	2.361711	0.0032889526
147203	2.374	2.3694405	0.0045595372
148147	2.384	2.3768479	0.0071520628
149173	2.394	2.3853047	0.0086953095
150166	2.404	2.3939422	0.010057791
151537	2.415	2.4066997	0.0083003217
153134	2.437	2.4229622	0.014037775
154103	2.448	2.4336696	0.014330381
155129	2.46	2.4457827	0.014217335
156132	2.472	2.4584703	0.013529696
157239	2.484	2.4735397	0.0104603
158297	2.496	2.4890872	0.0069127912
159122	2.51	2.5020545	0.0079454853
160186	2.525	2.5199602	0.0050398087
161155	2.54	2.5375153	0.0024846867
162165	2.556	2.5571813	-0.001181309
163217	2.573	2.5792651	-0.006265103
164194	2.59	2.6013472	-0.011347161
165140	2.61	2.6242756	-0.014275552
166350	2.633	2.655985	-0.022984981
167201	2.658	2.6799985	-0.02199848
168126	2.689	2.7078106	-0.018810593
169201	2.723	2.7425105	-0.019510486
170057	2.761	2.7720804	-0.011080427
171486	2.81	2.8255442	-0.015544151
172307	2.862	2.8587264	0.0032735623
173128	2.914	2.8938179	0.020182105
174083	2.98	2.9371598	0.042840198

TABLE XXVIII
 CRACK LENGTH VERSUS NUMBER OF CYCLES
 ALPHA = 20 DEGREES

<u>N</u> <u>(Cycles)</u>	<u>A</u> <u>(Inches)</u>	<u>Calculated A</u> <u>(Inches)</u>	<u>Error</u> <u>(Inches)</u>
37099	2.272	2.2547076	0.01729244
38674	2.275	2.2795022	-0.004502189
39831	2.278	2.296424	-0.018423996
41301	2.306	2.316651	-0.010650998
42113	2.324	2.3273337	-0.003333653
43344	2.345	2.3430299	0.0019700868
44131	2.359	2.3528347	0.006165306
45134	2.373	2.3651727	0.0078272573
46202	2.386	2.3782354	0.0077646493
47688	2.4	2.3965366	0.0034634061
49206	2.411	2.415734	-0.004733994
50121	2.434	2.4277153	0.0062846612
51174	2.445	2.4420215	0.0029784627
52133	2.453	2.4556394	-0.002639399
53211	2.482	2.4717452	0.010254804
54169	2.49	2.4868773	0.0031226532
55153	2.496	2.5033317	-0.007331714
56177	2.506	2.5215509	-0.015550908
57329	2.521	2.5435331	-0.022533128
58124	2.545	2.5597073	-0.014707303
58838	2.563	2.5749866	-0.011986627
59178	2.572	2.5825255	-0.010525485
59744	2.585	2.5954675	-0.010467474
60412	2.61	2.6113964	-0.001396403
61142	2.639	2.6296521	0.0093479241
61698	2.674	2.6441771	0.029822881
62238	2.681	2.6588184	0.022181635
62837	2.721	2.6756969	0.045303064
63754	2.721	2.7028893	0.018110722
64476	2.721	2.725501	-0.004501044
65233	2.74	2.7503967	-0.010396709
66033	2.77	2.7780815	-0.00808154
66706	2.81	2.8025075	0.0074925395
67461	2.839	2.8311904	0.0078096191
68331	2.855	2.8659832	-0.010983157
68804	2.882	2.8857066	-0.003706641
69542	2.895	2.9176513	-0.022651332
70172	2.927	2.9460804	-0.019080426
70755	2.972	2.9733659	-0.001365869
71492	3.013	3.009239	0.0037610358
72124	3.024	3.0412606	-0.017260598
72787	3.061	3.0761356	-0.015135567
73454	3.115	3.1125791	0.0024209347
74173	3.192	3.1534279	0.038572073

TABLE XXIX
 DA/DN VERSUS DELTA K
 ALPHA= 0 & 20 DEGREES

Plate Depth (Inches)	Delta K for Alpha = 0 degrees			Delta K for Alpha = 20 degrees		
	(a=2.188 in)	(a=2.625 in)	(a=2.850 in)	(a=2.309 in)	(a=2.625 in)	(a=2.8125 in)
0.000	17.533	31.518	45.235	18.327	38.604	50.064
0.025	17.550	31.545	45.273	18.311	38.488	50.032
0.050	17.605	31.640	45.403	18.355	38.520	50.132
0.075	17.705	31.810	45.640	18.421	38.664	50.268
0.100	17.892	32.135	46.095	18.530	38.848	50.480
0.125	18.183	32.638	46.800	18.667	39.080	50.784
0.150	19.195	34.425	49.350	18.850	39.508	51.160
0.175	19.483	34.893	49.978	19.115	40.284	52.280
0.200	20.920	37.388	53.480	19.580	40.820	52.916
0.225	17.548	31.235	44.553	20.165	45.648	59.992
0.250	19.883	35.350	50.320	24.116	41.820	49.824
0.275	16.150	28.660	40.500	22.334	45.268	55.308
<u>0.300</u>	<u>8.328</u>	<u>14.458</u>	<u>20.600</u>	<u>10.472</u>	<u>19.264</u>	<u>26.904</u>
(Average of 0 - 0.175)	18.143	32.576	46.722	18.572	39.000	50.650

Delta K	DA/DN	
	(Alpha=0 deg)	(Alpha=20 deg)
18.143	5.560E-06	
18.572		1.410E-05
32.576	2.550E-05	
39.000		2.510E-05
46.722	3.950E-05	
50.650		3.760E-05

**APPENDIX F--FORTRAN PROGRAM TO CALCULATE
CRACK GROWTH RATES**

```

C*****
C PROGRAM TO CALCULATE DA/DN FOR A GROWTH RATE TEST
C*****
      DIMENSION A(200),N(200),BB(3),DADN(200),DELK(200),ID(10)
      DIMENSION AA(10),NN(10)
      REAL N
      REAL NN
      INTEGER QQ
      INTEGER TYPE
      OPEN(5,FILE='AVSN.DAT',FORM='FORMATTED')
      OPEN(6,FILE='DADN.DAT',STATUS='NEW')
10  FORMAT(/A4, 9H SPECIMEN,5X,2HB=,F6.3,5H IN. ,5X,2HW=,F6.3,5H IN.
      ,5X,3HAN=,F6.3,5H IN. )
15  FORMAT(/,' SEVEN POINT INCREMENTAL POLYNOMIAL METHOD FOR DETERMINI
      * NG DA/DN ')
17  FORMAT(/)
20  FORMAT(/6H PMIN=,F6.3,4HKIPS,5X,5HPMAX=,F6.3,4HKIPS,5X,2HR=,F6.3,5
      * X,10HTEST FREQ=,F6.3,3HHZ.)
22  FORMAT(/7H TEMP=,F4.0,1HF,5X,12HENVIRONMENT=,A4)
25  FORMAT(A4,F5.1,F8.3,A4)
30  FORMAT(10A4,2I6)
35  FORMAT(/1H ,10A4,10X,14H NO.POINTS = ,I3)
40  FORMAT(4(F6.4,F9.0))
55  FORMAT(/8H OBS.NO., 3X,6HCYCLES,5X,8HA(MEAS.),3X,7HA(REG.),4X,6HM.
      * C.C.,5X,4HDELK,5X,5HDA/DN)
92  FORMAT(I4,6X,F8.0,2X,F8.3,3X,F8.3,3X,F8.6,2X,F8.2,3X,E8.3)
95  FORMAT(I4,6X,F8.0,2X,F8.3)
98  FORMAT(I4,6X,F8.0,2X,F8.3,3X,F8.3,3X,F8.6,2X,F8.2,3X,E8.3,2H *)
99  FORMAT(F6.3,F6.3,F6.1,F6.3,F6.3,F6.3)
200 FORMAT(/10H
      )
300 FORMAT(/45H * - DATA VIOLATE SPECIMEN SIZE REQUIREMENTS )
C TYPE=1 FOR CT AND 2 FOR A CCP
500 READ(5,30,END=1000)(ID(I),I=1,10),NPTS,TYPE
      READ(5,99)PMIN,PMAX,F,B,W,AM
C KIND=CT,CCP,ETC.
      READ(5,25)ENV,TEM,YS,KIND
      READ(5,40)(A(I),N(I),I=1,NPTS)
      WRITE(6,15)
      WRITE(6,35)(ID(II),II=1,10),NPTS
      WRITE(6,10)KIND,B,W,AM
      R=PMIN/PMAX
      WRITE(6,20)PMIN,PMAX,R,F
      WRITE(6,22)TEM,ENV
      WRITE(6,55)
      DO 31 I=1,NPTS
      A(I)=A(I) + AM
31  CONTINUE
      K=0
      PI=3.1416
      PP=PMAX-PMIN
      DO 110 I=1,3
      WRITE(6,95)I,N(I),A(I)
110 CONTINUE
      NPTS=NPTS-6

```

```

DO 100 I=1,NPTS
L=0
K=K+1
K1=K+6
DO 60 J= K,K1
L=L+1
AA(L) = A(J)
NN(L) = N(J)
60 CONTINUE
C1 = 0.5*(NN(1)+NN(7))
C2 = 0.5*(NN(7)-NN(1))
SX=0
SX2=0
SX3=0
SX4=0
SY=0
SYX=0
SYX2=0
DO 70 J=1,7
X = (NN(J)-C1)/C2
YY = AA(J)
SX = SX + X
SX2 = SX2 + X**2
SX3 = SX3 + X**3
SX4 = SX4 + X**4
SY = SY + YY
SYX = SYX + X*YY
SYX2 = SYX2 + YY*X**2
70 CONTINUE
DEN=7.0*(SX2*SX4-SX3**2)-SX*(SX*SX4-SX2*SX3)+SX2*(SX*SX3-SX2**2)
T2=SY*(SX2*SX4-SX3**2)-SYX*(SX*SX4-SX2*SX3)+SYX2*(SX*SX3-SX2**2)
BB(1) = T2/DEN
T3=7.0*(SYX*SX4-SYX2*SX3)-SX*(SY*SX4-SYX2*SX2)+SX2*(SY*SX3-SYX*SX2
*)
BB(2) = T3/DEN
T4=7.0*(SX2*SYX2-SX3*SYX)-SX*(SX*SYX2-SX3*SY)+SX2*(SX*SYX-SX2*SY)
BB(3) = T4/DEN
YB = SY/7.0
RSS = 0
TSS = 0
DO 75 J=1,7
X = (NN(J)-C1)/C2
YHAT = BB(1)+BB(2)*X+BB(3)*X**2
RSS = RSS+(AA(J)-YHAT)**2
TSS = TSS+(AA(J)-YB)**2
75 CONTINUE
R2 = 1.0-RSS/TSS
DADN(I)= BB(2)/C2 + 2.0*BB(3)*(NN(4)-C1)/C2**2
X=(NN(4)-C1)/C2
AR=BB(1)+BB(2)*X+BB(3)*X**2
S=1E+10
SNET=0
QQ=I+3
GOTO(1,2) ,TYPE

```

```

1  CONTINUE
   T = AR/W
   FT = ((2+T)*(0.886+4.64*T-13.32*T**2+14.72*T**3-5.6*T**4))/(1-T)**1.
* 5
   S = YS*SQRT(PI*W*(1-T))/2
   GOTO 190
2  CONTINUE
   T = 2*AR/W
   SEC = 1.0/(COS(PI*T/2))
   FT = SQRT((PI*T*SEC)/2.0)
   SNET = PMAX/(B*W*(1-T))
190 DELK(I) = (FT*PP)/(B*SQRT(W))
   AX = DELK(I)/(1-R)
   IF(AX.GE.S)GOTO 97
   IF(SNET.GE.YS)GOTO 97
91  WRITE(6,92)QQ,N(QQ),A(QQ),AR,R2,DELK(I),DADN(I)
   GOTO 100
97  WRITE(6,98)QQ,N(QQ),A(QQ),AR,R2,DELK(I),DADN(I)
100 CONTINUE
   J = NPTS+4
   K = NPTS+6
   DO 120 I=J,K
   WRITE(6,95)I,N(I),A(I)
120 CONTINUE
   WRITE(6,17)
   WRITE(6,300)
1000 CONTINUE
   STOP
   END

```

**APPENDIX G--STRESS INTENSITY FACTORS FOR SLANTED
CRACKS PROJECTED TO HORIZONTAL**

The following is a simple comparison of several actual Mode I/Mode II specimen stress intensity factors to the handbook solutions for a horizontal crack. Notice that the crack length a_{horz} is calculated by multiplying the slanted crack length $a_{slanted}$ by the cosine of the alpha angle.

TABLE XXX.
SIF'S FOR SLANTED CRACKS PROJECTED TO HORIZONTAL

Alpha (deg.)	a(slanted) (in.)	a(horz.) (in.)	a(horz.)/b	F(a(horz.)/b)	KI/Sigma (Handbook)	KI/Sigma* (Actual)
0	2.19	2.19	0.56	3.48	9.1	8.6
10	2.66	2.62	0.67	5.38	15.4	13.8
20	2.31	2	0.5	2.84	7.1	5.6
30	2.75	2.38	0.62	4.34	11.9	9.5
40	3.13	2.39	0.62	4.34	11.9	11.5

*Corrected for reduced cross section using a factor of .6

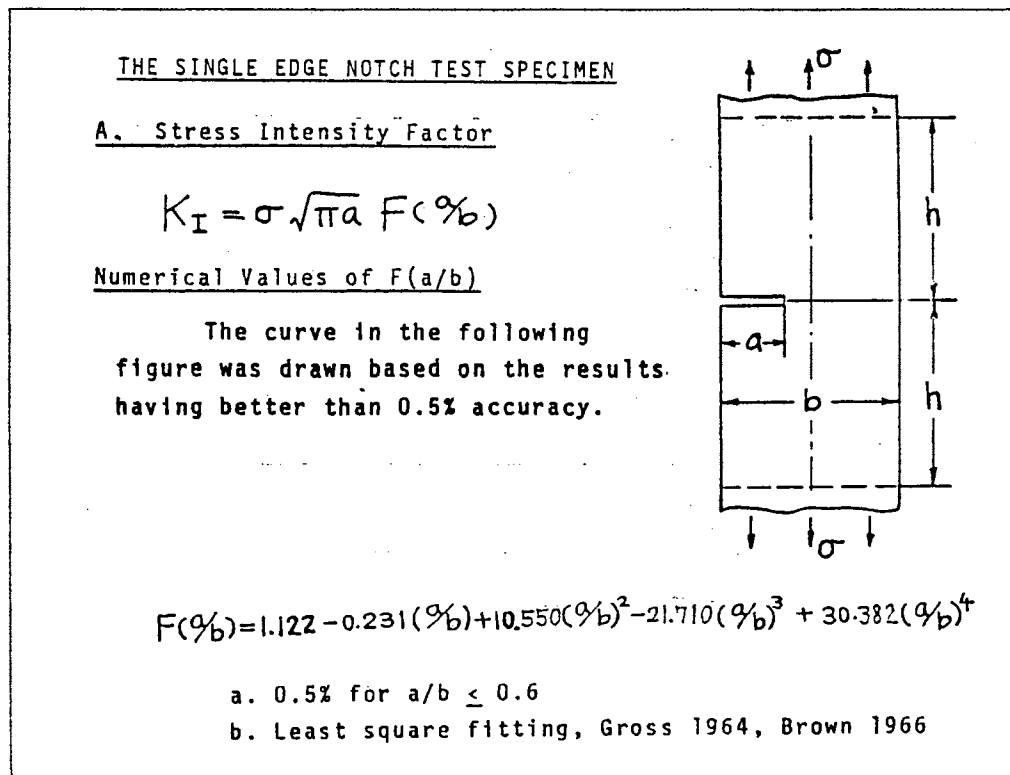


Figure 72. Handbook Solution for SIF's[94]

VITA 

Michael Allen Magill

Candidate for the Degree of

Doctor of Philosophy

Thesis: SUSTAINED MIXED MODE CRACK GROWTH IN FLAT PLATES

Major Field: Civil Engineering

Biographical:

Personal Data: Born in Fort Leonardwood, Missouri, May 29, 1958, the son of Vernon R. and Connie J. Magill. Married to Lisa L. Maeder on August 23, 1981. Father to Jessica, Tyler, and Marshall.

Education: Graduated from Putnam City West High School, Bethany, Oklahoma, in May 1976; received Bachelor of Science Degree in Mechanical Engineering from Oklahoma State University in December, 1980; received Master of Science Degree in Mechanical Engineering from Oklahoma State University in July, 1988; completed requirements for the Doctor of Philosophy Degree at Oklahoma State University in May, 1995.

Professional Experience: Machinist, Induction Engineering/American Wind Turbine, Stillwater, Oklahoma, August, 1977, to February, 1980; Summer Engineer, J.M. Huber Corporation, Borger, Texas, May, 1979, to August, 1979; Summer Engineer, Dow Chemical Company, Freeport, Texas, May, 1980, to August, 1980; Production Systems Engineer, Amoco Production Company, Rocky Mountain Region, January, 1981, to July, 1984; Structural Engineer/Project Supervisor, Engineering and Construction Division of the National Park Service, May, 1992, to August 1992 and May, 1993, to August, 1993; Assistant Professor, Division of Engineering Technology, Oklahoma State University, August, 1984 to present.

Professional Organizations: Registered Professional Engineer in the State of Oklahoma, American Society of Civil Engineers, American Society of Engineering Educators, Society of Manufacturing Engineers.